UTS UNIVERSITY OF TECHNOLOGY SYDNEY

Comparative Study of Morphological, Photophysiological, and Transcriptomic Responses to Varied Light Spectra in Two Filamentous Cyanobacteria from the Nostocales Order.

by Amber Brierley

Thesis submitted in fulfilment of the requirements for
the degree of

Master of Science (Research)

under the supervision of A. Prof. Mathieu Pernice and Dr. Andrei Herdean

University of Technology Sydney
Faculty of Science

December 2023

CERTIFICATE OF ORIGINAL AUTHORSHIP

I, Amber Brierley, declare that this thesis is submitted in fulfilment of the requirements for the award of Master of Science (Research), in the School of Life Sciences at the University of Technology Sydney.

This thesis is wholly my own work unless otherwise referenced or acknowledged. In addition, I certify that all information sources and literature used are indicated in the thesis.

This document has not been submitted for qualifications at any other academic institution.

This research is supported by the Australian Government Research Training Program.

Signature:

Production Note:
Signature removed prior to publication.

Date: 04/12/23

Acknowledgements

First and foremost, I would like to thank my supervisors, Mathieu Pernice and Andrei Herdean for their unwavering support and guidance throughout this Masters degree. With numerous setbacks, difficulties, troubleshooting and figuring out processes together they both stayed calm, cool, collected and managed to keep a sense of humour. Our weekly meetings involved regular check ins (both related to the project and life in general), staying on top of the project, a few laughs and lots and lots of chocolate. Without their help both in these meetings, with admin and chasing up other people on my behalf, to aiding me in the lab even when there wasn't really time, I wouldn't have been able to complete this thesis to the degree it is without them. Both Mathieu and Andrei made this a truly enjoyable experience and a bitter sweet moment to be approaching the end of this era.

Whilst two years has flown by, it wouldn't have had it not been for the friendships formed throughout this degree. A big thank you to Nicole Di Lernia, Amanda Grima, Chiara Duijser, Natasha Bartels, Laura La Motta, Kieran Chau, Bernardo Campos, Don Davis, Hadley England, Lorna Howlett, Axel Olander, Lili Hoch, Antonio Sacco, Clara Belotto for lunch at 12pm, 2pm coffees on the daily, Friday arvo drinks, starting a social soccer team, many a camping trip and all the help with the stresses of HDR candidature ship that we all know too well. Without all of these great people this experience would have been a whole lot worse.

Thank you to those who helped with some of my work, most notably Mikael Kim. A special thanks also to Lucia Bennar, Vishal Gupta, Unnikrishnan Kuzhiumparambil and Taya Lapshina for their assistance.

Finally, of course, to my biggest supporters – my parents Carolyn and Tony, my sister Jasmine and my partner Mark – who always asked how my work was going even if they knew they were not going to fully understand my answer. For all their support and encouragement throughout, this has meant a lot.

Table of Contents

List of Figures and Tables

List of Figures

List of Tables

List of Supplementary Figures

List of Supplementary Tables

across strains and across light conditions within each strain. Different letters indicate significance for the mentioned comparisons. N=10

Supplementary Table 6: Maximum fluorescent points from the Excitation / Emission heat maps in Figure 5

Supplementary Table 7: Genes commonly upregulated in both *Tolypothrix* sp. 481 and *Phormidium* 590 as obtained from Venny in relation to Figure 8.

Supplementary Table 8: Genes uniquely upregulated in *Tolypothrix* sp. 481 RL compared to WL as obtained from Venny in relation to Figure 8.

Supplementary Table 9: Genes uniquely upregulated in *Phormidium* 590 RL compared to WL as obtained by Venny in relation to Figure 8.

Supplementary Table 10: Genes commonly downregulated in *Tolypothrix* sp. 481 and *Phormidium* 590 as obtained by Venny in relation to Figure 8.

Supplementary Table 11: Genes uniquely downregulated in *Tolypothrix* sp. 481 RL compared to WL as obtained by Venny in relation to Figure 8.

Supplementary Table 12: Genes uniquely downregulated in *Phormidium* 590 RL compared to WL as obtained by Venny in relation to Figure 8.

Supplementary Table 13: List of proteins involved in the phycobilin biosynthetic pathway as referenced by a previous paper [1] accompanied by log Fold Change for *Tolypothrix* sp. 481 RL compared to WL

Supplementary Table 14: List of proteins involved in the phycobilin biosynthetic pathway as referenced by a previous paper [1] accompanied by log Fold Change for *Phormidium* 590 RL compared to WL

Thesis Abstract

Tolypothrix sp. (also known as *Fremyella diplosiphon*) is a cyanobacteria that undergoes chromatic acclimation (CA) - a process observed in certain cyanobacteria that allows them to adjust their light harvesting pigments in response to changes in light conditions. As a result, *Tolypothrix* sp. can synthesise both Phycocyanin (PC) and Phycoerythrin (PE) when under red (RL) and green light (GL) respectively. In contrast, another cyanobacteria of the same taxonomic order (Nostocales), *Phormidium* sp. (also known *Fremyella diplosiphon* on the UTEX culture collection website where both strains were purchased), has received limited investigation and cannot perform CA, unable to produce PE. In order to provide new insights into these two strains and their capabilities for chromatic adaption, in this study I experimentally exposed them to different light spectra (white light, WL; Red light, RL and Green light, GL) to compare their photophysiological, morphological and molecular responses. This study aims to shed light on the differences in behaviour of these two strains that are closely related taxonomically. *Tolypothrix* sp. shows variation in morphology with GL cultures having significantly longer cells and filaments compared to RL. Interestingly, there were no significant changes in morphology observed for *Phormidium* sp.. The growth rate for *Tolypothrix* sp. 481 was higher in RL than GL. Again, for *Phormidium* sp. there was limited change in growth rate observed under different light conditions. The Electron Transport Rate (ETR) was measured with *Tolypothrix* sp., the GL culture having a higher maximum ETR than RL, which was similarly seen for *Phormidium* 590, however, the difference between GL and RLwas much smaller. These differences observed under changed light conditions led to a 3D excitation (Ex) emission (Em) scan that indicated the presence of PC, PE and chlorophyll *a* (chl *a*) in *Tolypothrix* sp. and displayed the potential energy transfer from PC and PE to chl *a* altering its usual Ex/Em points. Across *Phormidium* sp. there was no PE fluorescence visible under any light condition. The quantity of these pigments confirmed this. No PE was detected in *Phormidium* sp., with a higher quantity of chl *a* and PC under GL. For *Tolypothrix* sp. there was more chl *a* and PC in RL but more PE in GL. These responses to light were further investigated through RNA NovaSeq, focusing more particularly for the most changing conditions (RL vs WL). Looking at the transcripts, there was clear regulation in both strains under RL conditions when comparing to WL. There is upregulation in proteins involved in the phycobilin biosynthetic pathway for *Tolypothrix* sp., whereas in *Phormidium* sp. a downregulated trend is present. Transcripts for linker genes in *Tolypothrix* sp. and *Phormidium* sp. were detected – including: *CpeC*, *CpcG*, *CpcC*, and *CpcD*, which are involved in securing PC, PE and allophycocyanin (APC) together to form the phycobilisome. Interestingly, *Phormidium* sp. showed trends of downregulation for the PE linker protein which could suggested the presence

of mechanisms for PE synthesis, although no PE was detected in the photophysiological data. Further whole-genome investigation is needed to fully comprehend and associate the underlying molecular processes that contribute to the differences observed.

Chapter 1: Introduction

1.1. Cyanobacteria and their Significance

Cyanobacteria are one of the oldest organisms on the planet and have played a vital role in the evolution of higher organisms [1, 2, 3]. Cyanobacteria are gram-negative photoautotrophic prokaryotes that occur in a diverse set of morphologies; unicellular to multicellular, filamentous, colonial and different lifestyles; planktonic or benthic [2, 4]. Not only is their morphology diverse but cyanobacteria inhabit the widest range of habitats from hot to cold, alkaline to acidic, marine, freshwater, saline, terrestrial and symbiotic environments [2, 5, 6] and have been found in extreme locations including hot springs, deep-sea vents and polar habitats [7] to occupy across nearly all niches of the globe. Cyanobacteria are capable of numerous metabolic and adaptive mechanisms including nitrogen fixation, chromatic acclimation and the ability to form symbiotic associations with eukaryotic hosts including plants, fungi and protists [2].

For cyanobacteria, photosynthesis is their principal mode of energy metabolism [4] leading them to account for approximately 40% of the world's photosynthetic activity [5, 8], giving them essential roles for ecosystem functioning on earth. Cyanobacteria global commercial biomass has been calculated to be approximately a thousand million tonnes (10^{15} g) [5, 8] with expectations for this to increase. Cyanobacteria are categorized as a stand alone organism, however, they are often grouped within microalgae for their similar properties and photosynthetic capabilities as well as their novel emerging applications in the biotechnology industry and climate action [9].

In 2004, one estimate put the global production of microalgae at around 5000 tons (dry weight) and US$ 1.25 billion per year [10]. Since then, production is presumed to have surged significantly; nonetheless, obtaining dependable figures remains unexpectedly challenging [11]. Algae, including cyanobacteria are becoming increasingly popular in their interest for harvesting a range of products that they produce, which include polysaccharides, pigments, lipids and protein compounds that display a range of beneficial properties such as antioxidant activity, anti-cancer, antibacterial, antifungal, anti-inflammatory and antiviral activity, plant growth promoting substances and hormones. These algal extracts are already found in a range of different commercially available products that range from pharmaceuticals to nutraceuticals, animal and human feed, carbon sequestration and bioremediation uses [12], however, more research is needed in this area to make these products and their synthesis a more economically viable industry.

Algae production is increasing with the compound annual growth rate increasing by 4.3% in the period 2020-2027. According to a paper in 2022 [3]a growing sector of microalgae products is food and more particularly proteins with predictions that by 2050 (Fortune Business Insights,

Microalgae Food Market Size Report https://www.fortunebusinessinsights.com/industry-reports/microalgae-food-market-100802) algae could account for 18% of protein sources [3].

It was estimated that in 2020, dyeing agents are at the head of the list of microalgae products on the market, with USD 800 million, followed by pharmaceuticals/chemicals (USD 500 million), nutraceuticals (USD 300 million), and, finally, cosmetics (USD 30 million) [3, 13].

Commonly used dyeing agents include pigments, which in a bio-context are compounds that absorb light in different ranges of the visible spectrum. The unique molecular structure of these pigments allows them to absorb photons at various wavelengths. In microalgae there are generally three different types of pigments that can be present in the cell [14]. These are chlorophylls; a family containing five classes – chlorophyll *a*, *b*, c, d and *f* that are present in different types of plants and organisms. Chlorophyll *a* is the most abundant of these types and is responsible for absorbing light in the photosynthesis process. Chlorophyll *a* is found in all light harvesting complexes of photosynthetic organisms, and the reaction centres - photosystem I (PSI) and photosystem II (PSII) [15, 16]. Carotenoids, including but not limited to betacarotene, lycopene and astaxanthin - which can be grouped into primary or secondary carotenoids. Primary carotenoids play a role in photosynthesis as structural and functional components, and secondary carotenoids are produced through carotenogenisis that is induced through environmental stimuli and stress [17-19]. Finally, phycobilins which are accessory photosynthetic pigments unique to algae that are capable of transferring light energy to chlorophylls and enhance photosynthetic efficiency. Phycobilin pigments include phycerythrobilin, phycocyanobilin, phycourobilin and phycobilivilin and are not present in any other organism except for cyanobacteria and algae [14].

1.1.1. Taxonomy and Phylogeny of Cyanobacteria

Phylogenetically, cyanobacteria are a very old group that have gone through many rapid adaptations to environmental conditions and has created one of the most diverse group of organisms known to date [20]. This, combined with their ability to asexually reproduce produces a challenge to accurately and consistently evaluate their taxonomy. Initially, cyanobacteria taxonomy was purely based off morphological traits but this has since been deemed insufficient on its own for modern taxonomy with so many cyanobacteria strains continuously emerging [21, 22].

A molecular approach has commonly been used for some time now and should be used in conjunction with morphological traits. Most commonly, specific markers such as 16S and 23S are used [20], however, some consider these marker genes to not be variable enough to recognize

and identify the diversity at the species level in prokaryotes and deem whole genome sequencing a more reliable method to be used to determine cyanobacteria taxonomy [23].

The importance of having accurate and adaptable techniques for taxonomy is essential to produce acceptable and consistent research especially when cyanobacteria are so diverse. Cyanobacteria can be broken down into 7 Orders including Chroococcales, Entophysalidaless, Pleurocapsales, Dermocarpales, Siphononematales, Nostocales and Stigonematakes [24]. In 2023, a paper reviewed the newly identified species of cyanobacteria between 2000-2022, with the Nostocales order having the highest number of total species (n=1745) out of all the cyanobacteria orders and illuminates the vast range of organisms that form up the cyanobacterial radiation [22].

Currently, one species can have multiple different names or synonymous names that are often placed in different phylogenetic branches depending on what gene marker or identifier was used to make the groupings, with reassessments needed frequently [25, 26]. The two strains investigated in this project were provided by The University of Texas at Austin (UTEX) Culture Collection of Algae and are both named *Fremyella diplosiphon* (UTEX 481 and UTEX 590) and have similar morphologies however, these organisms behave and adapt very differently. Using the 23S partial sequence provided by UTEX for both organisms their taxonomical classification produced by NCBI Blast (see Materials and Methods for details) is as follows:

F. diplosiphon UTEX 481 (GenBank KY963612.1) has the following taxonomic classification
Bacteria; Cyanobacteria; Cyanophyceae; Nostocales; Tolypothrichaceae; Tolypothrix
Other common names for this strain include *Tolypothrix* sp. PCC 7601 and *Calothrix* sp.

F. diplosiphon UTEX 590 (GenBank KY963613.1) has the following taxonomic classification
Bacteria; Cyanobacteria; Cyanophyceae; Nostocales; Ruvykaruaceae, Microchaete.
Other common names for this strain include *Phormidium* sp. and *Microchaete diplosiphon*.

When blasted using NCBI software, the GenBank 23s rRNA sequences have a 96.14% identity and have been chosen for comparative purposes due to the percentage identity and taxonomy identities yet noted physiological differences. Their phylogenetic relationship can be visualized in Figure 1. The two Nostocales strains will here on be referred to as *Tolypothrix* sp. UTEX 481 for *F. diplosiphon* UTEX 481 and *Phormidium* 590 For *F. diplosiphon* 590 to avoid confusion. As will be seen through the results, these organisms behave extremely differently

morphologically, photophysiologically and transcriptomically which emphasizes the importance for accurate nomenclature that differentiates cyanobacteria strains.

1.2 Pigments found in Cyanobacteria

These prokaryotes have a classical oxygenic photosynthetic process [6, 16], and they have evolved specialized photosynthetic proteins called cyanobacteriochromes to enhance light capture [27] to aid in photosynthesis. The pigments used for photosynthesis include chlorophyll *a* which is embedded in thylakoid membranes, and phycobilins that are bound to phycobiliproteins that create the phycobilisome that connects to chlorophylls which transfer captured energy to the photosystems.

1.2.1 Chlorophylls

Chlorophylls are pigments that don't absorb green light and therefore appear green, are soluble in organic solvents and not easily in water. Currently, chlorophylls have no toxic side effects and are being more widely used in the food industry for colourants of beverages and cakes along with maintaining the colouration of canned fruits and vegetables [14].

All cyanobacteria contain the light-harvesting pigment chlorophyll-a, as do all photosynthetic organisms, with the last common ancestor for cyanobacteria being nonphotosynthetic [28]. However, there are several types of chlorophylls found in nature, and not all organisms have the same kind. Among these, the most recognized types are chlorophyll-a, chlorophyll-b, chlorophyll-c1, chlorophyll-c2, chlorophyll-d, and the divinyl versions of chlorophyll-a and b. For cyanobacteria, chl *a* is the most commonly produced chlorophyll [14, 29]. Each of the chlorophylls has a different maximum absorption wavelength from the light spectrum, giving them different profiles and properties. Both *Tolypothrix* sp. PCC 7601 and *Phormidium* sp. contain chl *a* which has an absorption maximum (A_{max}) at two different wavelengths, 450 nm and 660 nm [30] with an excitation and emission wavelength for fluorescence at 430 and 670 nm respectively.

Chlorophyll *a* molecules are integral to the photosystems, serving distinct roles in light absorption and energy conversion. Within the photosystems, several chlorophyll *a* molecules are embedded in the antenna complexes, such as CP43 and CP47 proteins, where they function to capture and funnel light energy towards the reaction centres. Additionally, specialized pairs of chlorophyll a molecules located in the reaction centres are pivotal for charge separation and the initiation of electron transport, crucial steps in converting light energy into chemical energy [31].

1.2.2 Pigmented Protein Assemblages: The Phycobilisome

Phycobiliproteins aggregate to form structures known as phycobilisomes, which are associated with the thylakoid membrane in cyanobacteria [30]. These structures have an absorption range of 500-660nm. The phycobilisomes forms an antenna like shape which allows light energy to be transported to Photosystem II with great efficiency [30].

The structure of the phycobilisome (PBS) (Fig. 1) consists of two main units: the core and rods [32]. Within these units there are phycobiliproteins that carry three different chromophores with individual absorbance maximums (A_{max}) - phycoerythrin (A_{max} 565 nm), PC (A_{max} 620 nm), and Allophycocyanin (APC) (A_{max} 650 nm) [33-35]. APC forms the core of the PBS and is attached to the reaction center. Then there is constitutive PC (PCc) that forms the proximal part of the rods that are linked to the core. In some cyanobacteria capable of chromatic acclimation, the outer rods can be formed of either inducible PC (PCi) or PE depending on the incoming light spectral quality [36]. Each phycobiliprotein forms a stacked disc-like structure composed of six monomers, which are further stacked as two cylindrical trimers. Each monomer, in turn, consists of an alpha and beta subunit with linker proteins binding the rods to the core and the core to the thylakoid membrane [8, 37, 38].

1.2.3 Phycobilins

A group of pigments only found in algae are a class of photosynthetic pigment known as phycobilins which include phycoerythrin (PE), phycocyanin (PC), phycourobilin (PUB) and phycobiliviolin (PVB). Phycobiliproteins are bioactive proteins that bind to pigments and contain some essential amino acids that the human body needs. The market value of phycobiliproteins in 2018 was USD 30 million with the compound annual growth rate of 21.3% [14, 39]. Phycobiliproteins (PBP) are water soluble [30] and can account for 50% of total protein in cyanobacteria cells [40].

1.2.3.1 Phycoerythrin

There are a number of different phycoerythrins that can bind Phycoerythrobilin (PEB), phycourobilin (PUB) or both of these, that have an absorption maximum in the range of 495-575 nm [30, 41] and appears red or intense pink in colour. PE is an autofluorescing protein with fluorescence maximum at Excitation and Emission wavelengths of 543 and 575nm respectively

[41]. PE can prevent oxidative stress, cell damage and inhibit reactive oxygen species generation, as well as be applied to more commercial aspects such as food dyes and product colourants [14].

1.2.3.2 Phycocyanin

Phycocyanin is more commonly found in cyanobacteria than PE with R-PC found in red algae having a light absorption maximum between 533 – 544 nm, and C-PC found in cyanobacteria with a light absorption maximum between 610 - 620 nm [30, 41, 42] and appears as an intense blue colour. PC is also an autofluorescing protein with fluorescence maximum at Excitation and Emission of 633 and 645nm respectively [41]. PC has been of increasing interest due to its anti-inflammatory, antioxidant, antibacterial applications, along with the previously mentioned food-industry related uses [14].

1.2.3.3 Allophycocyanin

Allophycocyanin (APC) is a phycobiliprotein binding exclusively to phycocyanobilin that fluoresces inred light with an Excitation/Emission maximum of 651/660nm [41] and is also a water soluble accessory pigment.

1.3 Cyanobacteria Photosynthesis

Like other organisms, the photosynthetic system in cyanobacteria is tightly connected to other metabolic pathways [43]. Using the measured fluorescence of chlorophylls can provide rapid information about acclimation and photosynthesis of cyanobacteria with the cellular Phycobilin (PBP) content influencing the fluorescent yield of the cell [31]. Cyanobacteria have phycobilisomes as the main complex to capture light [31, 44] and are the only prokaryote known to undergo oxygenic photosynthesis [45] and respiration in a single compartment which not a lot of other organisms are capable of [46].

The initial step in the photosynthetic light reactions of cyanobacteria involves the absorption of light by large antennas called phycobilisomes, however, these do not exist in all cyanobacteria. These phycobilisomes are made up of phycobilins which are the chromophores of PBP, that have the ability to capture light energy. Carotenoids are also able to act as accessory pigments and capture light energy to be transferred to chlorophyll [17-19]. The captured light is then transferred to PSII and PSI complexes, which are embedded in the thylakoid membrane and it has been documented that PBP are capable of transferring light energy to chl *a* with almost 100% efficiency [47, 48]. PSII is responsible for the oxidation of water in photosynthesis through the removal of

electrons from water and is the start of a chain of reaction centres for the electron transport chain, with chlorophylls transferring their captured light energy to PSII [49, 50]. In cyanobacteria, the number of PSII complexes is lower compared to PSI, and the majority of PBPs are associated with PSII. However, under specific conditions, the phycobilisomes can be redistributed to PSI, thereby regulating the efficiency of energy transfer between the two photosystems [28, 46, 51, 52]. Cyanobacteria have also evolved several electron transport pathways in order to avoid over supply of light energy which could be harmful to continued function and energy capture [53]. As another protective measure, carotenoids quench chlorophyll or disperse excess energy that would be unused in photosynthesis.

1.4 Chromatic Acclimation

Complementary chromatic adaptation (CCA) is a process by which certain cyanobacteria can adjust their pigment composition in response to changes in the ambient light spectrum, an ability that enables these organisms to optimize their light capture efficiency under various light conditions [32, 54, 55]. This process has been updated to Chromatic Acclimation (CA) to be more scientifically correct. There have been many researchers looking into the process of CA, mainly focusing on the green-red light changes. However, more types of CA have been uncovered and are becoming more widely understood as scientific tools are further advanced. The molecular mechanisms behind the CA process are being recognized and been made aware of for most of the known types of CA, however, the challenge that still remains lies in understanding the fitness impacts of cyanobacteria that undergo CA – being both costs and benefits [56].

Extensive studies and reviews on these adaptations have shed light on the mechanisms behind this process [56-62]. A more recent paper reviewed the types of CA that can occur in cyanobacteria, and summarized these into six main types [56]. Chromatic Acclimation type 1 (CA1) is a changing in the rod-core linker CpcL quantity where there is low abundance of the linker in red light and high abundance in green light. CA2 changes phycoerythrin levels to be low in red light and high in green light. CA3 changes Phycobilisome (PBS) rod and chromophore composition (Fig. 1) to be phycocyanin rich in red and phycoerythrin rich in green light. CA 1-3 can be categorized as green/red acclimation and is observed in some freshwater cyanobacteria. CA4 changes chromophore composition in some marine cyanobacteria to be PEB rich in green light and PUB rich in blue light and is blue/green acclimation. CA4 does not rely on a change in the ratios of different phycobiliproteins, but on changes in phycobilins on the same phycobiliproteins. CA5 adds/removes rod proteins to be high PC in red light and low PC in far-red light. CA6 changes photosystem, PBS core and chlorophyll composition to be chlorophyll *a*

containing in red light, chlorophyll *d- f-* containing organisms in far-red light and fall under red/far-red acclimation, which is useful in terrestrial and symbiotic environments [32, 34, 63, 64].

CA3 is the main focus of this study and this type chromatic acclimation alters the structure of the phycobilisomes by changing the ratio of different phycobilins within the complex [65], however, only the rods of the PBS are altered. The cPC and APC core remain the same [66]. These changes in phycobiliprotein ratios result in changes in pigment composition, altering the absorption spectrum of the phycobilisomes. CA has been seen to increase the photon capturing efficiency drastically for photosynthesis and should be considered an important contributor to global primary productivity [56, 67].

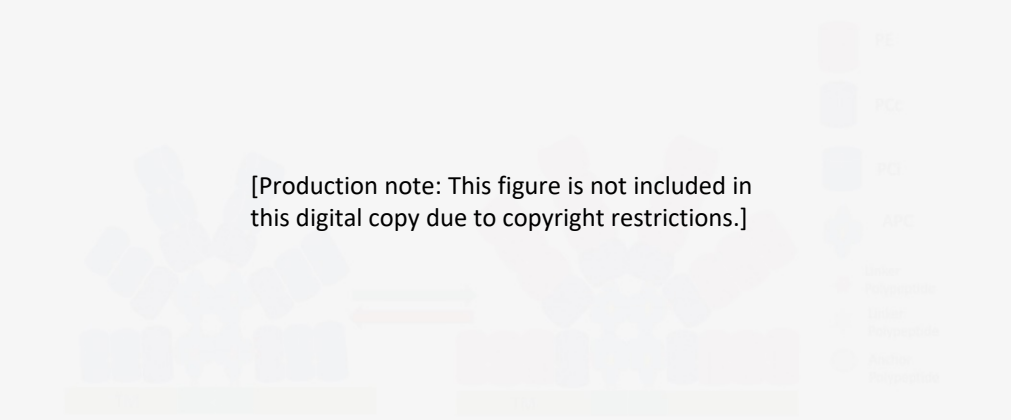

Figure 1: The structure of the phycobilisomes (PBS). The composition pf PBS is shown to be altered by the red and green light signals representing the changes observed under CA3. In RL, the rod is made up of constitutive phycocyanin (PCc) and inducible phycocyanin (PCi), compared to green light where the rod consists of PCc and phycoerythrin (PE). The core remains unchanged and is always made up of allophycocyanin (APC). The PBS is attached to the thylakoid membrane (TM). Figure adapted from previously published paper [1].

In addition, recent research has revealed that complementary chromatic acclimation can also be influenced by other factors such as nutrient availability, temperature, and oxidative stress [64, 68]. These findings highlight the complexity and importance of CA in the survival and growth of photosynthetic organisms in diverse environments. Temperature has also been found to affect CA in cyanobacteria with changes in temperature resulting in changes in pigment composition [69]. It was published in 2019 that increasing levels of hydrogen peroxide led to a decrease in PBP gene expression in *Synechocystis* sp. PCC 6803 - the authors suggest that this may be dues to the fact that oxidative stress can damage the PBS and decrease their expression [70].

1.4.1 Regulatory Pathways: Rca System

RcaE is a photoreceptor identified in CA3 and was found to be similar to phytochrome and ethylene receptors, which are known to play important roles in light sensing and signalling in plants [34, 58, 71]. A 2004 paper demonstrated that RcaE is necessary for responsiveness to both green and red light [60]. The study showed that RcaE is involved in modulating the expression of genes encoding the phycobiliprotein pigments, phycoerythrobilin and phycocyanobilin, in response to changes in light conditions. In particular, the researchers found that RcaE participates in a regulatory pathway that controls the transcription of the *cpc* and *cpe* genes, which encode the alpha and beta subunits of phycocyanin and phycoerythrin, respectively. This, among other papers [54, 69, 72-74] proposed a model for the role of RcaE in controlling chromatic acclimation, which involves a feedback loop between RcaE and the expression of phycobilin genes involved in the pychobilisome structure and regulation, with notes on RcaE is involved in photoregulating cellular morphology [60, 75, 76].

The phosphorelay pathway includes RcaE, as mentioned previously, a histidine kinase sensor protein, which senses changes in the light spectrum [77]. Upon detecting the light signal, RcaE autophosphorylates and subsequently transfers the phosphate group to the RcaC protein, a histidine-containing phosphotransfer (HPt) domain. Finally, the phosphate group is transferred to the response regulator, Rca, which then modulates the expression of phycobilisome genes accordingly [78, 79]. A studyinvestigated the role of RcaC in CA [55]. They found that deleting the *rcaC* gene in *Tolypothrix* sp. UTEX 481 resulted in impaired chromatic acclimation, with the mutant strain showing a reduced ability to change its pigment composition in response to different light colors. This study highlighted the importance of the phosphorelay system in regulating CA in *F. diplosiphon*.

The regulation of the CA3 pathway is induced in response to incoming light spectra. Red light signals the start of the phosphorelay cascade of RcaE whilst simultaneously inhibiting the synthesis of PEB at the translation of *cpeC* gene (Fig. 2). In green light, there is no phosphorelay signal triggered and therefore, RcaC is unable to, and has no signal to inhibit the transcription of the *cpeC* gene which goes onto synthesis PEB production [54, 56, 69].

Whilst the mechanisms and pathways of CA are quite well known (Fig. 2) and a deep understanding of the pathways and that lead to the changes seen in the PBS rod composition, not a lot is known about how these transcriptional changes impact the photophysiology of organisms [73, 76].

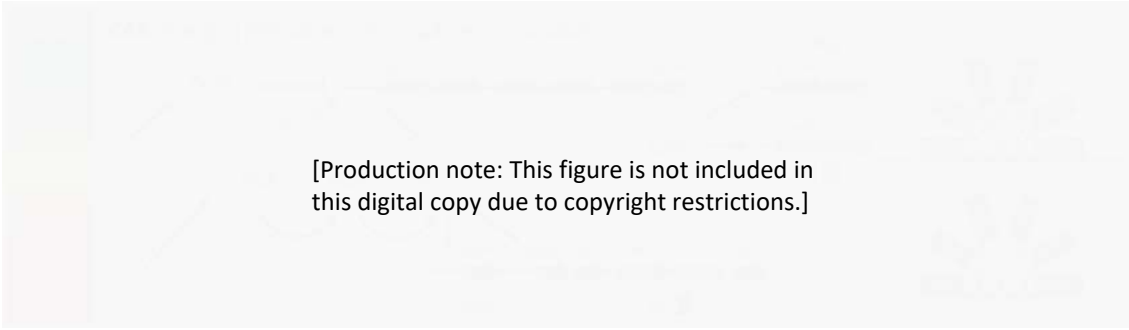

Figure 2: Regulatory mechanisms controlling CA3 in *Tolypothrix* sp. UTEX 481 uses the CBCR RcaE and two response regulators, RcaF and RcaC, to regulate the composition of the rod proteins and chromophores composition (PEB or PCB). The Cgi pathway also represses production of phycoerythrin containing rods and involves repression by an IF3 translation initiation factor. Figure adapted from previously published paper [56].

1.5 *Tolypothrix* sp. UTEX 481

The filamentous freshwater cyanobacteria *Fremyella diplosiphon UTEX* 481 undergoes CA3 [80, 81] and is the focus of this thesis. In this type of CA, phycocyanin synthesis is activated by red light, while phycoerythrin production is activated by green light. The changes in pigmentation are regulated at the transcription level through a phosphorelay regulation pathway that is not yet fully understood. According to a 2003 paper, maximum phycoerythrin synthesis is triggered by 550 nm green light, while maximum phycocyanin synthesis is triggered by 640 nm red light [54]. Furthermore, these pigmentation changes are known to impact the cell morphology with red light inducing shorter, more rounded cells and green light producing longer, rectangular brick like cells [65, 66, 82].

1.6 *Phormidium* sp. UTEX 590

Phormidium sp. UTEX 590 is another filamentous cyanobacteria that has not been documented to undergo CA. *Phormidium* sp. also contain PBS as their pigment housing structure and contains the core APC and the rods are comprised of PCc and PCi with no changes seen to this composition under different lights [83]. There are numerous genera in the *Phormidium* group that have different attributes in regards to pigmentation composition and behaviour under different conditions with limited research on *Phormidium* sp. UTEX 590 to understand the transcriptomic responses to light and morphological and photophysiological responses to light [84]. This Nostocales strain of cyanobacteria provides an interesting, closely related yet highly different behaving model for responses to light, especially as the morphology is so similar to *Tolypothrix* sp. PCC 7601.

1.7 Genetic Variation

Despite advances in understanding chromatic acclimation (CA), a paper from 2001 pointed out that some questions are still unresolved [85]. These include the precise light wavelengths to which photoreceptors respond, the regulatory proteins they interact with, and the possibility that responses to different light spectra might be unique to particular strains or species. There is information on the photoreceptors involved in the CA process of *F. diplosiphon* - being the cyanobacteriochromes (CBCRs) [86], which can sense different wavelengths of light and initiate signaling pathways to regulate the expression of genes encoding light-harvesting proteins. CBCRs are classified into three subfamilies based on the type of chromophore they contain: phycocyanobilin (PCB), phycoviolobilin (PVB), or biliverdin (BV). Each subfamily absorbs light at different wavelengths, allowing *F. diplosiphon* to sense a broad range of colors in its light environment. For example, the green light-absorbing CBCR RcaE (PVB-containing) and the red light-absorbing CBCR RcaF (BV-containing) are important for CA in *F. diplosiphon* [87].

1.8 Project Objective

Cyanobacteria play one of the most significant roles in oxygen production on Earth and can be found in almost every environment across the globe [88, 89]. The application of cyanobacteria pigments and their uses in renewable markets requires further research and optimisation to drive the progress of the bio-pigment industry [40]. Looking at the potential impacts light has on the functioning of two Nostocales strains of cyanobacteria and understanding the genetic beginnings of this process is key to furthering understanding of how similar looking organisms behave and adapt in different ways.

In this study, to gain a deeper understanding of CA, a comparison was made between *F. diplosiphon* 481, a well-documented CA undergoing cyanobacterium, and *F. diplosiphon* 590, a taxonomically related strain (Fig. 3), which does not appear to undergo CA. By comparing the two strains, the aim was to determine the physiological impacts of CA and shed more light on the specie specific molecular responses to different light spectra. This study has also illuminated the plasticity and adaptability of different cyanobacteria and their responses to different light.

The genetic adaptations and responses to light seen between the two Nostocales strains will deepen the understanding we have about the optimal fitness level of these organisms and their pigment production for future and novel applications that can improve the bio-pigment industry and its economic viability. This is necessary with increasing demand for more sustainable and

environmentally friendly products used in everyday life by industry and the general population. With research being conducted into the halotolerance of *Tolypothrix* sp. UTEX 481 and its suitability as use for biofuel, understanding the mechanisms behind pigment synthesis is detrimental to increasing the understanding of how this organism functions. CA has the ability to allow organisms to be cultured in varying light qualities, limiting restrictions for mass production and scalability. This will be extremely beneficial to industry applications like the mentioned biofuel research. Comparing this to another related cyanobacteria will illuminate differences between the two organisms and may pave the way for areas of genetic mutation to increase the flexibility of *Phormidium* sp. 590 to be used in similar applications as *Tolypothrix* sp. 481.

The specific aims for this project were to:

1. To compare morphological and photophysiological changes under different light colours for *Tolypothrix 481* and *Phormidium 590*.

This section focusses on determining if different light colours impact the functioning of these two organisms through looking at cell morphology, growth rate, electron transport rate and pigment fluorescence and quantity.

2. To understand the genes activated under different light colours through transcriptomics and determine how these genes play a role in the differences in morphology and physiology.

This objective aims to link the genetic functioning to the morphological and physiological changes that occur in both tested organisms. This will contribute to a deeper understanding of how CA works and the role of pigment composition on morphology and photophysiology. The long-term aim and a major future direction of this project is to contribute knowledge that will further the application and sustainable use of cyanobacteria pigments in the biotechnology industry.

Chapter 2: Experimental Design, Materials and Methods

2.1 Culture conditions

The freshwater filamentous cyanobacteria *Fremyella diplosiphon* UTEX B481 and *Fremyella diplosiphon* UTEX B590 from the UTEX culture collection at the University of Texas in Austin USA, was cultured in Standard BG-11 media (UTEX BG-11 Liquid Medium Recipe where stocks were made to the same final concentration https://utex.org/products/bg-11-medium?variant=30991786868826#recipe). For trace metal solution, the same final concentration was used however $Na_2MoO_4.4H_2O$ was used and $CoCL_2.6H_2O$ were used in substitute for $Na_2MoO_4.2H_2O$ and $Co(NO_3)_2.6H_2O$ respectively. Cultures were grown in 250 mL Schott bottles (part number: 21 801 365, DURAN Group GmbH, Mainz, Germany) with aeration (GL45 screw cap lids with aperture 2 ports, PSI, Drasov, Czech Republic) at 0.1 bar pressure at 24 ^oC under 20 $\mu mol\ m^{-2}\ s^{-1}$ [90, 91] (measured using a 2 pi LI-190R Quantum Sensor Q 44416 with LI-250A Light Meter S/N LM2- 4668, LI-COR Biosciences, Lincoln, NE, USA) at spectral wavelengths of 437 and 535 nm (together), 663 nm, and 518 nm (Supplementary Figure 1)– hereon referred to as white light, red light and green light respectively - supplied by Hydra 64HD Smart Reef LED lamps (Aquaillumination D89760042A02 & D89760015D60 Bethlehem PA, USA) unless otherwise specified. Parent cultures were in exponential phase and pre-acclimated to either WL, RL or GL prior to subculturing. Cultures were inoculated from parent cultyres and grown for 5 days, at the end of which all of the physiological and RNA data was collected. It should be noted that all experiments were carried out on cells already fully acclimated to the light conditions tested for the purposes of strain comparison.

2.2 Calibration Curve & Data Normalisation

A dilution series for both *Fremyella diplosiphon* strains were created using 4 dilutions with 5 replicates for each dilution under each light colour. These dilutions had their optical density measured in BD Falcon 96 Flat Transparent 96 well plates (cat. No. 353072, Corning New York, USA) using Spark Multimode microplate reader (Tecan Trading AG, Switzerland). The samples were then frozen at -80^oC to then be placed onto a Christ Alpha 2-4 LD plus Freeze-dryer (Part No. 101542, Serial No. 22110 Martin Christ Gefriertrocknungsanlagen GmbH, Osterode, Germany) at -80^oC with 0.10 mbar pressure for 5 days. The freeze-dried samples were then weighed and a calibration curve for each strain was developed using the biomass dry weight (g) plotted against the optical density (680 nm). These curves were used to normalise the data obtained (Supplementary Figure 2).

2.3 Morphology & Microscopy

Cultures were observed at a similar growth phase (OD 680 of 0.1) for all cell morphology measurements. Live *F. diplosiphon* cells were imaged with a Nikon Ni U upright microscope (H600L, Nikon, Japan) using Differential Interference Contrast (DIC) optics with a 100x oil immersion objective. Morphology was measured through cell length, filament length and number of cells per filament using the inbuilt microscope measuring software on 30 filaments for each light condition.

Cultures were monitored daily under the microscope simultaneously when measuring optical density and fluorescence with the use of an Olympus IX73 Inverted Fluorescent Microscope (SN 0G48540 Olympus, Tokyo, Japan), imaged through Infinity 5 Teledyne Lumenera camera on Teledyne Lumenera Infinity Analyze 7 (Telendyne Lumenera, Ottowa, Canada). Wells were viewed under 40x magnification in a Nunclon 96 Flat Black well plate (Product code: 10281092 ThermoFisher Scientific, Goteborg Sweden) containing 200 uL of culture to check and monitor growth and possible contamination.

2.4 Growth Curve

White- red- and green- light grown cultures were each cultured in 200 mL Schott bottles using a 1:10 dilution). The optical density (OD) at 680 and 720 nm was recorded daily for the duration of the experiment using Spark Multimode microplate reader (SN 2012002080, Tecan Trading AG, Grodig, Austria). The daily optical density readings were plotted to give the growth curve for each organism under each light condition from Day 0 – Day 5.

These optical densities were used to measure specific parameters. OD at 680 nm: This wavelength is close to the peak absorption of chlorophyll *a*, making it useful for estimating the concentration of chlorophyll *a* in the sample. By measuring OD at this wavelength, we are directly relating the measurement to the absorption properties of chlorophyll *a*, which is crucial for photosynthesis in cyanobacteria and other photosynthetic organisms. OD at 720 nm: This wavelength is typically used as a reference for correcting the light scattering effect, which is more pronounced at longer wavelengths. By measuring OD at 720 nm, we are aiming to estimate the biomass more accurately, as this measurement helps to account for the scattering effects that are not directly related to chlorophyll absorption but are indicative of the total biomass.

2.5 Excitation & Emission 3D scans

Excitation Emission Matrices (EEM) data was obtained through excitation wavelengths from 400 to 600 nm in 10 nm increments. For each excitation wavelength the emission fluorescence was measured from 550 to 750 nm in 10 nm increments. This measurement gives a wholistic idea of the fluorescence profile of an organism which is useful when there is more than one fluorescent protein present in the organism. Instrument signal gain was set to manual and maintained at the same level across all measurements. Measurements were taken using 200 µl of white- red- and green-light grown cultures in a Nunclon 96 Flat Black well plate (Product code: 10281092 ThermoFisher Scientific, Goteborg Sweden) using a Spark Multimode microplate reader (Tecan Trading AG, Switzerland). All obtained data was normalised using a global normalization strategy by averaging the entire matrix data set per measurement, per strain, per condition and then dividing each data point by the average. This measurement was replicated 3 times and an average of these replications was taken. Data was processed using Excel with heat maps being produced using the matrix function on OriginPro 2022b (Learning Edition). Fluorescent spectra of the cultures is presented in Supplementary Figure 3.

2.5.1 Pigment Standards

This process was completed on commercial pigment standards of chl *a* (DK-2970 Chlorophyll *a* Batch no. chla-126 conc: 1.737 mg/mL, Horsholm, Denmark), PC (AAT-2553: C-PC [C-Phycocyanin] *CAS 11016-15-2* (1mg) 20mg/mL, Jomar Life Research Victoria, Australia) and PE (52412 1MG-F R-Phycoerythrin, Sigma, Missouri, USA) to determine the precise excitation and emission values for these pigments using the Spark Multimode microplate reader (Tecan Trading AG, Switzerland). These were done in isolation and also in combination including; chl *a* only, PE only, PC only, chl *a* and PE, chl *a* and PC, PE and PC, chl *a*, PE and PC. This provided a basis for the positioning of these pigments in isolation and when combined together to allow identification of these in *F. diplosiphon* cultures. The heat maps of the pigment fluorescence is found in Supplementary Figure 4. This process was then repeated on the live *F. diplosiphon* cultures under each light condition to demonstrate the different pigment profile through the fluorescence given off by the cultures under different excitation values. For the standards, a 1:1 ratio of water and 90% acetone was created to form a 45% acetone solution, as PE and PC are water soluble and chl *a* is soluble in acetone Standards testing was conducted to confirm the fluorescence emission and excitation peaks of these pigments as these profiles were being displayed differently in the two organisms.

2.6 Relative Pigment Quantification

To determine the quantity of chl *a*, PE and PC within the organisms a relative approach was taken. Standard curves were created using the standard for each pigment. A range of dilutions were prepared using diluted acetone and the standards had their fluorescence measured at the excitation and emission previously determined through the EEM method described above. A graph was made of the standard curve (Supplementary Figure 5) obtained for each pigment and the line of best fit equation was used to determine the quantity of each pigment within the culture. The cultures fluorescence was measured daily and the data was normalised to OD720- this involved the values obtained from the standard curve being divided by the Day 5 OD720nm reading for the respective cultures to ensure comparison of results was accurate.

Firstly, a 1:1 ratio of water and 90% acetone was created to form a 45% acetone solution. Into a Nunclon 96 Flat Black well plate199 µl of 45% acetone was added and 1 µl of pigment standard and mixed. 100 µl was taken from this well and mixed with 100 µl of 45% acetone to create a final solution of 22.5% acetone and 0.5 µl of stock pigment and was used to create a series of dilutions. Eight dilutions were created. The wells had their fluorescence measured at Excitation and Emission (Ex/Em) of 430/670, 540/580 and 620/580 nm as determined from the pigment standard Section 2.6.1 Excitation Emission steps in Section 2.6.1 using a Spark Multimode microplate reader (SN 2012002080, Tecan Trading AG, Grodig, Austria). All three pigment Ex/Em points were measured for each pigment sample to ensure there was no increase or decrease in the pigments to act as a negative control. The concentration of the standards was then multiplied by the dilution factor to give the final concentration in µg/ml and plotted against the fluorescence values.

It must be noted that the fluorescence intensity of free proteins and pigments cannot be directly compared to those of the same proteins and pigments in an in vivo context. However, due to equipment and time restraints this was the best option available to provide data and further measurements should be undertaken using more scientifically accurate methods such as HPLC.

2.7 Optical Fingerprinting

This measurement combines two instruments concurrently running individual custom protocols as documented in published literature [92]. Cultures were normalised to OD680 0.1 24 hours prior to being tested. For each light adapted culture 200 µl of the sample was added in each well of a Hard-shell Polymerase Chain Reaction (PCR) 96 microwell plate (HSP9655, Bio-Rad Laboratories, Inc, Hercules, CA, USA).

Prior to the measurements, the Walz Imaging PAM lens (Heinz Walz, Effeltrich, Germany) was focused on the sample with the near infra-red LEDs turned on to generate a clear image on the screen (780 nm). Far-red light was used for pre-illumination to oxidise PSII at (730 nm). Blue LED array provided the actinic light and saturation pulses at a peak wavelength of 470 nm. A customised protocol was used which included 5 minutes of dark adaptation and temperature acclimation, followed by a rapid light curve (RLC). The light protocol was as follows: 11, 35, 59, 83, 132, 180, 252, 349. 445, 662, 903 µmol photons m^{-2} s^{-1} for the duration of 5 s at each intensity. These well plates were run on the Eppendorf Mastercycler thermocycler (ABI Veriti, Applied Biosystems,Waltham, MA, USA) which was programmed for every pair of columns to reach and hold a temperature gradient across 7 to 40 °C. The RLC was commenced after the 5 min incubation period. This temperature range was chosen based on the optimal growth temperature for the cyanobacteria, and creating an upper and lower deviation from this [92]. The PAM measurement data which includes F_v, F_o and F_m is then used to portray chl *a* fluorescence to infer relative electron transport rate (rETR).

2.8 DNA Extraction & Sequencing

2.8.1 DNA Extraction

Aliquots of 40 mL of each White Light (WL) culture for each Nostocales strain was collected and the Dneasy PowerSoil Pro Kit (50) (Cat. No. 47014, Qiagen, Hilden, Germany) used for Deoxyribonucleic acid (DNA) extraction as per the instructions with several amendments made to the procedure. Two cycles of freeze/thawing at -80°C were carried out prior to the listed protocol. The quantity of C6 (10 mM Tris) solution added was 50 uL. Samples were measured on the nano-drop 2000 Spectrophotometers (Cat. No. ND-2000C, Thermo Scientific, Massachusetts, USA) for quantity of DNA and purity. This measures the 10nm absorbance of the samples from 220-350nm with interest in the ratio of A260/280 for an indication of purity with ~1.8 being considered pure and the ratio of A260/230 to detect any contamination from other agents such as phenols and salts with acceptable samples having a ratio of 2.0-2.2. Samples were then frozen at -30°C.

2.8.2 PCR

Primers were designed based on previous papers to target specific genes and proteins that have been documented to play a role in CA [61, 87, 93] and are listed in Supplementary Table 1. Primers were centrifuged for 30 s at 6000 x g. Working stocks with a volume of 10 uL were made and added to 90 uL ultrapure water. A total reaction volume of 50 uL was used which included: GoTaq Green Master Mix 2X 25uL, 2uL of each upstream and downstream primer (10 uM) 2 uL

DNA template and nuclease free water to 50uL. Samples were placed in a PCR Thermocycler (need actual name/make/model and protocol).

2.8.3 Gel Electrophoresis

PCR products were checked using gel electrophoresis with 0.8% agarose gel made following the Thermo Scientific 'General Recommendations for DNA Electrophoresis' protocol. Ladder d3937-1 vl "directload(tm) 1 kb DNA ladder (Merck, Victoria, Australia). PCR amplicons with appropriate band size were then sent to Ramaciotti Centre for Genomics (UNSW Sydney, Australia) [94] for purification and Sanger Sequencing using 2uL of each primer per Nostocales strain (primers designed and listed in Supplementary Table 1).

2.8.4 Phylogenetic Tree Construction

A phylogenetic tree was constructed to illustrate the closeness in relationship between the two Nostocales strains using the primers and sequences obtained from the DNA extraction and PCR process. The phylogenetic trees were constructed based on curated RcaE genes (Supplementary Table 3, RcaE-5 primer) as this has been documented to regulate CA via a photochromic photocycle [61]. This tree was confirmed by two approaches Maximum Likelihood (ML) and Maximum Parsimony (MP). ML was conducted via IQ-tree version 2.3.0 with 1000 times of bootstrapping and MP was conducted via RAxML version 8.2.13 with 1000 times of bootstrapping. The tree is rooted at Nostoc_commune_HK-02.

2.9 RNA Extraction & Sequencing

Volumes that provided equivalent biomass of each strain for WL and RL were collected and centrifuged at 3000 x g for 3 min at 4°C (thermoFisher Scienctific Multifuge X4R Pro Centrifuge 75009915 Ref, TX-1000 4 x 1000 mL Swinging Bucket Rotor cat. No. 75003017, Harz, Germany). Supernatant was discarded and the pellet was snap frozen in liquid nitrogen and stored at -80°C until further processing.

For RNA extraction steps, samples were transferred into a Retsch John Morris Scientific Mixer Mill MM200 (Article no. 20.738.0001, Rheinische, Germany) that was pre-frozen in liquid nitrogen (BOC Gases Refrigerated Liquid Nitrogen Unit no. 1977) and shaken for 3 min at 30 Hz. The following procedure was conducted on ice in a fume hood. Samples were then transferred to 2 mL Eppendorf tubes and 1.5 mL trizol was added and homogenised with a pipette. Samples were incubated at room temperature for 5 min. Next, 300 ul of Chloroform was added and samples inverted for 15 s to mix. Samples were then incubated at room temperature for 15 min. Samples

were centrifuged using a ThermoFisher Scientific Multifuge X Pro Series (SN 42700118, Osterode, Germany) at 12,000 x g for 15 min at 4°C. The upper aqueous phase was then transferred to clean 2 mL Eppendorf tubes. An equal volume of absolute ethanol was added and the samples were inverted to mix. Samples were then transferred to a Rneasy mini column in a 2 mL collection tube 650 ul at a time and centrifuged at 8,000 x g for 30 s at 4°C. This step was repeated until all of the liquid had passed through the column.

Using the RNeasy Mini Kit (50 74104, Qiagen PTY LTD, Chadstone Centre, Victoria, Australia) and following the provided protocol 350 ul of Buffer RW1 was added to the column and samples were centrifuged at 8,000 x g for 15 s at 4°C and flowthrough was discarded. Then 500 ul of Buffer RPE was added to the column and centrifuged at 8,000 x g for 15 s at 4°C and flowthrough was discarded. Another 500 ul of Buffer RPE was added to the column and centrifuged at 8,000 x g for 2 min at 4°C and flowthrough was discarded. The column was then placed in a new 1.5 mL Eppendorf tube and 30-50 ul of Rnase free water was added directly to the column membrane. Samples were centrifuged at 8,000 x g for 1 minute to elute RNA. Concentration of the sample was checked using the nano-drop 2000 Spectrophotometers (Cat. No. ND-2000C, Thermo Scientific, Massachusetts, USA) for quantity of DNA and purity. This measures the 10nm absorbance of the samples from 220-350nm with interest in the ratio of A260/280 for an indication of purity with ~2.0 being considered pure and the ratio of A260/230 to detect any contamination from other agents such as phenols and salts with acceptable samples having a ratio of 2.0-2.2. Quality control was run by Ramaciotti using RNA Bioanalyzer.

The following RNA samples were sent to Ramaciotti Centre for Genomics (UNSW Sydney, Australia) [94] for Illumina Stranded Total RNA library prep with RibZero Plus NovaSeq 6000 SP 2x100bp lane sequencing. 481 WL, 481 RL, 590 WL, 590 RL (n=5, total n=20) as selected from the differences seen in the photophysiology results. Due to an issue arising at Ramaciotti, the included data uses 19 samples, with only 4 WL *Tolypothrix* sp. UTEX 481 samples being used instead of 5.

2.10 Bioinformatics Data Analysis

Fastq files were trimmed using Trimmomatic with minimum phred score of 30. Quality control of fastq files was performed using FastQC v0.11.931 pre- and post-trimming, and reports compiled by MultiQC v1.1132. Fastq reads were then aligned to the reference genome for *Tolypothrix tenuis PCC 7101* using BWA aligner and read count for each transcript were

generated using FeatureCounts. The differential expression among the transcript counts were determined using Deseq2.

It is noted that both PCC7910 and PCC7601 were checked as suitable mapping candidates for both strains, however, PCC7101 had a higher percentage match as well as higher gene annotation, and highest number of total genes.

2.10.1 Gene Regulation

To compare the genes present under the different conditions a Venn diagram was created utilising the significantly regulated genes where $-2 \leq$ Fold Change ≥ 2 and $p < 0.05$. These genes were then separated into either upregulated (Fold Change ≥ 2) or downregulated (Fold Change ≤ -2). These were copied from the excel file containing the gene data from the Gene Ontology (GO) column. The GO is a way of grouping and describing a specific conceptualization of gene products in a way where there is no overlap and is easily understandable to scientists [95]. The GO terms are obtained from the annotation file where the information for gene IDs being attributed to metabolic pathways and their corresponding GO terms are collected from the uniport database (https://www.uniprot.org/). The GO terms were then pasted onto the software Venny (https://www.biotools.fr/misc/venny) which generated the Venn diagram figure for the different comparisons used. This software also gave a list of each of the genes that overlapped in each segment which was filtered through to determine shared genes of interest.

2.10.2 Gene Identity

Identification of genes related to the phycobilin biosynthesis pathway were identified based on the pathway described in a 2019 paper [1].. Based on the listed proteins in the pathway, a search within the gene Excel document was conducted for each term in the find tool on Excel (Microsoft Corporation…). The same process was done for PE and PC related genes based on the Kegg database with searches for Phycoerythrin and Phycocyanin (https://www.genome.jp/kegg/kegg2.html).

Chapter 3: Results

The two organisms compared come from the same taxonomic order and can be visualised as to how closely they are related through the constructed phylogenetic tree (Fig. 3). This tree uses a primer targeted to the *RcaE* gene which is known to play a role in CA in *Tolypothrix* sp. UTEX 481.

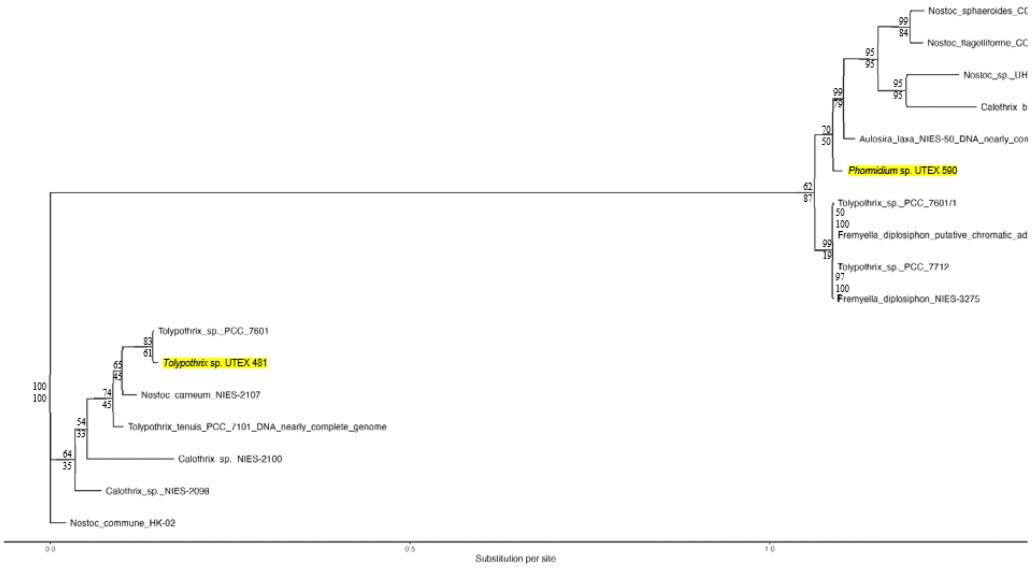

Figure 3: Phylogenetic tree based on RcaE sequences (Supplementary table). *Tolypothrix* sp. UTEX 481 and *Phormidium* sp. UTEX 590 are both highlighted in yellow. Maximum likelihood (top) and maximum parsimony (bottom) values are indicated at each fork. Tree is rooted at Nostoc_commune_HK-02.

3.1 Morphological Changes in Response to Light Spectral Quality

Tolypothrix sp. UTEX 481 demonstrated differing responses to light quality in regard to the morphology and size of the organism, whereas *Phormidium* sp. UTEX 590 did not show changes under these light conditions. Microscopy was used to visually document changes in cell shape and colour and to quantify cell measurements to determine if the different light colours altered the morphology of these organisms.

3.1.1 Morphology & Microscopy

The morphology of the two Nostocales strains was documented using microscopy for red- white- and green- light grown cultures to determine Chromatic Acclimation's (CA's) impact on phenotype (Fig. 4) and compare these differences between the two Nostocales strains. Visually, it is observed that the *Tolypothrix* sp. UTEX 481 morphology differs across light conditions. In Figure 1a the white light culture appears red in colour with elongated, rectangular looking cells

which is a trait observed more intensely in the green light culture as well. In comparison, the red-light culture appears green and has smaller, rounded cells. These morphological changes have occurred due to CA. When looking at the morphology of *Phormidium* sp. UTEX 590 there is limited change in the visual appearance of the cells with white, red and green light (fig. 1D-F) all displaying small, green, round cells within the filaments.

Quantifying this through measurements of cell length, filament length and the number of cells per filament shows a significant difference (Fig. 4G-I). Interestingly, *Tolypothrix* sp. UTEX 481 exposed to green light showed a significantly larger cell length (10.01 ± 0.45 μm) compared to both white and red-light cultures (6.71 ± 0.25 μm and 6.68 ± 0.40 μm respectively). The longer cell length in green light resulted in a significantly smaller number of cells per filament (23 ± 1.637) compared to white light (31 ± 2.598) and red light (31 ± 2.592). The longer but fewer cells per filament in green light seemed to result in a longer total filament length (222.63 ± 16.55 μm) compared to white and red light which tended to show shorter filament lengths (205.97 ± 16.05 μm and 199.40 ± 16.43 μm), however, these differences were not significant. White and red-light cultures followed a similar trend, with green light producing differing observations. Whilst the cellular morphology seemed to differ across the three light conditions, these changes were not significantly different ($p>0.05$) but highlighted one of the many differences CA could have on the phenotype of *Tolypothrix* sp. UTEX 481

These changes in morphology were not seen in *Phormidium* sp. UTEX 590, which did not display any signs of reacting to different light spectra. The altering light conditions did not have any significant impact on cell length with white- red- and green light all being within 0.405 μm of each other (4.940 ± 0.19, 4.529 ± 0.25, 4.880 ± 0.16 μm respectively). Filament length had some small variation with Green light having 94.67 ± 11.22 μm filament length and white and red having 78.37 ± 6.822 and 88.62 ± 12.07 μm filament length respectively. As expected, green light had more cells per filament at 20 ± 2.455 with white and red having 16 ± 1.146 and 19 ± 3.765 cells per filament respectively. When compared to *Tolypothrix* sp. UTEX 481, overall *Phormidium* sp. UTEX 590 cell length was significantly shorter across all light conditions. Cells were 6.71 ± 0.25 and 4.940 ± 0.19 μm long under white light, 6.68 ± 0.40 and 4.529 ± 0.25 under red light, and 10.01 ± 0.45 and 4.880 ± 0.16 μm under green light respectively for *Tolypothrix* sp. UTEX 481 and *Phormidium* sp. UTEX 590. There was a significantly lower number of cells per filament for white and red light– 16 ± 1.146 and 19 ± 3.765 μm for *Phormidium* sp. UTEX 590 and 31 ± 2.598 and 31 ± 2.592 μm for *Tolypothrix* sp. UTEX 481 respectively for white and red light. Whilst *Phormidium* sp. UTEX 590 still had less cells per filament in green light (20 ± 2.455 compared to 23 ± 1.637 for *Tolypothrix* sp. UTEX 481)

this was not significant. Filament lengths were significantly shorter once again across all light colours for *Phormidium* sp. UTEX 590 and a shorter filament length across all light colours.

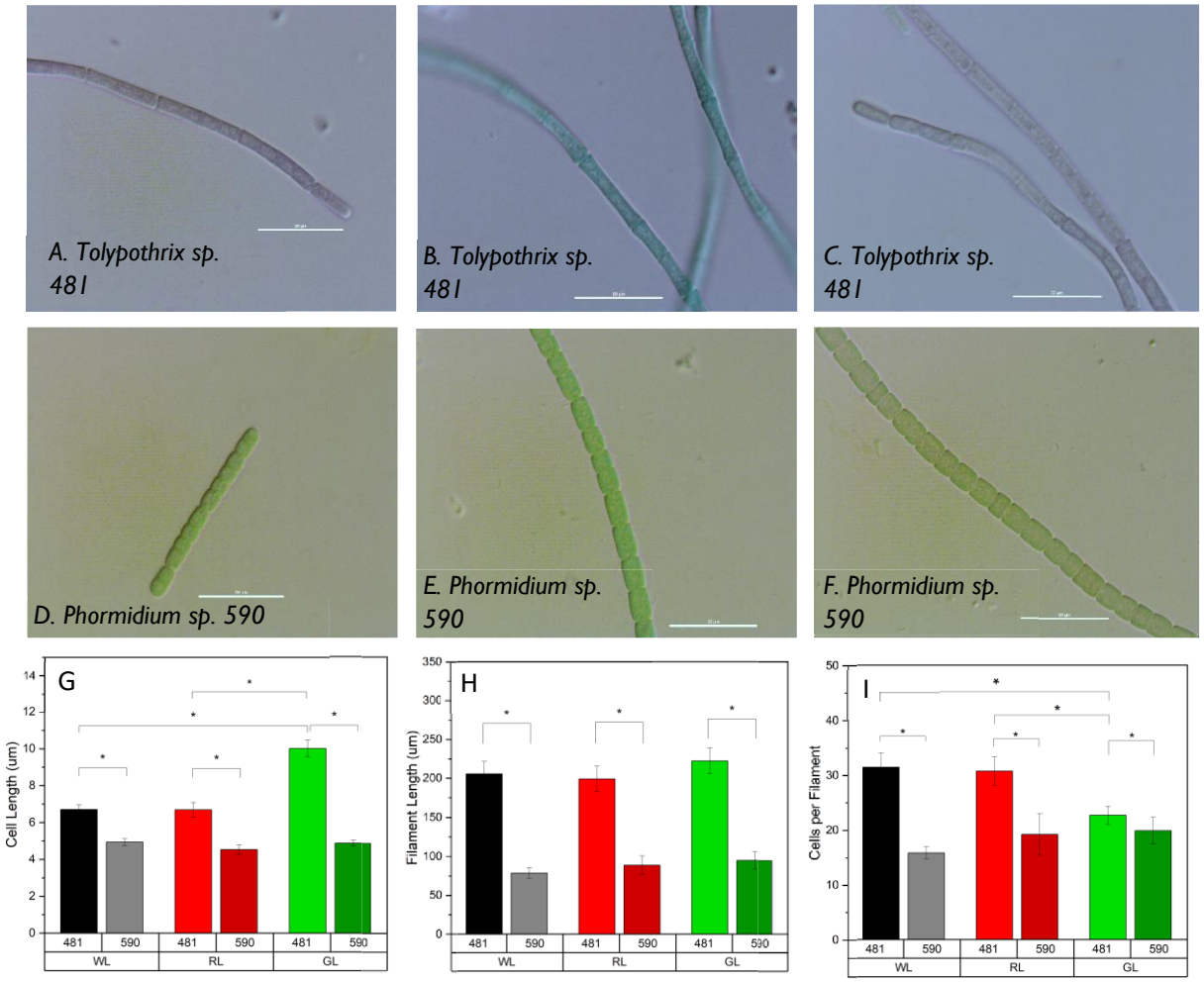

Figure 4: Microscope images under 100x oil immersion for *Tolypothrix sp.* UTEX 481 A) WL, B) RL, C) GL and *Phormidium sp.* UTEX 590 D) WL E) RL, F) GL. G, H, I represent cell measurements for cell length, filament length and cells per filament respectively, comparing *Tolypothrix sp.* UTEX 481 and *Phormidium sp.* UTEX 590 for WL, RL and GL as indicated. N=20. All images and measurements used Nikon Ni U Upright Microscope software. Bars with asterisks indicate significance, $p<0.05$ from one-way Anova. Scale bar = 20 µm

3.2 Photophysiological Responses to Light

After measuring morphological differences under different light quality, next I observed photophysiological and growth responses of these two Nostocales strains when exposed to different light quality. As both organisms are photosynthetic, their capability to grow, photosynthesise and produce the necessary pigments for survival are impacted by the light they receive. The following results explore lights impact on these functions.

3.2.1 Growth Rate and Electron Transport Rate

The growth of both organisms can be seen in Figure 5A-C. Over the 5 days the cultures were growing, *Tolypothrix* sp. UTEX 481 grew best under white light conditions with the highest OD720 reaching 0.3978 ± 0.0374. The red-light culture had a lower maximum OD720 of 0.2494 ± 0.0534 and the green light culture had the lowest maximum OD720 of 0.1984 ± 0.0207 growing the slowest over the time period. These differences in growth rate are another impact of CA on this organism. When looking at *Phormidium* sp. UTEX 590 the white light culture has a slightly higher maximum OD720 of 0.1656 ± 0.0580 whereas the red and green light cultures sit at 0.1062 ± 0.0238 and 0.1023 ± 0.0203 respectively. The main comparison however is the differences seen between the two organisms. *Tolypothrix* sp. UTEX 481 max OD720 in white light is significantly higher ($P<0.05$) than *Phormidium* sp. UTEX 590 (0.3978 ± 0.0374 and 0.1656 ± 0.0580), *Tolypothrix* sp. UTEX 481 red light is just at double *Phormidium* sp. UTEX 590 (0.2494 ± 0.0534 and 0.1062 ± 0.0238) and under green light is *Tolypothrix* sp. UTEX 481 is significantly higher ($P<0.05$) than *Phormidium* sp. UTEX 590 (0.1984 ± 0.0207 and 0.1023 ± 0.0203). These vast differences highlight the advantage towards *Tolypothrix* sp. UTEX 481 for growth under different light conditions due to having a greater range of photosynthetic pigments, a higher absorbance cross section and higher Electron Transport Rate (ETR) which will be explored further, compared to *Phormidium* sp. UTEX 590.

The ETR measured as the relative ETR of Photosystem II (PII) is determined through measuring chlorophyll fluorescence and represents an important parameter reflecting the photosynthetic efficiency of an organism [96]**.** As cyanobacteria are phototrophs, in order to better understand the impact of light colours on these two Nostocales, we also measured ETR in addition to growth. Figure 5D-I are the heat maps that represent the relative electron transport rate (ETR) across increasing light intensities (y axis) and temperatures (x axis). *Tolypothrix* sp. UTEX 481 has the highest ETR max 211.7 across all light colours when exposed to white light, which coincides with the highest growth rate. The red light *Tolypothrix* sp. UTEX 481 culture has an ETR max

lower than WL and GL of 163.1, with the RL profile being significantly different to both WL and GL (p-value 4.98^{-05} and 9.58^{-09} respectively) whilst having the second highest growth rate. Green light has a maximum ETR of 202.6 but the lowest growth rate for *Tolypothrix* sp. UTEX 481.

The *Phormidium* sp. UTEX 590 cultures have no significant differences across light conditions for their ETR profiles. For white light the ETR max is the highest at 95.94. The red light is slightly lower 90.82 whilst quite similar to the green light of 91.50. These correlate to the trend seen in the growth rate of this organism. This indicates that the light *Phormidium* sp. UTEX 590 cells are exposed to, does not alter their ETR. When looking at the ETR for *Phormidium* sp. UTEX 590, these heat maps (Fig 5G-I) have the same axis as the *Tolypothrix* sp. UTEX 481 culture of the same light condition. As a result, it can be noted that in general *Phormidium* sp. UTEX 590 has a much lower ETR max than the *Tolypothrix* sp. UTEX 481 cultures across all light conditions. This is also consistent with *Phormidium* sp. UTEX 590 having a lower growth rate than *Tolypothrix* sp. UTEX 481 under each light condition.

Not only is the ETR max an important piece of information, but our data set also demonstrates the capabilities of these two Nostocales strains to photosynthesise at different light intensities and different temperatures. For *Tolypothrix* sp. UTEX 481, the maximum ETR is found at 662 µmol photons m^{-2} s^{-1} across the three light conditions, whereas for *Phormidium* sp. UTEX 590 the maximum light intensity for the greatest ETR was at 445 µmol photons m^{-2} s^{-1} displaying a difference in the photoprotection capabilities and functioning of these organisms. More importantly are the differences in higher ETR values across temperature ranges. For both *Tolypothrix* sp. UTEX 481 and *Phormidium* sp. UTEX 590 the WL cultures observed a maximum ETR at 34°C whereas GL cultures for both *Tolypothrix* sp. UTEX 481 and *Phormidium* sp. UTEX 590 and the *Phormidium* sp. UTEX 590 RL culture have their maximums at 35°C. Interestingly, the *Tolypothrix* sp. UTEX 481 RL culture maximum occurs at 39°C – again having a significantly different profile to WL and GL (supplementary table), indicating a different response to temperature than the WL and GL cultures for *Tolypothrix* sp. UTEX 481 and all the *Phormidium* sp. UTEX 590 RL culture.

As delineated in the reference methodology paper, the design is inherently focused on enabling the simultaneous measurement of multiple light curves at various temperatures. This experimental framework is not intended to explore the acclimation states of the organisms to specific temperatures over prolonged periods. Instead, this approach aims to elucidate the immediate,

transitional responses of microalgae to concurrent shifts in both the rmal and light conditions.This investigation into transitional states rather than acclimation states is pivotal for a couple of reasons:

Immediate Response Versus Long-term Acclimation: It allows us to distinguish between the inherent capacity of microalgae to rapidly adjust their photosynthetic machinery in response to sudden environmental changes and their ability to acclimate over extended periods. This distinction is crucial for understanding microalgal resilience and survival strategies in their natural, frequently fluctuating environments.

Ecological and Environmental Relevance: The natural habitats of microalgae are characterized by dynamic changes in light and temperature, often occurring within short periods. By simulating these rapid transitions, the experiment reflects more accurately the challenges microalgae face in situ, providing insights into their adaptive photobiological mechanisms.

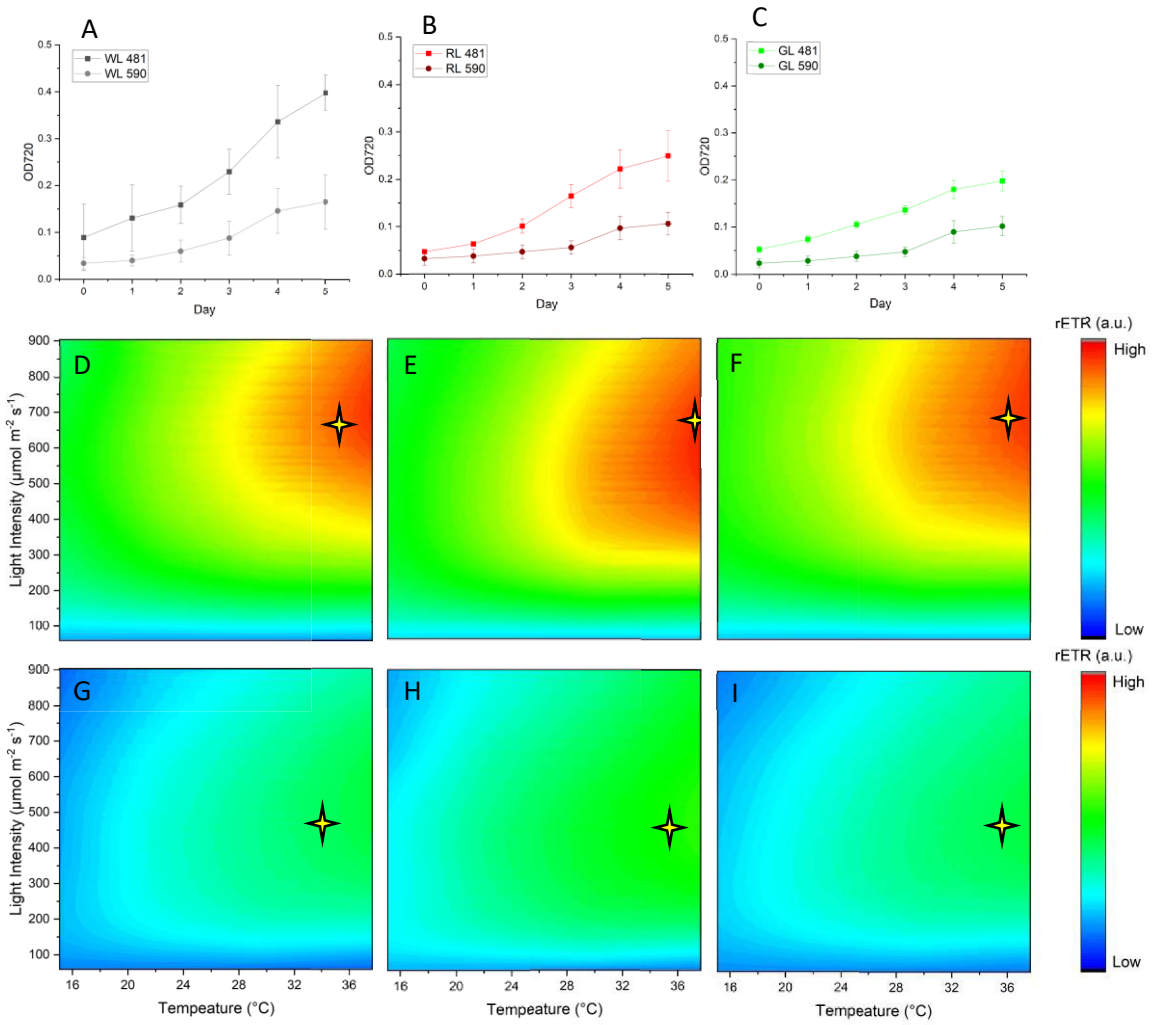

Figure 5: Growth curve measured by OD720 for *Tolypothrix sp.* UTEX 481 and *Phormidium sp.* UTEX 590 under A) WL, B) RL, C) GL. Relative Electron Transport Rate (rETR) for *Tolypothrix sp.* UTEX 481 and *Phormidium sp.* UTEX 590 measured through chlorophyll *a* fluorescence. Heat maps displayed *Tolypothrix sp.* UTEX 481 D) WL E) RL F) GL and *Phormidium sp.* UTEX 590 G) WL H) RL I) GL. Heat maps in line vertically have the same axis; D & G are 0-212, E & H are 0-163, and E & I are 0-203. Stars indicate the position of the maximum rETR value. For growth curves, all *Tolypothrix* sp. UTEX 481 conditions are significantly different. *Phormidium* sp. UTEX 590 WL is significantly different to RL and GL. All strain comparisons are significantly different. For rETR, *Tolypothrix* sp. UTEX 481 RL is significantly different to WL and GL. Statistical significance determined through one-way anova (A-C) and Kolmogorov-Smirnov test (D-I), p-values found in supplementary table

3.2.2 Excitation and Emission

The differences in pigment contents under different light spectra was measured through an excitation / emission matrix to visualise the difference in phycobilin placement through fluorescent profiling. To begin, an excitation and emission heat map was created based on 3D fluorescent scans of the pigment standards known to be found in *Tolypothrix* sp. UTEX 481

and *Phormidium* sp. UTEX 590 (Fig 6A-C). Chlorophyll *a* (chl *a*) standard was determined to have two maximum fluorescent points at 430 nm, 670 nm Ex/Em and between 600-650 nm Ex with Em 670-720 nm. This process was repeated for standard Phycoerythrin (PE), which presented one maximum fluorescence point of 540 nm, 580 nm Ex/Em. This was again repeated for Phycocyanin (PC) standard, which presented one maximum fluorescence point of 610 nm, 650 nm Ex/Em. The fluorescence scan was repeated for these standards in combination in order to represent the interactions of these pigments that may be seen in the cell and the Ex/Em heat maps can be found in Supplementary Figure 2. These fluorescent excitation and emission maximums from the standards of each pigment were then used to identify and label the pigment fluorescence maximums in the organisms that underwent the same fluorescent scan.

These can be seen in Figure 6D-I with each heat mapped labelled, with each pigment's maximum excitation and emission fluorescence point. For *Tolypothrix* sp. UTEX 481 under WL (Fig 6D) it can be seen that there is a small amount of fluorescence where the PE pigment should be fluorescing. There is fluorescence for chl *a* at 430, 670 nm however this is not visually seen due to the other fluorescent pigments havng higher fluorescence levels at this point. The upper fluorescent point of chl *a*, usually found between 600-650 nm and 670-720 nm Ex/Em respectively appears to move in line with the PE fluorescence, getting excited at 540 nm. This could indicate that the PE and chl *a* are part of a system that is energetically coupled together and the PE is transferring energy and fluorescence to Chl *a* which result in the shift in Ex/Em for the pigment. This is possible as PE is an accessory pigment and is known to transfer energy to chl *a*. There is also fluorescence where PC is expected at 610, 650 nm Ex/Em, however the maximum fluorescence lies somewhere between all three pigments at 570, 670 nm again indicating the possible binding of chl *a* to both PE and PC combined with the transfer of energy from both of these PBP to chl *a* to shift its fluorescent profile. The *Tolypothrix* sp. UTEX 481 green light culture (Fig 6F) appears fairly similar to the WL profile, however it has a greater fluorescence maximum (indicated by the more intense red zone in the heat map) and there appears to be slightly less fluorescence in the PC region indicated by the lighter blue colouring compared to the green seen in the WL heat map.

In contrast, the red-light culture has a significantly different profile to GL (p-value 0.0029) with no fluorescence at the PE Ex/Em point but has a high fluorescence point where PC should be at 610, 650 nm. Compared to the PC standard, the RL culture has a fluorescence that extends further across the emission spectrum (Fig 6E). This would be from chl *a* and the energy transfer that occurs from the two pigments. Again, there is chl *a* fluorescence at 430, 670 nm Ex/Em that is much lower than the maximum point that it does not visually appear on the heat map. The

Tolypothrix sp. UTEX 481 cultures indicate there is a difference in their pigment profiles through the fluorescence excitation under different light conditions.

For *Phormidium* sp. UTEX 590 the pigment profiles appear slightly different across the light conditions. For all of *Phormidium* sp. UTEX 590 (Fig 6G-I) there appears to be greater fluorescence for chl *a* at 430, 670 nm Ex/Em which was less pronounced in the *Tolypothrix* sp. UTEX 481 cultures. This could be a result of the relative amounts of the phycobilisome to chl *a* pigments between the two strains. For *Phormidium* sp. UTEX 590 WL (Fig 6G) there is a very small fluorescent spot where PE is located, however there are two peaks at the PC point and slightly lower. This is the same for *Phormidium* sp. UTEX 590 GL (Fig 6I). The red-light culture for *Phormidium* sp. UTEX 590 (Fig 6I) has a different profile to that of the WL and GL cultures and has a significantly different profile to both these conditions (p-value 0.0026 and 0.00060 respectively). Similarly, to *Tolypothrix* sp. UTEX 481, the RL for *Phormidium* sp. UTEX 590 has no visible PE fluorescence and has a strong PC fluorescence along with the chl *a* fluorescence mentioned earlier.

When comparing between organisms, the WL scan for *Tolypothrix* sp. UTEX 481 has one single maximum peak from a combination of three fluorescent pigments. The *Phormidium* sp. UTEX 590 WL has two distinct maximums and a greater chl *a* fluorescence. For RL, the two organisms display similar profiles, however, *Phormidium* sp. UTEX 590 again has greater chl *a* fluorescence at the lower Ex/Em point (540,580 nm). GL is similar to the WL, where *Tolypothrix* sp. UTEX 481 has one maximum peak and *Phormidium* sp. UTEX 590 has two with higher chl *a* fluorescence.

These differences observed in excitation and emission fluorescence signatures indicate the impact light has on the organism's pigment profile. *Tolypothrix* sp. UTEX 481 has drastic changes with accessory pigments binding and shifting chl *a* fluorescence while *Phormidium* sp. UTEX 590 has less evident changes and is different for *Tolypothrix* sp. UTEX 481 especially with higher chl *a* fluorescence.

Again, it must be noted that while the fluorescence coefficients of the three molecules are dramatically different when they are free and where they are coupled *in vivo* in the photosynthetic machinery, the method used does not provide an absolute quantification. However, this method allowed us to highlight major differences across the 2 strains under the different conditions. It is also noted that absolute values of chl *a* could have been used here to be more accurate.

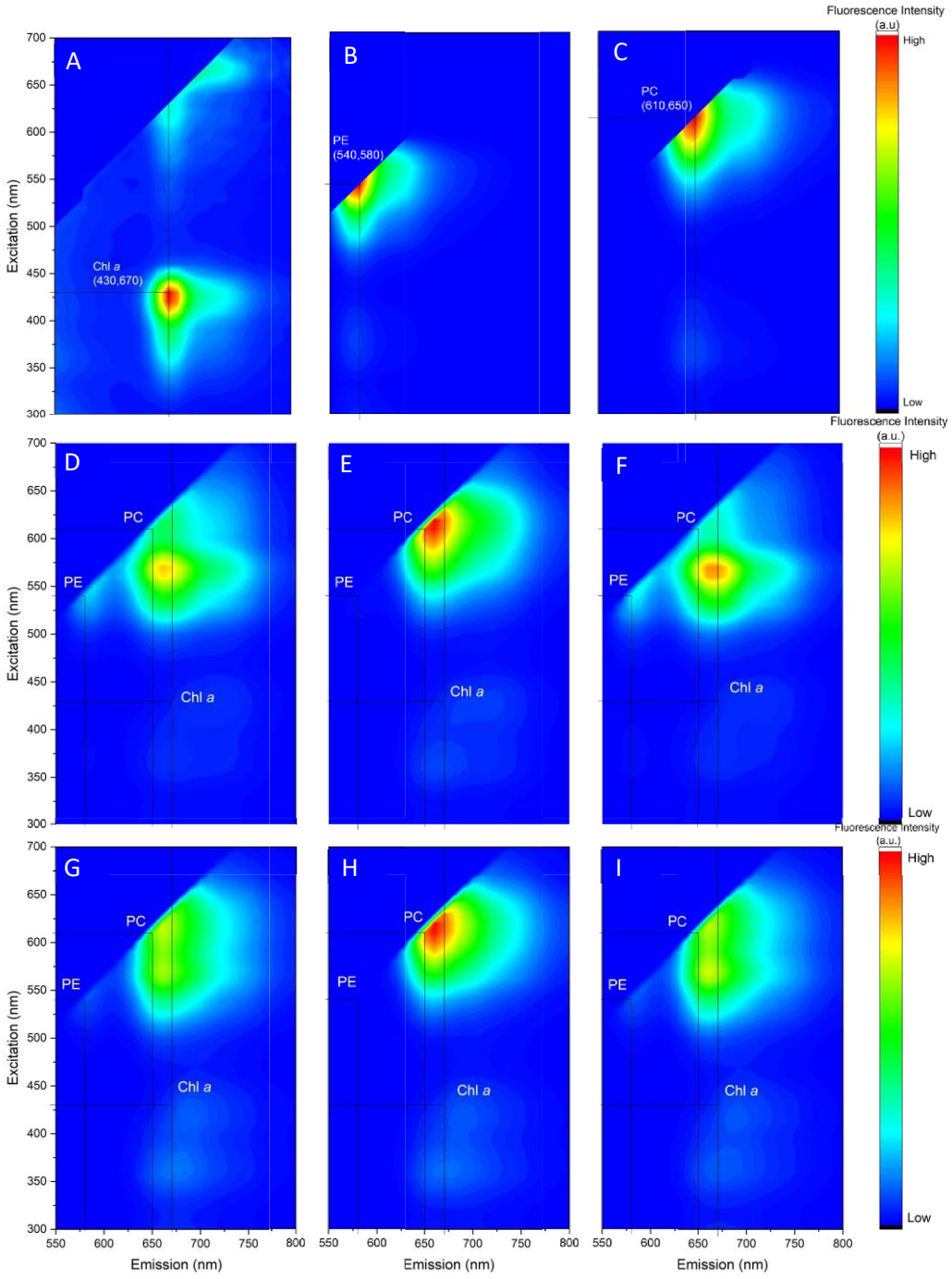

Figure 6: 3D Fluorescent scan of excitation and emission (EEM) of pigment composition displayed as heat maps for A) Chl *a* standard, B) PC standard, C) PE standard, followed by *Tolypothrix sp.* UTEX 481 D) WL E) RL F) GL and *Phormidium sp.* UTEX 590 G) WL H) RL I) GL. Each data point was normalised to the average of its dataset. Labelling of pigments according to pigment standard EEM. N=5. *Tolypothrix* sp. UTEX 481 RL and GL are significantly different. *Phormidium* sp. UTEX 590 RL is significantly different to WL and GL. Statistical tests conducted using Kolmogorov-Smirnov test, p-values found in supplementary table.

3.2.3 Pigment Quantification

After observing differences in excitation and emission fluorescence signatures for the two organisms under different light conditions, the next step was to quantify the different pigments found in these cyanobacteria. The quantification was done through relative methods using a standard curve for each of the standards and measuring the fluorescence at the Ex/Em for that specific pigment. This was used as a proxy for pigment quantities and normalised to OD 720 of the culture in order to determine the relative quantity of these pigments in each of the cultures for the differing lights at the final time point. The Ex/Em values used were those established by the fluorescent 3D scan mentioned above (Fig 6A-C).

For chl *a* (Fig. 7A), in *Tolypothrix* sp. UTEX 481 the culture exposed to white light had the least amount of chlorophyll *a* with the GL culture having a significantly higher amount of chl *a* 0.0083 ± 0.0004 μg/OD720. RL has the highest amount of chl *a* for *Tolypothrix* sp. UTEX 481 of 0.0311 ± 0.0018 μg/OD720, being significantly higher than both WL and GL 0.0105 ± 0.0004 μg/OD720. This coincides with the fluorescent pigment profiling where there is a slightly more visible chl *a* fluorescence at the lower Ex/Em as previously mentioned (Fig 6E). In *Phormidium* sp. UTEX 590 WL has the lowest chl *a* content of 0.0119 ± 0.0008 μg/OD720 with RL having a slightly higher of 0.0152 ± 0.0017 μg/OD720. GL has a significantly higher amount of chl *a* compared to GL at 0.0207 ± 0.0017 μg/OD720.

Comparing *Tolypothrix* sp. UTEX 481 and *Phormidium* sp. UTEX 590 to each other, WL and GL *Phormidium* sp. UTEX 590 cultures have significantly higher quantities of chl *a* than the *Tolypothrix* sp. UTEX 481 cultures under the same light conditions. However, under RL, the *Tolypothrix* sp. UTEX 481 culture has significantly more chl *a* than the *Phormidium* sp. UTEX 590 culture. Once again, the fluorescent profiling indicates the *Phormidium* sp. UTEX 590 cultures had the greater chl *a* fluorescent point.

Moving to the quantity of PE found within the organisms (Fig. 7B), when looking at *Tolypothrix* sp. UTEX 481 there is a clear impact on the quantity based on the light conditions. The WL culture has 0.7799 ± 0.0667 μg/OD720 amount of PE, which is significantly higher than the RL culture (no PE detected). The GL culture produces significantly more PE than both WL and RL at 1.785 ± 0.0568 μg/OD720. This is to be expected as a result of CA. When looking at 590 there is no PE detected under WL, RL or GL making this organism significantly different in its PE content compared to *Tolypothrix* sp. UTEX 481 – except under RL.

Finally, PC varied across all organisms and conditions (Fig. 7C). For *Tolypothrix* sp. UTEX 481 WL had significantly less PC than RL and GL with 106.2 ± 10.53 µg/OD720. RL had significantly more PC with 435.6 ± 10.53 µg/OD720 compared to GL (43.43 ± 13.73 µg/OD720) and WL with. On a whole, *Tolypothrix* sp. UTEX 481 had significantly higher quantities of PC under all light conditions, when comparing the amount of PC to that found in *Phormidium* sp. UTEX 590. For *Phormidium* sp. UTEX 590, WL had significantly more PC than both RL and GL of 143.8 ± 64.31 µg/OD720**.** GL (204.45 ± 91.43 µg/OD720) had significantly more PC than RL (539.18 ± 90.65 µg/OD720). This was less clear in the fluorescent scans as WL and GL had two peak fluorescent points whereas RL had the main PC fluorescence point.

Overall, major significant differences were observed (i) for *Tolypothrix* sp. UTEX 481 when exposed to different light colours and (ii) between *Tolypothrix* sp. UTEX 481 and *Phormidium* sp. UTEX 590 when exposed to the same light. This indicates the changes in *Tolypothrix* sp. UTEX 481 due to CA, while the comparison between the two Nostocales strains that can produce multiple PBP highlight that *Phormidium* sp. UTEX 590 does not change in the same way.

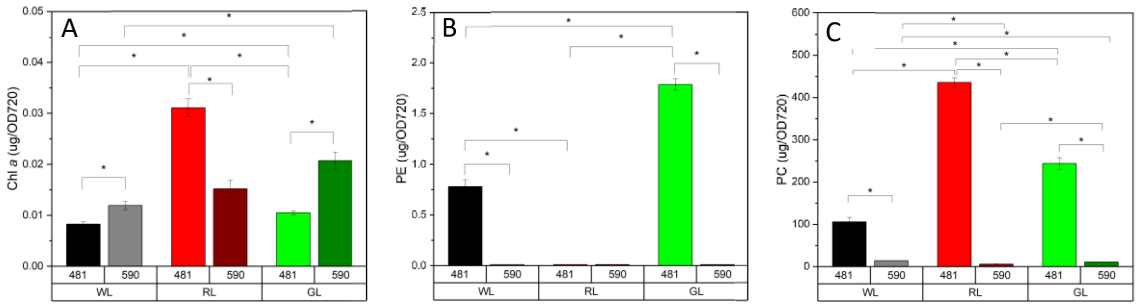

Figure 7: Relative pigment quantification for A) Chl *a*, B) PE, C) PC for *Tolypothrix* sp. UTEX 481 and *Phormidium* sp. UTEX 590 under WL, RL and GL. Quantification based off pigment standard curves found in Supplementary Figure 3. Bars indicate significance p <0.05 from One-Way ANOVA with Tukey test.

3.3 Transcriptomic Responses to Light

Knowing the differences in morphology, growth and photophysiology observed between *Tolypothrix* sp. UTEX 481 and *Phormidium* sp. UTEX 590 under different light conditions, the next key step in this study was to explore the molecular mechanisms potentially driving these differences. Using RNA sequencing from both organisms under WL and RL, the transcriptomic responses to light have been analysed. Although there were clear differences in the responses between RL and GL for *Tolypothrix* sp. UTEX 481, the WL cultures are compared to the RL in order to compare these changes to a control sample (WL).

3.3.1 Transcript Variation

Visualising the variation and separation in the transcriptomic regulation for both Nostocales strains suggests there is different gene regulation in response to light spectra for both strains (Fig. 8). The PCA plots show separation between the WL and RL conditions for *Tolypothrix* SP. UTEX 481 (Fig. 8a) indicating there is a difference in RNA expression between the two group of samples under the two light spectra for this strain. Similarly, the PCA plot for *Phormidium* SP. UTEX 590 (Fig. 8b) also indicates a separation between the WL and RL conditions with majority of this separation occurring between different light conditions (horizontal axis) with 36.8% and 39.2% of the differences explained due to light for the two strains respectively.

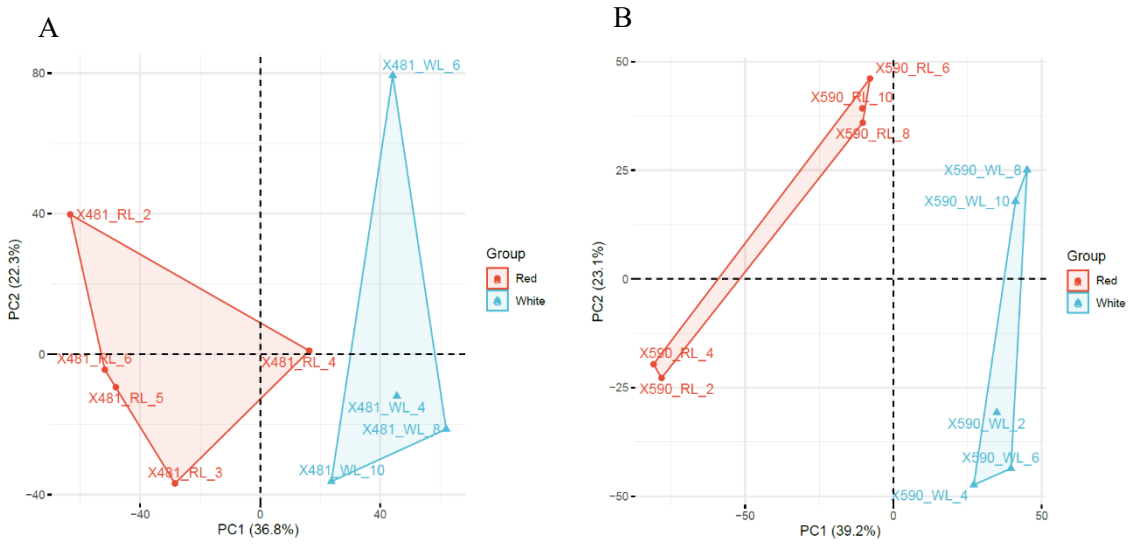

Figure 8: Principal Component Analysis (PCA) plots displaying the variance of transcriptomic data for A *Tolypothrix* sp. UTEX 481 RL vs. WL and B *Phormidium* sp. UTEX 590 RL vs. WL.

3.3.2 Transcript Regulation

Based on the different gene regulation observed for both strains under WL compared to RL, we further investigated how these genes are regulated. The volcano plots (Fig. 9) shows genes found in both WL and RL transcriptomes for *Tolypothrix* SP. UTEX 481 (Fig. 9a) and *Phormidium* UTEX 590 (Fig. 9b) as being either upregulated (red) or downregulated (green) in RL compared to WL with a $-2 \geq$ fold change ≥ 2 and p-value < 0.05. From these plots, for *Tolypothrix* SP. UTEX 481 we can see that out of the 259 significantly regulated genes, 178 of the genes are upregulated under RL, with an apparent cluster of genes highly regulated (28 genes over 20-fold change) under RL with the remaining 81 being downregulated.

When looking at the volcano plot for *Phormidium* SP. UTEX 590, there is both up- and down-regulation of genes similar to *Tolypothrix* SP. UTEX 481 but without any apparent highly

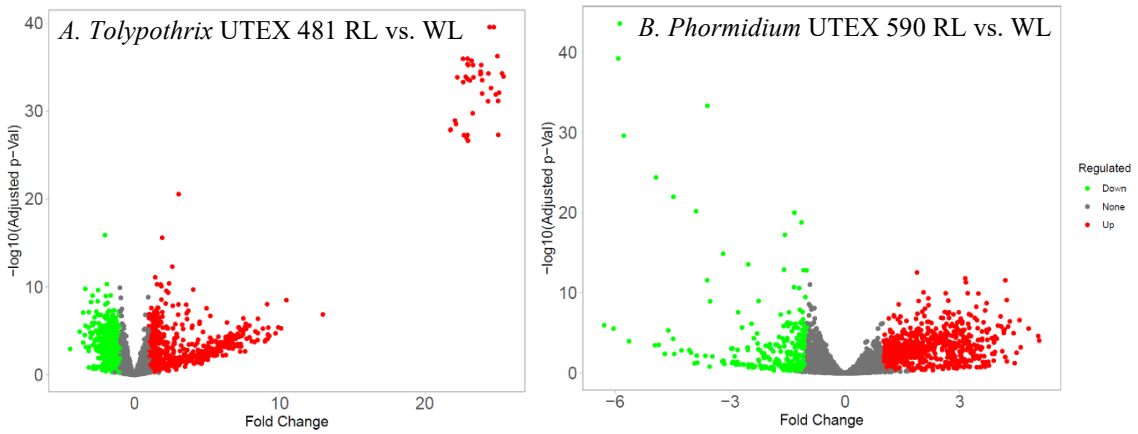

Figure 9: Volcano plots indicating the up- (red) and down- (green) regulation of genes for A) *Tolypothrix* UTEX 481 RL vs. WL and B) *Phormidium* SP. UTEX 590 RL vs. WL. Cut off -2 ≤ Fold Change ≥ 2 and $p < 0.05$.

upregulated cluster. There are several genes that are highly downregulated for *Phormidium* sp. UTEX 590, however, these are not to the same extent as the other strain, with maximum fold change at -6. Out of the 336 significantly regulated genes, 302 are upregulated with a maximum log fold change of 5 and 34 genes are downregulated. Comparing the two Nostocales strains, it is clear that there are greater changes in the gene regulation for *Tolypothrix* 481 based on the apparent cluster for in the upregulation region with fold change being over 20 apparent cluster of genes in Fig. 9A that are upregulated in *Tolypothrix* 481 RL compared to WL can be found in Table 1**.** As previously mentioned, there are 28 genes in the cluster with a fold change >20 however, these genes have been curated to exclude the ones classified as an unknown protein and/or had missing Gene Ontology (GO), leaving only 8 identified genes highly regulated. Of interest, the gene coding for the protein Pheophorbide a oxygenase (GO:0010277) is upregulated fold change of 22.8. The gene encoding the short chain dehydrogenase/reductase SDR protein has the oxidoreductase activity (GO:0016491), with oxidoreductase known to be part of the phycobilin biosynthetic pathway [86].

Table 1: Proteins and their corresponding gene ontology annotation that are clustered in Figure 9A indicating Upregulation in 481Tvs481W with a fold change >20 and $p<0.05$.Accession number AP018248..

Gene ID	Protein Names	Gene Ontology [GO]	Fold Change
NIES37_19430	histidine kinase (EC 2.7.13.3)	phosphorelay sensor kinase activity [GO:0000155]	24.44
NIES37_66790	Short-chain dehydrogenase/reductase SDR	oxidoreductase activity [GO:0016491]	24.38
NIES37_03540	Type I site-specific deoxyribonuclease, HsdR family protein	DNA restriction-modification system [GO:0009307]	23.35

NIES37_23220	Pheophorbide a oxygenase	membrane [GO:0016020], 2 iron, 2 sulfur cluster binding [GO:0051537], chlorophyllide a oxygenase [overall] activity [GO:0010277], metal ion binding [GO:0046872]	23.20
NIES37_72340	Phosphoenolpyruvate synthase	ATP binding [GO:0005524], kinase activity [GO:0016301], phosphorylation [GO:0016310]	23.18
NIES37_20210	DUF1350 domain-containing protein	membrane [GO:0016020]	22.81
NIES37_19660	Nitrogenase protein alpha chain (EC 1.18.6.1)	molybdenum-iron nitrogenase complex [GO:0016612], carbonyl sulfide nitrogenase activity [GO:0018697], iron-sulfur cluster binding [GO:0051536], metal ion binding [GO:0046872], nitrogenase activity [GO:0016163], nitrogen fixation [GO:0009399]	22.44
NIES37_27230	DUF3592 domain-containing protein	membrane [GO:0016020]	22.24
NIES37_59800	Lipoxygenase-like protein	metal ion binding [GO:0046872], oxidoreductase activity, acting on single donors with incorporation of molecular oxygen, incorporation of two atoms of oxygen [GO:0016702], lipid oxidation [GO:0034440]	10.54
NIES37_23040	Short-chain dehydrogenase/reductase SDR	oxidoreductase activity [GO:0016491]	9.81
NIES37_48210	Formate acetyltransferase (EC 2.3.1.54) (Pyruvate formate-lyase)	cytoplasm [GO:0005737], formate C-acetyltransferase activity [GO:0008861], glucose metabolic process [GO:0006006]	8.62
NIES37_30120	Winged helix-turn helix domain-containing protein	nucleic acid binding [GO:0003676]	8.49
NIES37_73070	Helix-turn-helix domain-containing protein	DNA binding [GO:0003677]	7.63
NIES37_16740	HigA2-like helix-turn-helix domain-containing protein	DNA binding [GO:0003677]	7.54
NIES37_19690	Cysteine desulfurase (EC 2.8.1.7) (Nitrogenase metalloclusters biosynthesis protein NifS)	cysteine desulfurase activity [GO:0031071], iron-sulfur cluster binding [GO:0051536], lyase activity [GO:0016829], metal ion binding [GO:0046872], pyridoxal	7.54

		phosphate binding [GO:0030170], amino acid metabolic process [GO:0006520]	
NIES37_38330	Molybdopterin-dependent oxidoreductase alpha subunit	4 iron, 4 sulfur cluster binding [GO:0051539], formate dehydrogenase (NAD+) activity [GO:0008863], molybdenum ion binding [GO:0030151], molybdopterin cofactor binding [GO:0043546]	7.04
NIES37_65350	Phosphinothricin N-acetyltransferase	acyltransferase activity, transferring groups other than amino-acyl groups [GO:0016747]	6.66
NIES37_37740	Ubiquinone biosynthesis protein	ubiquinone biosynthetic process [GO:0006744]	6.38
NIES37_68400	AraC family transcriptional regulator	DNA-binding transcription factor activity [GO:0003700], sequence-specific DNA binding [GO:0043565]	6.33
NIES37_44100	ABC transporter-like protein	membrane [GO:0016020], ABC-type transporter activity [GO:0140359], ATP binding [GO:0005524], ATP hydrolysis activity [GO:0016887]	5.98

3.3.3 Transcript Differentiation

The Venn diagram (Fig. 10) compares the genes significantly up- and down- regulated for *Tolypothrix* 481 RL conditions compared to WL with *Phormidium* 590 RL compared to WL conditions. Out of the 40 genes unique to the upregulation in *Tolypothrix* 481 RL (Fig. 10A green) 3 may be related to light harvesting and photosynthesis as well as 1 gene involved in phycobilin biosynthesis (oxidoreductase activity [GO:0016702]) [1].

There are 62 uniquely upregulated genes in *Phormidium* 590 RL compared to WL (Fig. 10A blue) with 9 relating to photosynthesis and the PBS that have roles in chlorophyll biosynthesis, electron transport pathway of photosynthesis and light energy transfer. There is also 1 gene present that is part of the phycobilin biosynthetic pathway (oxidoreductase activity [GO:0016722]).

Out of the 18 genes unique to *Tolypothrix* 481 that are downregulated in WL (Fig. 10B green) 2 are related to the biosynthetic pathway for phycobilins (heme binding [GO:0020037], oxidoreductase activity with incorporation or reduction of molecular oxygen [GO:0016705]) [1].

There are 17 genes uniquely downregulated in *Phormidium* 590 RL compared to WL (Fig. 10B blue) with 2 of these relating to the light harvesting complex that houses PC and PE. The biosynthesis of phycobilins has 4 genes downregulated in these conditions (oxidoreductase activity, [GO:0016636], phytochromobilin biosynthetic process [GO:0010024], heme oxygenase (decyclizing) activity [GO:0004392] and heme oxidation [GO:0006788]) [1].

Between *Tolypothrix* 481 RL compared to WL and *Phormidium* 590 RL compared to WL there are 16 genes that are commonly upregulated (Fig. 10A overlap) with 2 being involved in light absorption and the transfer of light energy within the phycobilisomes and 1 component involved in the phycobilin biosynthetic pathway (oxidoreductase activity [GO:0016491]). There are 2 shared genes between *Tolypothrix* 481 RL downregulation and *Phormidium* 590 RL downregulation (Fig. 10B overlap), which are membrane (GO:0016020) gene encoding for a family of light harvesting-like proteins and DNA binding gene responsible for the DNA binding present in transcriptional regulators (GO:0003677).

3.3.4 Phycocyanin and Phycoerythrin Regulation

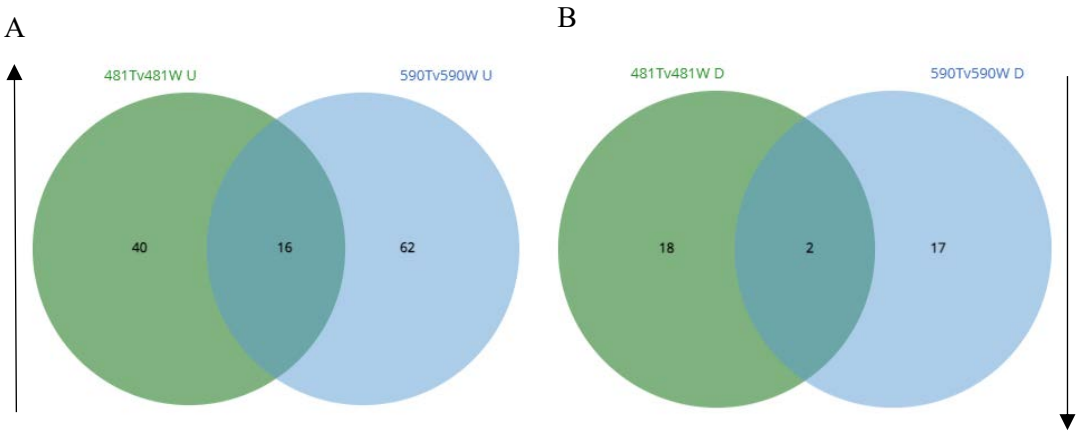

Figure 10: Venn diagram representing the overlap in genes significantly regulated, $-2 \leq$ fold change ≥ 2 and p-value < 0.05 that are; A Upregulated in *Tolypothrix sp.* 481Tvs481W (green) and upregulated in *Phormidium* sp. UTEX 590 (blue) and B downregulated in *Tolypothrix sp.* 481Tvs481W (green) and downregulated in *Phormidium sp.* 590Tvs590W (blue). Where T represents Treatment sample (RL) and W represents control or WL sample.

A previous publication investigated the components of the phycobilisomes for both *Tolypothrix* 481 and *Phormidium* 590 and developed a clear schematic representation of the PBS structure, annotated with linker genes as previously proposed [97, 98]. The *CpeC* gene codes for the PC-PE linker that is downregulated and significantly downregulated in *Tolypothrix* 481 RL compared to

WL and *Phormidium* 590 RL compared to WL respectively. The *CpcG* gene is the linker between APC (core of the PBS) and PC which is downregulated in both strains. The *CpcC* gene is the PC-PC linker and is downregulated in *Tolypothrix* 481 RL compared to WL but upregulated in *Phormidium* 590 RL compared to WL and the *CpcD* gene is a PC linker that limits the length of the peripheral rods which is upregulated in 590 and is present in 481 as up- and down- regulated. Whilst this means for *Phormidium* 590 under RL there is more PC-PC linkage, there is less APC-PC linkage, securing the PC to the core of the PBS which could correspond to the lower quantity of PC found in the *Phormidium* 590 RL culture. Conflictingly, for *Tolypothrix* 481 under RL there is downregulation for all the linker genes even though there is a significant amount more of PC under RL compared to WL (Fig. 6C). These genes however are not significantly regulated. Majority of these genes encoding these linkers, chains and subunits in relation to PE and PC have Gene Ontology that relate to the phycobilisomes (GO:0030089), thylakoid membrane (GO:0031676) and photosynthesis (GO:0015979). Alvey et al. (2003) determined the upregulation of genes encoding for PE and PBP biosynthesis elements (*CpeBA* and *pebA* and *pebB* respectively*)* occurs under GL in *Tolypothrix* 481 and may be a better comparison than the WL cultures to get a clearer picture of the differences in regulation for the phycobilin genes [99].

Interestingly, in *Phormidium* 590 RL compared to WL some downregulation for the PE linker proteins is present, indicating that the mechanics for PE synthesis exist within this organism and the process of synthesising multiple pigments via chromatic adaptation is possible. However, as there is no indication of PE based on the photophysiological data (Fig. 6B), however, there is significant downregulation for the PE linker proteins, indicating there is clearly something missing at the molecular level that results in PE not being transcribed and produced in this organism. The methods used may also not be sensitive enough to detect the quantities of this pigment. What exactly is missing, whether it be a specific gene, a pathway or a process cannot be determined from this data set but would be interesting to further explore and uncover with a more thorough investigation including whole-genome sequencing to clearly identify all the genes at play within the organism. The alpha and beta subunits of PE and PC were not significantly up- or down- regulated in either strain under the different light spectral qualities.

A clear pathway for the biosynthesis of phycobilins (PB) in *Fremyella diplosiphon* and the products, proteins and processes involved in these steps has been published previously [1]. This known pathway has been used to determine the important proteins to look for in the transcript regulation of the two strains (Fig. 11). When looking at the genes found in the two Nostocales strains from these pathways, there are subtle trends that can be seen for the regulation of Phycobilin biosynthesis. For *Tolypothrix* 481 RL compared to WL there is some upregulation seen in Uroporphyrinogen III synthase, Protoporphyrin IX and Heme oxygenase which are all involved in PB biosynthesis [1, 116]. As these genes are not significantly regulated, we see a

trend in the upregulation for *Tolypothrix* 481 RL, which aligns with the significantly higher PC production for this organism (Fig. 7C). Conversely, for *Phormidium* 590 RL compared to WL there is downregulation of δ-Aminolevulinic acid (ALA), Uroporphyrinogen III synthase, Protoporphyrin IX and significantly downregulated Heme oxygenase. This aligns with no PE production and less PC production in *Phormidium* 590 compared to *Tolypothrix* 481.

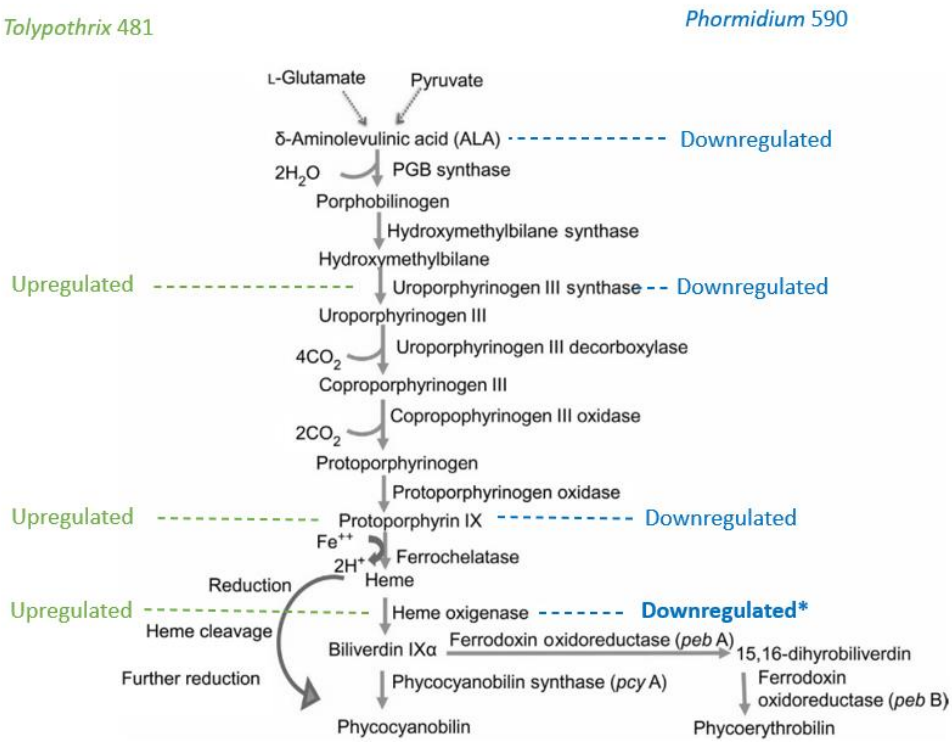

Figure 11: Biosynthetic pathway of phycobilins with the up- and down- regulation of these genes found in *Tolypothrix* 481 RL compared to WL (green) and *Phormidium* 590 RL compared to WL (blue). Figure adapted from previously published paper [1].. Asterisk indicates significant regulation.

Chapter 4: Discussion

4.1 Regulation of Morphology & Microscopy

From the results displayed in the microscopic measurements and images, there is a significant and clear difference between the size of cells and filaments of cyanobacteria strain SP. UTEX 481 when exposed to different light colours (Figure 4). This is in line with other publications [55, 82, 100-102] that document this phenomenon as a result of CA seen in this species. Research published in 2008 documented that when *F. diplosiphon* was grown in green light, the organism was approximately 9.2 times longer and contained 4 times as many cells as the red light grown cultures [55]. Others have noted cultures grown under red light can have filament lengths ten times shorter than green light [32, 73]. Whilst the numbers do not exactly match, the trend of GL having longer filaments than RL is consistent with our results. A possible reason why the red light filaments could be shorter might be that 20% of cells were converted to necridia – dead cells as a result of programmed cell death within the filaments that act as separation disks and break the filaments at these points creating shorter fragments [32, 71, 73].

The regulation of the morphology of 481 has been depicted to rely on similar pathways as CA, utilizing the Rca pathway [101, 103]. However, there is more evidence that suggests the morphology has its own regulators as well. In RL, there is an upregulation of reactive oxygen species (ROS) which may influence the regulation of morphology [104]. Others have suggested TonB and BolA regulate morphological changes [68, 105-107]. TonB is a family of proteins involved in membrane biogenesis and cell wall biosynthesis, which has been noted to be upregulated in GL [106]. BolA is known to play a role in spherical morphology adaptation, with lower levels of BolA noted under GL [106, 108]. This leads to the suggestion that while changes in morphology are linked to CA, the molecular mechanisms driving the responses to light in these two strains might be different.

Green light exposure results in significantly longer and more rectangular cells, while red light exposure leads to shorter, more rounded cell morphology. A review conducted in 2019 suggests that size regulation due to CA and light spectra may confer survival and fitness advantages [56]. At the water surface where there is more red light, the shorter, rounder cells of *F. diplosiphon 481* are therefore better equipped to increase their density and still be able to capture these longer and more abundant wavelengths without overcrowding and reducing light penetration

When moving deeper into the water column, the light shifts towards green light which has shorter wavelengths and is less abundant. *Tolypothrix* sp. 481 responds to this by elongating both its cells and filaments, resulting in an increased surface area that can better capture the little light that is available at greater depths and increase its ability to survive in the given environment [103]. This efficiency is supported by the rETR data, where GL had the highest rETR for *Tolypothrix* sp. UTEX 481. Cell size plays a crucial role in fitness and survival, as it determines the amount of thylakoid membrane surface available for PBS attachment [103, 109]. When exposed to green light, enhanced light capture is particularly important for this strain since chlorophylls are unable to absorb green light as efficiently compared to red light conditions [109, 110]. Another theory could relate the filament sizes and their location in the water column to buoyancy, which is something to be looked at further.

In contrast to *Tolypothrix* sp. 481, there was no significant difference between cell or filament length across differing light conditions for *Phormidium* sp. 590 cultures (Figure 1). This indicates this strain has no morphological response to light. When compared to *Tolypothrix* sp. 481, cell size is significantly smaller for *Phormidium* sp. 590 under all light conditions as is filament length, making this Nostocales strain smaller which could be to reduce light shading as these cells are unable to alter their morphology to absorb different light qualities.

As the adaptation of morphology under different light has been attributed to advantages towards survival [56], this would suggest that *Tolypothrix* sp. 481 has an adaptive advantage over *Phormidium* sp. 590 when exposed to prolonged periods of red and green light. To further confirm and support this notion, further experiments that focus on the comparative survivability and adaptability should be conducted.

4.2 Growth Rate & rETR

Different light colours impact the growth of *Tolypothrix* sp. 481 differently (Fig. 5). As WL is a combination of all the colours in the colour spectrum, it is not surprising that both *Tolypothrix* sp. 481 and *Phormidium* sp. 590 grew best under this light condition, as most organisms are cultured under WL. WL is widely accessible in nature and would be where you would expect to find these organisms. For *Tolypothrix* sp. 481, RL had the second highest growth rate and even with the advantage of larger cells under GL, the organism still has a lower growth rate under GL compared to the other light conditions and has been documented in other research [111].

Compared to this, *Phormidium* sp. 590 had a lower overall growth rate under all light conditions (Fig. 5). This was extremely lower in WL compared to *Tolypothrix* sp. 481, indicating *Tolypothrix* sp. 481 is better suited to these conditions. As there was very little difference in the growth rate across the light conditions for *Phormidium* sp. 590, with GL being slightly lower, this may be due to the lack of PE as well as the smaller cell size for this organism to capture and utilise light for as efficiently as *Tolypothrix* sp. UTEX 481. In this case, having the use of PE and PC to transfer light energy and the larger cell size in *Tolypothrix* sp. 481, a growth advantage is demonstrated under the used conditions. This again could further be confirmed by changing the conditions beyond the optimal growth settings for *Tolypothrix* sp. 481 and recording how adaptable and flexible both the Nostocales strains are to light and other biotic factors. Whilst there are differences in growth under the different spectral qualities, no testing was done to rule out other factors that could also contribute to growth or to find the optimum conditions for each light spectrum.

Cyanobacteria grow through photosynthesis, and the efficiency of an organism to carry out this process can be inferred through the rETR measured by chlorophyll *a* fluorescence. The information captured gives a picture of the temperature and light adaptability of the organism for short term durations. As would be expected, the *Tolypothrix* sp. 481 WL culture with the highest growth rate also had the highest rETR (Fig. 5A and 2D). The WL culture, as it is exposed to all wavelengths of colour, is able to capture light energy through chlorophyll *a* as well as transfer energy from PE and PC to chlorophyll *a* and enhance its rETR and growth. RL had the second highest rETR, along with the second highest growth rate. GL has the lowest growth rate and rETR. This may be due to the RL culture being able to transfer light energy from PC to chl *a* (Fig. 6e) [31] and capture light from chl *a* directly, whereas the GL culture would transfer light from PE to chl *a* and have less direct light capture from chl *a* under these light conditions [112].

For *Tolypothrix* sp. 481, there is a difference seen across light spectra for rETR activity. There is a difference in maximum values with white light having the highest rETR, followed by red light and then green light (Fig. 6). There's also ETR values across a greater temperature range for white light, with red and green light having low to no ETR at the low and high temperature spectrum. The PBS that contain PC and PE are attached to the thylakoid membrane and play a role in transferring energy to chlorophyll *a* [68].

In comparison, *Phormidium* sp. 590 has a much lower ETR under all light conditions compared to *Tolypothrix* sp. 481 (Fig. 5). This was consistent with the much lower growth rate produced by this Nostocales strain. When looking at *Phormidium* sp. 590 the ETR profiles are quite similar

across each of the light conditions, with similar maximum ETR's that occur at very similar temperature and light intensities indicating that light spectra does not impact the photosynthetic efficiency of this strain and that this Nostocales strain is less efficient at capturing and transferring light energy.

There are clear differences between the two strains with greater maximum ETR's in *Tolypothrix* sp. 481 across all lights compared to *Phormidium* sp. 590. This might be related to the content of photosynthetic pigments available to capture and transfer light energy among the two strains.

4.3 Excitation and Emission Matrix

Using the Ex/EM data of the standard pigments, a clear point at which these samples fluoresce is made evident and can be used to infer pigments content within the algal samples. This was used to determine the pigment composition and interactions within both Nostocales strains under different light conditions, and to provide potential reasons for some of the photophysiological data obtained. As observed, there is an interesting merging of fluorescence under WL (Figure 6D) and GL for *Tolypothrix* sp. 481 (Figure 6F), where the PE appears to be transferring light energy to chl *a*, which is known as the Förster resonance energy transfer (FRET) is a process where energy is transferred between chromophores through non-radiative dipole-dipole coupling. This mechanism enables efficient energy transfer over distances of 1-10 nm without the need for direct contact between the molecules [113]. In relation to this, it is worth noting that PE plays a crucial role in enhancing the light absorption capacity of chl a, but it achieves this without directly binding to it.In the matrices, this FRET appears to alter the fluorescence maximum to a different ex/em point for chl *a*. The RL profilePE appears to have shifted slightly, with the PC fluorescence shifting upward (Fig. 6E) which may explain why WL has a higher growth rate and RL has the lowest rETR.

For *Phormidium* sp. 590, there is very limited to no PE observed in the pigment scan, however, under WL and GL there is still a merging of pigment fluorescence, which is significantly different to the RL profile. . Merging but still distinct, there are clearly two pigments fluorescing here. This could potentially be a small amount of PE transferring energy to chlorophyll *a* as seen in *Tolypothrix* sp. 481. However, as the overall fluorescence is lower it may appear as two separate fluorescent spots where as in *Tolypothrix* sp. 481 they are so intense they merge into one big point. RL (Fig. 6H) appears to be similar to *Tolypothrix* sp. 481 (Fig. 6E) where there is one maximum fluorescence spot, displaying PC and chl *a* in their expected spots.

The precise excitation and emission wavelengths of each of the pigments was determined using pigment standards to pin point the pigments seen in the samples. In the initial scan for *Tolypothrix* sp. 481, it is visually seen that this sample has a different pigment profile compared to the initial scan for WL and GL. For the GL, the initial scan appears to be extremely similar to the WL scan [90, 114, 115]. The pigment interactions for both organisms will have an influence on other photophysiological data.

4.4 Pigment Quantification

Whilst most other references that have quantified the pigments within *F. diplosiphon* have done so as ug/ug chlorophyll [91, 114] these publications also used a more specific quantification method. The method used here was relative quantification to establish which organism and light colour produced more of which pigment. For *Tolypothrix* sp. 481 there is significantly more chl *a* under RL than any other light condition, with GL having significantly more chl *a* than WL (Fig. 7).

For *Tolypothrix* sp. 481, only WL and GL treatments showed detectable level of PE (Fig. 7). This is to be expected as exposure to RL does not induce the synthesis of PE, it actually inhibits this process [56] and *Phormidium* sp. 590 does not seem to have the capability to produce PE. GL produces significantly more PE than the WL culture, which is likely due to receiving more green light wavelengths under GL as opposed to a variety of wavelengths under WL. For *Tolypothrix* sp. 481, PC content is maximal under the RL conditions, while exposure to GL produces significantly more PC than WL conditions (Fig. 7C), as a result of the CA mechanisms.

The slower growth rate, lower ETR and smaller filaments observed across light conditions for *Phormidium* sp. 590 compared to *Tolypothrix* sp. 481 are consistent with pigment levels detected for this Nostocales strain, which were significantly lower than *Tolypothrix* sp. 481 under all light conditions (Except for PE under RL as neither organism produces PE here).

These results indicate *Phormidium* sp. 590 does not undergo CA and does not have the high functioning pigment synthesis for both PE and PC under different light spectra as seen in strain *Tolypothrix* sp. 481. Future work incorporating more specific and complex quantification method like HPLC is recommended for sensitive and conclusive comparisons between strains.

4.5 Transcriptomic Responses

When isolating the top 20 significantly regulated genes (either up- or down- wards) for *Tolypothrix* 481, the top 20 are all upregulated whereas for *Phormidium* 590 there are 12

upregulated genes and 8 downregulated genes. Of the top regulated, for *Tolypothrix* 481 oxidoreductase involved in phycobilin biosynthesis and chlorophyllide a oxygenase involved in chlorophyll *b* synthesis are the genes that are of importance in relation to PE and PC synthesis. The presence of chlorphyll *b* is surprising as it is not commonly present in cyanobacteria and could be due to the bias of the partial gene annotation results. For *Phormidium* 590, the downregulation of 2 phycobilisome proteins and 2 phycobilisome linkers that all relate to photosynthesis are of interest as they potentially play a role in pigment quantity and arrangement.

4.5.5 Phycobilin Biosynthetic Pathway

In *Tolypothrix* 481, whilst there is more PE in WL than RL (Fig. 7B), the differences are greater in the PC quantity, potentially accounting for the trend in the upregulation of the proteins for this synthesis pathway in RL opposed to GL. As for *Phormidium* 590, as there is significantly higher PC under WL compared to RL, it would make sense as to why the proteins in the synthesis pathway have the trend of downregulation. Interestingly, the inverse trends in regulation for the two strains could account for the different levels in phycobilins determined from the photophysiological data (Fig. 6 & 7) and these additional phycobilins in the form of PC and PE have the potential to increase the photosynthetic efficiency through light transfer which would aid in raising the growth of *Tolypothrix* 481 as seen in Figure 5.

4.5.6 Other Biological Processes

In *Tolypothrix* 481 RL compared to WL the transcript for the Orange Carotenoid Protein (OCP) N-terminal that is part of the phycobilisomes and plays a role in Non-Photochemical Quenching (NPQ) [19], is involved in chloride ion binding as part of the light absorption process is significantly upregulated. The protein pheophorbide a oxygenase is also significantly upregulated and plays a role in the degradation of chlorophylls. Genes such as the phycobilisomes, thylakoid membrane and photosynthesis contribute to the generation of the linker and beta chain proteins for PC. These are all important, significantly regulated genes to the organism's response to light, however, due to the limited annotation of the genome, the specific roles and functions of these genes could not be determined. As there is an upregulation for genes that impact photosynthesis in *Tolypothrix* 481 this could propose a reason as to why the RL culture has higher PC and chl *a* quantity (Fig. 7A & C). As the photosynthetic efficiency inferred by ETR is higher in WL (Fig. 5D & E), this could be due to the presence of PC and PE both capturing light for chl *a* to utilise, whereas RL has only PC and chl *a* to contribute to this process.

For Phormidium 590 RL compared to WL, the proteins related to the phycobilisome structure and PE linker protein have 4 replicates of the transcript that are significantly downregulated. The presence of the PE linker at all in this strain is surprising due to this organism not synthesising this pigment, and could again be due to the gene annotation limitations. The gene encoding for the fluorescence recovery protein which has a role in NPQ – the process where excess absorbed light energy is transferred to heat energy - and is also significantly downregulated [19, 117]. The photosynthetic genes involved in chlorophyll biosynthesis, and the oxidoreductase activity as well as heme binding gene contributing to the biosynthesis of phycobilins are significantly upregulated. The gene encoding proteins involved in the electron transfer activity, specifically electron donors are part of the electron transport chain which could contribute to photosynthesis is significantly upregulated too. The gene encoding the OCP N-terminal protein are the phycobilisome cellular component that has the function of chloride ion binding in the light absorption process and is significantly upregulated. Finally, the electron transporter that transfers electrons within the cyclic electron transport pathway of photosynthesis activity has two transcripts that are significantly upregulated. As for *Phormidium* 590, there is more chl *a* under RL (Fig. 7A) which coincides with the upregulation of genes involved in chlorophyll biosynthesis. Interestingly, however, WL has a higher ETR max (Fig. 5G & H) and greater chl *a* fluorescence than RL cultures (Fig. 6G & H) despite RL having a greater quantity of chl *a*. Exploring further the role and relationship between the energy transfer of phycobilins to chl *a* may provide understanding to these differences.

The regulation and stimulation of PBP production is caused by light that triggers a phosphorelay system cascade [54, 118-120]. With multiple repeats of genes for phosphorelay systems and activation in both Nostocales strains, it is clear that this is a highly regulated process for both organisms despite only *Tolypothrix* 481 showing signs of CA. Again, this alludes to *Phormidium* 590 having the capabilities to carry out changes in pigmentation as a result of changing light quality, however, there are missing pieces or genes to the process.

4.5.7 Limitations of Transcriptomics Analysis

This analysis comes with its limitations. Unfortunately, there are some genes that appear to be both up- and down- regulated at the same time, which is contradictory. This occurs in *Tolypothrix* 481 RL compared to WL with the helicase activity [GO:0004386] gene which appears to be significantly regulated in both directions. For *Phormidium* 590 RL compared to WL this occurs with the gene's transcripts for the plasma membrane [GO:0005886] and nitrate transmembrane transporter activity [GO:0015112].

For the mapping against the reference genome - *Tolypothrix tenuis PCC 7101* - which will not be fully accurate for either strain, however had >90% match and is closely related. Due to the gene annotation not being truly accurate, this has resulted in some genes appearing to be simultaneously up- and down- regulated in both Nostocales strains, making it somewhat difficult to draw clear conclusions about some genes and their regulation in particular with the biosynthesis pathway and PE and PC genes. The main reasoning behind this is also due to the type of RNA sequencing used. The Illumina sequencing used only looks at 100bp fragments, which are extremely short compared to the size of the whole gene. As a result of this, fragments could have high similarity within the 100bp sequence but do not encode for the same gene. To avoid this and improve the mapping quality, complementing this approach with a sequencing option that reads longer sequences (>1000bp) would be ideal to use and provide much more accurate reads.

Overall, there are more differences than similarities in the regulation of genes between the two Nostocales strains that could account for the differences seen in photophysiology and pigment production behaviour. The important differences related to light absorption, pigment composition and pigment synthesis are not significantly regulated. More in depth genome analysis is required to draw solid, significant conclusions as to the impacts light has on these transcripts and how this links clearly to specific responses.

4.6 Conclusions

Overall, *Tolypothrix* sp. 481 demonstrates adaptability and changes in morphology, photophysiology and transcriptomics in response to different light spectra. There are drastic differences between *Tolypothrix* sp. 481 and *Phormidium* sp. 590, with the later strain not adapting as well to tested conditions. Not only that, there were no significant changes observed for *Phormidium* sp. 590 under the different light conditions. Changing morphology and cell size provides an advantage for *Tolypothrix* sp. UTEX 481. It allows for higher growth rate, more efficient photosynthesis through ETR and intense differences in pigment composition and quantity.

Chapter 5: Synthesis

This research had several limitations which included spending the first few months of my candidature trying to get *Phormidium* sp. 590 to produce PE only to discover this was not the strain it was thought to be – then having to order the correct strain. I then focussed the direction of my thesis to be a comparative study; had this not happened I believe I would have been able to run more experiments and look at some more parameters that may be impacted by the CA process. This research presented many challenges and setbacks but these also provided new avenues and opportunities for this research. Another challenge was the contamination of my cultures with *Synechocystis* after already sending my RNA extractions to be sequenced. After cleaning my cultures and repeating experiments, *Phormidium* sp. 590 appeared to behave differently (as it was heavily contaminated before). Following on from this observation, looking at co-culture interactions between *Phormidium* sp. 590 and *Synechocystis* would be interesting to determine the changes in photophysiological behaviour. Additionally, creating a co-culture of both Nostocales strains and determining if CA provides an adaptive and survivability advantage would also be an interesting experiment.

As mentioned with the gene annotation, the mapping reference organism was slightly different, combined with short fragment read which resulted in co-regulation of a number of genes. Developing a more accurate gene map for both of these Nostocales strains would be interesting and may also shed more light onto the regulation of genes under different light conditions. Furthermore, investigating the genome of *Phomridium* 590 in regards to CA and PE production would give a clearer picture if this organism contains the genes for PE but is unable to synthesise this pigment under the light conditions investigated, which may provide some unique and interesting findings. This in-depth analysis of the genomes for both organisms is needed to rectify any uncertainties and to link more clearly the true relatedness of these two organisms. In this respect, in Figure 10, a phylogenetic tree using another marker gene, RcaE, known to have higher resolution than 16S in cyanobacteria displays a clearer picture of the evolutionary relationship between the two Nostocales strains. One key aspect for future experimentation is to determine the full impact of CA through colour shift experiments where these measurements are taken on cultures that have not already been acclimated to the light spectral quality they are tested in. This would be extremely interesting to look at the transcriptomic side of the colour shift experiments.

Further research that explores areas that may relate to but are outside of direct correlation with the CA process are monitoring and measuring metabolomics and/or volatilomics under different light colours to see changes in this component of organisms. Investigating the impact of different nutrients on both growth and pigment production may provide insights to some of the changes

seen, with papers indicating calcium and iron have impacts on photosynthesis [121-123], nitrate on phycobilin production [124] as well as the photoreceptor RcaE being involved in the acclimation to iron deficiency [125-127], sulfur limitation inducing the expression of an operon encoding PC [128, 129]. Looking at some of the mutated forms of *Tolypothrix* 481 [130] and determining how these mutations impact photophysiological behaviour may shed more light onto how this organism functions and perhaps explain the lack of PE found in *Phormidium* sp. 590. Testing if there is a correlation between growth rate and rETR would be intriguing for both strains and may shed more light onto the differences observed.

Conducting an action spectra on both of these Nostocales strains would also be an exciting test to determine the efficiency at which they photosynthesise under different light conditions [131] (this measurement was initially planned for *Tolypothrix* sp. 481; however, this was not possible due to equipment failure). Attempting mutations to these strains to see if they are capable of adapting to far red light, which has been documented in some cyanobacteria [132, 133]. Looking into the non-photochemical quenching properties of the cultures under different lights as there is note of differences under red and green light in *Tolypothrix* 481 [134]. As previously mentioned, Reactive Oxygen Species (ROS) have been documented to impact the morphology and pigmentation production in *F. diplosiphon* [135] and would be interesting to explore further and determine if the genes involved in this are also linked to the CA process. Looking into the isolation location for both of these Nostocales strains and comparing the habitats these organisms are naturally found in would link the processes to the functioning for both of these Nostocales strains. Exploring more downstream applications for this organism and its pigments would also be an exciting and potentially novel prospect.

References

1. Kumar, V., et al., *Photomorphogenesis in the cyanobacterium Fremyella diplosiphon improves photosynthetic efficiency*, in *Cyanobacteria*. 2019, Elsevier. p. 131-143.
2. Gupta, V., et al., *New insights into the biodiversity and applications of cyanobacteria (blue-green algae)—Prospects and challenges.* Algal research, 2013. **2**(2): p. 79-97.
3. Hachicha, R., et al., *Biomolecules from microalgae and cyanobacteria: Applications and market survey.* Applied Sciences, 2022. **12**(4): p. 1924.
4. Waterbury, J.B., *The cyanobacteria—isolation, purification and identification.* The prokaryotes, 2006. **4**: p. 1053-1073.
5. Whitton, B.A. and M. Potts, *Introduction to the cyanobacteria*, in *Ecology of cyanobacteria II: their diversity in space and time*. 2012, Springer. p. 1-13.
6. Chorus, I. and M. Welker, *Toxic cyanobacteria in water: a guide to their public health consequences, monitoring and management*. 2021: Taylor & Francis.
7. Tan, H.T., et al., *Characterisation and selection of freshwater cyanobacteria for phycobiliprotein contents.* Aquaculture International, 2023. **31**(1): p. 447-477.
8. Dagnino-Leone, J., et al., *Phycobiliproteins: Structural aspects, functional characteristics, and biotechnological perspectives.* Computational and Structural Biotechnology Journal, 2022.
9. Castenholz, R.W. and F. Garcia-Pichel, *Cyanobacterial responses to UV radiation*, in *Ecology of cyanobacteria II: Their diversity in space and time*. 2012, Springer. p. 481-499.
10. Pulz, O. and W. Gross, *Valuable products from biotechnology of microalgae.* Applied microbiology and biotechnology, 2004. **65**: p. 635-648.
11. Ullmann, J. and D. Grimm, *Algae and their potential for a future bioeconomy, landless food production, and the socio-economic impact of an algae industry.* Organic Agriculture, 2021. **11**(2): p. 261-267.
12. Michalak, I. and K. Chojnacka, *Algae as production systems of bioactive compounds.* Engineering in Life Sciences, 2015. **15**(2): p. 160-176.
13. Levasseur, W., P. Perré, and V. Pozzobon, *A review of high value-added molecules production by microalgae in light of the classification.* Biotechnology advances, 2020. **41**: p. 107545.
14. Chen, Z., et al., *Recent advances of natural pigments from algae.* Food Production, Processing and Nutrition, 2023. **5**(1): p. 39.
15. Pareek, S., et al., *Chlorophylls: Chemistry and biological functions.* Fruit and Vegetable Phytochemicals: Chemistry and Human Health, 2nd Edition, 2017: p. 269-284.
16. Whitton, B.A. and M. Potts, *The ecology of cyanobacteria: their diversity in time and space*. 2007: Springer Science & Business Media.
17. Henríquez, V., et al., *Carotenoids in microalgae.* Carotenoids in nature: biosynthesis, regulation and function, 2016: p. 219-237.
18. Frank, H.A. and R.J. Cogdell, *Carotenoids in photosynthesis.* Photochemistry and photobiology, 1996. **63**(3): p. 257-264.
19. Bao, H., M.R. Melnicki, and C.A. Kerfeld, *Structure and functions of Orange Carotenoid Protein homologs in cyanobacteria.* Current opinion in plant biology, 2017. **37**: p. 1-9.
20. Komárek, J., *A polyphasic approach for the taxonomy of cyanobacteria: principles and applications.* European Journal of Phycology, 2016. **51**(3): p. 346-353.
21. Oren, A. and G.M. Garrity, *Uncultivated microbes—in need of their own nomenclature?* The ISME Journal, 2018. **12**(2): p. 309-311.
22. Kaštovský, J., *Welcome to the jungle!: An overview of modern taxonomy of cyanobacteria.* Hydrobiologia, 2023: p. 1-15.
23. Dvořák, P., et al., *Population genomics meets the taxonomy of cyanobacteria.* Algal Research, 2023: p. 103128.

24. Strunecký, O., A.P. Ivanova, and J. Mareš, *An updated classification of cyanobacterial orders and families based on phylogenomic and polyphasic analysis.* Journal of Phycology, 2023. **59**(1): p. 12-51.
25. Hauer, T., et al., *Reassessment of the cyanobacterial family M icrochaetaceae and establishment of new families T olypothrichaceae and G odleyaceae.* Journal of Phycology, 2014. **50**(6): p. 1089-1100.
26. Layer, A. and B.L. Montgomery, *Homologs of Phycobilisome Abundance Regulator PsoR Are Widespread across Cyanobacteria.* Microbiology Research, 2022. **13**(2): p. 167-182.
27. Ikeuchi, M. and T. Ishizuka, *Cyanobacteriochromes: a new superfamily of tetrapyrrole-binding photoreceptors in cyanobacteria.* Photochemical & Photobiological Sciences, 2008. **7**(10): p. 1159-1167.
28. Soo, R.M., et al., *On the origins of oxygenic photosynthesis and aerobic respiration in Cyanobacteria.* Science, 2017. **355**(6332): p. 1436-1440.
29. Saini, D.K., S. Pabbi, and P. Shukla, *Cyanobacterial pigments: Perspectives and biotechnological approaches.* Food and chemical toxicology, 2018. **120**: p. 616-624.
30. Hsieh-Lo, M., et al., *Phycocyanin and phycoerythrin: Strategies to improve production yield and*

chemical stability. Algal Research, 2019. **42**: p. 1-11.
31. Campbell, D., et al., *Chlorophyll fluorescence analysis of cyanobacterial photosynthesis and acclimation.* Microbiology and molecular biology reviews, 1998. **62**(3): p. 667-683.
32. Kehoe, D.M. and A. Gutu, *Responding to color: the regulation of complementary chromatic adaptation.* Annu. Rev. Plant Biol., 2006. **57**: p. 127-150.
33. Glazer, A.N., *Structure and molecular organization of the photosynthetic accessory pigments of cyanobacteria and red algae.* Mol Cell Biochem, 1977. **18**(2-3): p. 125-40.
34. Six, C., et al., *Diversity and evolution of phycobilisomes in marine Synechococcusspp.: a comparative genomics study.* Genome biology, 2007. **8**(12): p. 1-22.
35. Stomp, M., et al., *Colorful niches of phototrophic microorganisms shaped by vibrations of the water molecule.* The ISME journal, 2007. **1**(4): p. 271-282.
36. Mishra, S.K., et al., *Effect of preservatives for food grade C-Phycoerythrin, isolated from marine cyanobacteria Pseudanabaena sp.* International journal of biological macromolecules, 2010. **47**(5): p. 597-602.
37. Liu, L.-N., et al., *Characterization, structure and function of linker polypeptides in phycobilisomes of cyanobacteria and red algae: an overview.* Biochimica et Biophysica Acta (BBA)-Bioenergetics, 2005. **1708**(2): p. 133-142.
38. Kronfel, C.M., *Characterization of cpeY and cpeZ mutants in Fremyella diplosiphon strain UTEX 481.* 2013.
39. Patel, A., et al., *Purification and characterization of C-Phycocyanin from cyanobacterial species of marine and freshwater habitat.* Protein expression and purification, 2005. **40**(2): p. 248-255.
40. Pagels, F., et al., *Phycobiliproteins from cyanobacteria: Chemistry and biotechnological applications.* Biotechnology Advances, 2019. **37**(3): p. 422-443.
41. Bordowitz, J.R. and B.L. Montgomery, *Exploiting the autofluorescent properties of photosynthetic pigments for analysis of pigmentation and morphology in live Fremyella diplosiphon cells.* Sensors, 2010. **10**(7): p. 6969-6979.
42. Glazer, A.N. and C.S. Hixson, *Characterization of R-phycocyanin. Chromophore content of R-phycocyanin and C-phycoerythrin.* Journal of Biological Chemistry, 1975. **250**(14): p. 5487-5495.
43. Zhang, C.-C., et al., *Carbon/nitrogen metabolic balance: lessons from cyanobacteria.* Trends in plant science, 2018. **23**(12): p. 1116-1130.
44. Mulkidjanian, A.Y., et al., *The cyanobacterial genome core and the origin of photosynthesis.* Proceedings of the National Academy of Sciences, 2006. **103**(35): p. 13126-13131.

45. Sánchez-Baracaldo, P. and T. Cardona, *On the origin of oxygenic photosynthesis and Cyanobacteria.* New Phytologist, 2020. **225**(4): p. 1440-1446.
46. Vermaas, W.F., *Photosynthesis and respiration in cyanobacteria.* e LS, 2001.
47. Bryant, D.A., *Phycoerythrocyanin and Phycoerythrin: Properties and Occurrence in Cyanobacteria.* Journal of General Microbiology, 1982. **128**: p. 835-844.
48. Porter, G., et al., *Picosecond time-resolved energy transfer in Porphyridium cruentum. Part I. In the intact alga.* Biochimica et Biophysica Acta (BBA)-Bioenergetics, 1978. **501**(2): p. 232-245.
49. Yamamoto, Y., *Quality control of photosystem II.* Plant and Cell Physiology, 2001. **42**(2): p. 121-128.
50. Shevela, D., et al., *Photosystem II.* eLS, 2021. **2**(7): p. 1-16.
51. Shevela, D., R.Y. Pishchalnikov, and L.A. Eichacker, *Oxygenic photosynthesis in cyanobacteria*. 2013: CRC Press Boca Raton.
52. Ting, C.S., et al., *Cyanobacterial photosynthesis in the oceans: the origins and significance of divergent light-harvesting strategies.* Trends in microbiology, 2002. **10**(3): p. 134-142.
53. Nikkanen, L., et al., *Regulatory electron transport pathways of photosynthesis in cyanobacteria and microalgae: Recent advances and biotechnological prospects.* Physiologia Plantarum, 2021. **173**(2): p. 514-525.
54. Grossman, A.R., *A molecular understanding of complementary chromatic adaptation.* Photosynthesis research, 2003. **76**(1): p. 207-215.
55. Bordowitz, J.R. and B.L. Montgomery, *Photoregulation of cellular morphology during complementary chromatic adaptation requires sensor-kinase-class protein RcaE in Fremyella diplosiphon.* Journal of bacteriology, 2008. **190**(11): p. 4069-4074.
56. Sanfilippo, J.E., et al., *Chromatic acclimation in cyanobacteria: a diverse and widespread process for optimizing photosynthesis.* Annual review of microbiology, 2019. **73**: p. 407-433.
57. Appleby, J.L., J.S. Parkinson, and R.B. Bourret, *Signal transduction via the multi-step phosphorelay: not necessarily a road less traveled.* Cell, 1996. **86**(6): p. 845-848.
58. Kehoe, D.M. and A.R. Grossman, *Similarity of a chromatic adaptation sensor to phytochrome and ethylene receptors.* Science, 1996. **273**(5280): p. 1409-1412.
59. Cobley, J.G., et al., *CpeR is an activator required for expression of the phycoerythrin operon (cpeBA) in the cyanobacterium Fremyella diplosiphon and is encoded in the phycoerythrin linker-polypeptide operon (cpeCDESTR).* Molecular microbiology, 2002. **44**(6): p. 1517-1531.
60. Terauchi, K., et al., *RcaE is a complementary chromatic adaptation photoreceptor required for green and red light responsiveness.* Molecular microbiology, 2004. **51**(2): p. 567-577.
61. Hirose, Y., et al., *Green/red cyanobacteriochromes regulate complementary chromatic acclimation via a protochromic photocycle.* Proceedings of the National Academy of Sciences, 2013. **110**(13): p. 4974-4979.
62. Ariyanti, D., K. Ikebukuro, and K. Sode, *Artificial complementary chromatic acclimation gene expression system in Escherichia coli.* Microbial Cell Factories, 2021. **20**(1): p. 1-12.
63. Hirose, Y., et al., *Diverse chromatic acclimation processes regulating phycoerythrocyanin and rod-shaped phycobilisome in cyanobacteria.* Molecular Plant, 2019. **12**(5): p. 715-725.
64. Wang, F. and M. Chen, *Chromatic Acclimation Processes and Their Relationships with Phycobiliprotein Complexes.* Microorganisms, 2022. **10**(8): p. 1562.
65. Grossman, A.R., et al., *The phycobilisome, a light-harvesting complex responsive to environmental conditions.* Microbiological reviews, 1993. **57**(3): p. 725-749.
66. Federspiel, N.A. and A.R. Grossman, *Characterization of the light-regulated operon encoding the phycoerythrin-associated linker proteins from the cyanobacterium Fremyella diplosiphon.* Journal of bacteriology, 1990. **172**(7): p. 4072-4081.

67. Kehoe, D.M., *Chromatic adaptation and the evolution of light color sensing in cyanobacteria.* Proceedings of the National Academy of Sciences, 2010. **107**(20): p. 9029-9030.
68. Singh, S.P. and B.L. Montgomery, *Morphogenes bolA and mreB mediate the photoregulation of cellular morphology during complementary chromatic acclimation in F remyella diplosiphon.* Molecular microbiology, 2014. **93**(1): p. 167-182.
69. Grossman, A.R., D. Bhaya, and Q. He, *Tracking the light environment by cyanobacteria and the dynamic nature of light harvesting.* Journal of Biological Chemistry, 2001. **276**(15): p. 11449-11452.
70. Li, W., et al., *Phycobiliproteins: Molecular structure, production, applications, and prospects.* Biotechnology Advances, 2019. **37**(2): p. 340-353.
71. Schuergers, N., et al., *Cyanobacteria use micro-optics to sense light direction.* Elife, 2016. **5**: p. e12620.
72. Singh, S.P. and B.L. Montgomery, *Determining cell shape: adaptive regulation of cyanobacterial cellular differentiation and morphology.* Trends in microbiology, 2011. **19**(6): p. 278-285.
73. Gutu, A. and D.M. Kehoe, *Emerging perspectives on the mechanisms, regulation, and distribution of light color acclimation in cyanobacteria.* Molecular plant, 2012. **5**(1): p. 1-13.
74. Montgomery, B.L., *Reflections on Cyanobacterial Chromatic Acclimation: Exploring the Molecular Bases of Organismal Acclimation and Motivation for Rethinking the Promotion of Equity in STEM.* Microbiology and Molecular Biology Reviews, 2022. **86**(3): p. e00106-21.
75. Campbell, D., J. Houmard, and N.T. De Marsac, *Electron transport regulates cellular differentiation in the filamentous cyanobacterium Calothrix.* The Plant Cell, 1993. **5**(4): p. 451-463.
76. Montgomery, B., *Shedding new light on the regulation of complementary chromatic adaptation.* Open Life Sciences, 2008. **3**(4): p. 351-358.
77. Tandeau de Marsac, N. and J. Houmard, *Adaptation of cyanobacteria to environmental stimuli: new steps towards molecular mechanisms.* FEMS microbiology reviews, 1993. **10**(1-2): p. 119-189.
78. Singh, S.P. and B.L. Montgomery, *Temporal responses of wild-type pigmentation and RcaE-deficient strains of Fremyella diplosiphon during light transitions.* Communicative & integrative biology, 2011. **4**(5): p. 503-510.
79. Chang, C.-W., et al., *Tracking the secondary photodynamics of the green/red cyanobacteriochrome RcaE from Fremyella diplosiphon.* Chemical Physics Letters, 2016. **644**: p. 225-230.
80. Bennett, A. and L. Bogorad, *Complementary chromatic adaptation in a filamentous blue-green alga.* Journal of cell biology, 1973. **58**(2): p. 419-435.
81. Lomax, T., et al., *Isolation and characterization of light-regulated phycobilisome linker polypeptide genes and their transcription as a polycistronic mRNA.* Journal of bacteriology, 1987. **169**(6): p. 2675-2684.
82. Rohnke, B.A., et al., *RcaE-dependent regulation of carboxysome structural proteins has a central role in environmental determination of carboxysome morphology and abundance in Fremyella diplosiphon.* MSphere, 2018. **3**(1): p. e00617-17.
83. Ramu Ganesan, A., et al., *Phycoerythrin: A pink pigment from red sources (rhodophyta) for a greener biorefining approach to food applications.* Critical Reviews in Food Science and Nutrition, 2022: p. 1-19.
84. Marquardt, J. and K.A. Palinska, *Genotypic and phenotypic diversity of cyanobacteria assigned to the genus Phormidium (Oscillatoriales) from different habitats and geographical sites.* Archives of microbiology, 2007. **187**: p. 397-413.
85. Mullineaux, C.W., *How do cyanobacteria sense and respond to light?* Molecular microbiology, 2001. **41**(5): p. 965-971.

86. Hirose, Y., et al., *Cyanobacteriochrome CcaS is the green light receptor that induces the expression of phycobilisome linker protein.* Proceedings of the National Academy of Sciences, 2008. **105**(28): p. 9528-9533.
87. Wiltbank, L.B. and D.M. Kehoe, *Two cyanobacterial photoreceptors regulate photosynthetic light harvesting by sensing teal, green, yellow, and red light.* MBio, 2016. **7**(1): p. e02130-15.
88. Papke, R.T., et al., *Geographical isolation in hot spring cyanobacteria.* Environmental Microbiology, 2003. **5**(8): p. 650-659.
89. Rindi, F., *Diversity, distribution and ecology of green algae and cyanobacteria in urban habitats*, in *Algae and cyanobacteria in extreme environments*. 2007, Springer. p. 619-638.
90. Beguin, S., et al., *Chromatic adaptation in a mutant of Fremyella diplosiphon incapable of phycoerythrin synthesis.* Biochimie, 1985. **67**(1): p. 109-117.
91. Bruns, B.U., W.R. Briggs, and A.R. Grossman, *Molecular characterization of phycobilisome regulatory mutants of Fremyella diplosiphon.* Journal of bacteriology, 1989. **171**(2): p. 901-908.
92. Herdean, A., D.L. Sutherland, and P.J. Ralph, *Phenoplate: An innovative method for assessing interacting effects of temperature and light on non-photochemical quenching in microalgae under chemical stress.* New Biotechnology, 2022. **66**: p. 89-96.
93. Bussell, A.N. and D.M. Kehoe, *Control of a four-color sensing photoreceptor by a two-color sensing photoreceptor reveals complex light regulation in cyanobacteria.* Proceedings of the National Academy of Sciences, 2013. **110**(31): p. 12834-12839.
94. *Ramaciotti Centre for Genomics*. Available from: https://www.ramaciotti.unsw.edu.au/.
95. Gruber, T., *What is an Ontology*. 1993.
96. Gorbunov, M.Y. and P.G. Falkowski, *Using chlorophyll fluorescence kinetics to determine photosynthesis in aquatic ecosystems.* Limnology and oceanography, 2021. **66**(1): p. 1-13.
97. Pérez-Gómez, B., et al., *A proteomic approach to the analysis of the components of the phycobilisomes from two cyanobacteria with complementary chromatic adaptation: Fremyella diplosiphon UTEX B590 and Tolypothrix PCC 7601.* Photosynthesis research, 2012. **114**(1): p. 43-58.
98. Glazer, A.N., *Light harvesting by phycobilisomes.* Annual review of biophysics and biophysical chemistry, 1985. **14**(1): p. 47-77.
99. Alvey, R.M., et al., *Lesions in phycoerythrin chromophore biosynthesis in Fremyella diplosiphon reveal coordinated light regulation of apoprotein and pigment biosynthetic enzyme gene expression.* The Plant Cell, 2003. **15**(10): p. 2448-2463.
100. Singh, S.P. and B.L. Montgomery, *Distinct salt-dependent effects impair Fremyella diplosiphon pigmentation and cellular shape.* Plant signaling & behavior, 2013. **8**(7): p. e24713.
101. Pattanaik, B., M.J. Whitaker, and B.L. Montgomery, *Light Quantity Affects the Regulation of Cell Shape in Fremyella diplosiphon.* Front Microbiol, 2012. **3**: p. 170.
102. Rohnke, B., *Environmental Determination and Dynamic Regulation of the Carbon Concentrating Mechanism in Fremyella diplosiphon*. 2019: Michigan State University.
103. Bordowitz, J.R., M.J. Whitaker, and B.L. Montgomery, *Independence and interdependence of the photoregulation of pigmentation and development in Fremyella diplosiphon.* Communicative & integrative biology, 2010. **3**(2): p. 151-153.
104. Walters, K.J., et al., *Light intensity and reactive oxygen species are centrally involved in photoregulatory responses during complementary chromatic adaptation in Fremyella diplosiphon.* Communicative & Integrative Biology, 2013. **6**(5): p. e25005.
105. Montgomery, B.L., *Mechanisms and fitness implications of photomorphogenesis during chromatic acclimation in cyanobacteria.* Journal of experimental botany, 2016. **67**(14): p. 4079-4090.

106. Pattanaik, B. and B.L. Montgomery, *FdTonB is involved in the photoregulation of cellular morphology during complementary chromatic adaptation in Fremyella diplosiphon.* Microbiology, 2010. **156**(3): p. 731-741.
107. Pattanaik, B., M.J. Whitaker, and B.L. Montgomery, *Regulation of phycoerythrin synthesis and cellular morphology in Fremyella diplosiphon green mutants.* Biochemical and biophysical research communications, 2011. **413**(2): p. 182-188.
108. Singh, S.P. and B.L. Montgomery, *Regulation of BolA abundance mediates morphogenesis in Fremyella diplosiphon.* Frontiers in microbiology, 2015. **6**: p. 1215.
109. Maurya, P.K., et al., *Green and blue light-dependent morphogenesis, decoupling of phycobilisomes and higher accumulation of reactive oxygen species and lipid contents in Synechococcus elongatus PCC 7942.* Environmental and Experimental Botany, 2023. **205**: p. 105105.
110. Terashima, I., et al., *Green light drives leaf photosynthesis more efficiently than red light in strong white light: revisiting the enigmatic question of why leaves are green.* Plant and cell physiology, 2009. **50**(4): p. 684-697.
111. DIAKOFF, S. and J. SCHEIBE, *Cultivation in the Dark of the Blue-green Alga Fremyella diplosiphon. A Photoreversible Effect of Green and Red Light on Growth Rate.* Physiologia Plantarum, 1975. **34**(2): p. 125-128.
112. Cunningham Jr, F.X., et al., *Growth under red light enhances photosystem II relative to photosystem I and phycobilisomes in the red alga Porphyridium cruentum.* Plant physiology, 1990. **93**(3): p. 888-895.
113. Şener, M., et al., *Förster energy transfer theory as reflected in the structures of photosynthetic light-harvesting systems.* ChemPhysChem, 2011. **12**(3): p. 518-531.
114. Balabas, B.E., et al., *CotB is essential for complete activation of green light-induced genes during complementary chromatic adaptation in Fremyella diplosiphon.* Molecular microbiology, 2003. **50**(3): p. 781-793.
115. Bennett, A. and L. Bogorad, *Properties of subunits and aggregates of blue-green algal biliproteins.* Biochemistry, 1971. **10**(19): p. 3625-3634.
116. Cornejo, J. and S.I. Beale, *Phycobilin biosynthetic reactions in extracts of cyanobacteria.* Photosynthesis research, 1997. **51**: p. 223-230.
117. Tietz, S., et al., *NPQ (T): a chlorophyll fluorescence parameter for rapid estimation and imaging of non-photochemical quenching of excitons in photosystem-II-associated antenna complexes*. 2017, Wiley Online Library.
118. Parkinson, J.S. and E.C. Kofoid, *Communication modules in bacterial signaling proteins.* Annual review of genetics, 1992. **26**(1): p. 71-112.
119. Grossman, A.R. and D.M. Kehoe, *Phosphorelay control of phycobilisome biogenesis during complementary chromatic adaptation.* Photosynthesis research, 1997. **53**(2): p. 95-108.
120. Kehoe, D.M. and A.R. Grossman, *New classes of mutants in complementary chromatic adaptation provide evidence for a novel four-step phosphorelay system.* Journal of Bacteriology, 1997. **179**(12): p. 3914-3921.
121. Brand, J.J. and D.W. Becker, *Evidence for direct roles of calcium in photosynthesis.* Journal of bioenergetics and biomembranes, 1984. **16**(4): p. 239-249.
122. Ferreira, F. and N.A. Straus, *Iron deprivation in cyanobacteria.* Journal of Applied Phycology, 1994. **6**(2): p. 199-210.
123. González, A., et al., *The challenge of iron stress in cyanobacteria.* Cyanobacteria, 2018: p. 109-138.
124. FUJITA, Y. and A. HATTORI, *Formation of phycoerythrin in pre-illuminated cells of Tolypothrix tenuis with special reference to nitrogen metabolism.* Plant and cell physiology, 1960. **1**(4): p. 281-292.
125. Busch, A.W. and B.L. Montgomery, *The tryptophan-rich sensory protein (TSPO) is involved in stress-related and light-dependent processes in the cyanobacterium Fremyella diplosiphon.* Frontiers in microbiology, 2015. **6**: p. 1393.

126. Busch, A.W. and B.L. Montgomery, *Distinct light-, stress-, and nutrient-dependent regulation of multiple tryptophan-rich sensory protein (TSPO) genes in the cyanobacterium Fremyella diplosiphon.* Plant signaling & behavior, 2017. **12**(3): p. 1393-84.
127. Michel, K.P. and E.K. Pistorius, *Adaptation of the photosynthetic electron transport chain in cyanobacteria to iron deficiency: the function of IdiA and IsiA.* Physiologia plantarum, 2004. **120**(1): p. 36-50.
128. Casey, E.S. and A. Grossman, *In vivo and in vitro characterization of the light-regulated cpcB2A2 promoter of Fremyella diplosiphon.* Journal of Bacteriology, 1994. **176**(20): p. 6362-6374.
129. Mazel, D. and P. Marliére, *Adaptive eradication of methionine and cysteine from cyanobacterial light-harvesting proteins.* Nature, 1989. **341**(6239): p. 245-248.
130. Cobley, J. and R. Miranda, *Mutations affecting chromatic adaptation in the cyanobacterium Fremyella diplosiphon.* Journal of bacteriology, 1983. **153**(3): p. 1486-1492.
131. Haury, J.F. and L. Bogorad, *Action Spectra for Phycobiliprotein Synthesis in a Chromatically Adapting Cyanophyte, Fremyella diplosiphon.* Plant Physiol, 1977. **60**(6): p. 835-9.
132. Gan, F. and D.A. Bryant, *Adaptive and acclimative responses of cyanobacteria to far-red light.* Environmental microbiology, 2015. **17**(10): p. 3450-3465.
133. Mascoli, V., et al., *The antenna of far-red absorbing cyanobacteria increases both absorption and quantum efficiency of Photosystem II.* Nature Communications, 2022. **13**(1): p. 1-8.
134. Campbell, D., *Complementary chromatic adaptation alters photosynthetic strategies in the cyanobacterium Calothrix.* Microbiology, 1996. **142**(5): p. 1255-1263.
135. He, Y.-Y. and D.-P. Häder, *UV-B-induced formation of reactive oxygen species and oxidative damage of the cyanobacterium Anabaena sp.: protective effects of ascorbic acid and N-acetyl-L-cysteine.* Journal of Photochemistry and Photobiology B: Biology, 2002. **66**(2): p. 115-124.

Supplementary Data

Supplementary Figures

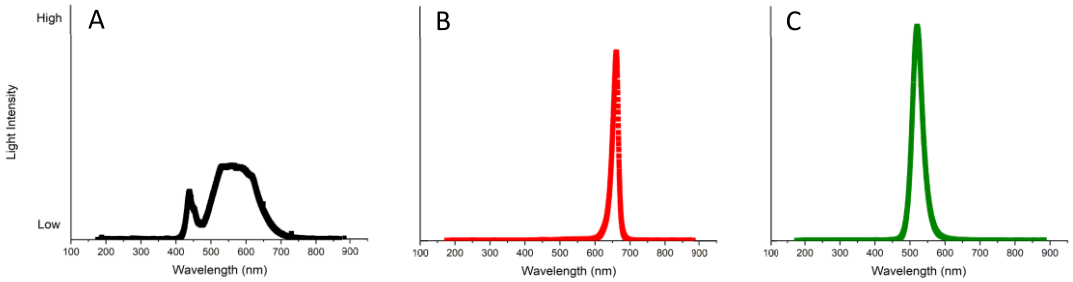

Supplementary Figure 1: Emission of light sources used throughout the experiment for A) WL, B) RL and C) GL.

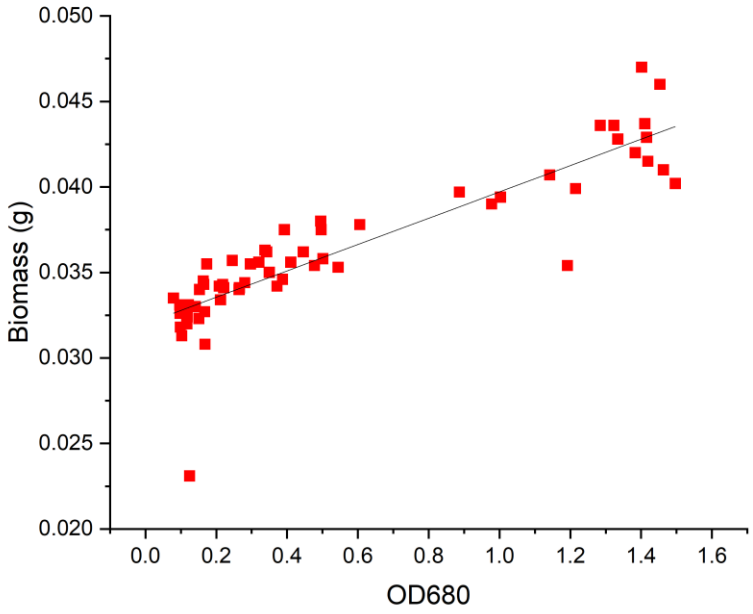

Supplementary Figure 2: Calibration curve linking Optical Density (OD) at 680nm to biomass (g). Curve was created using *Tolypothrix* UTEX 481 with WL, RL and GL cultures. Line of best fit equation y = 0.0114x + 0.0304 $R^2 = 0.9301$

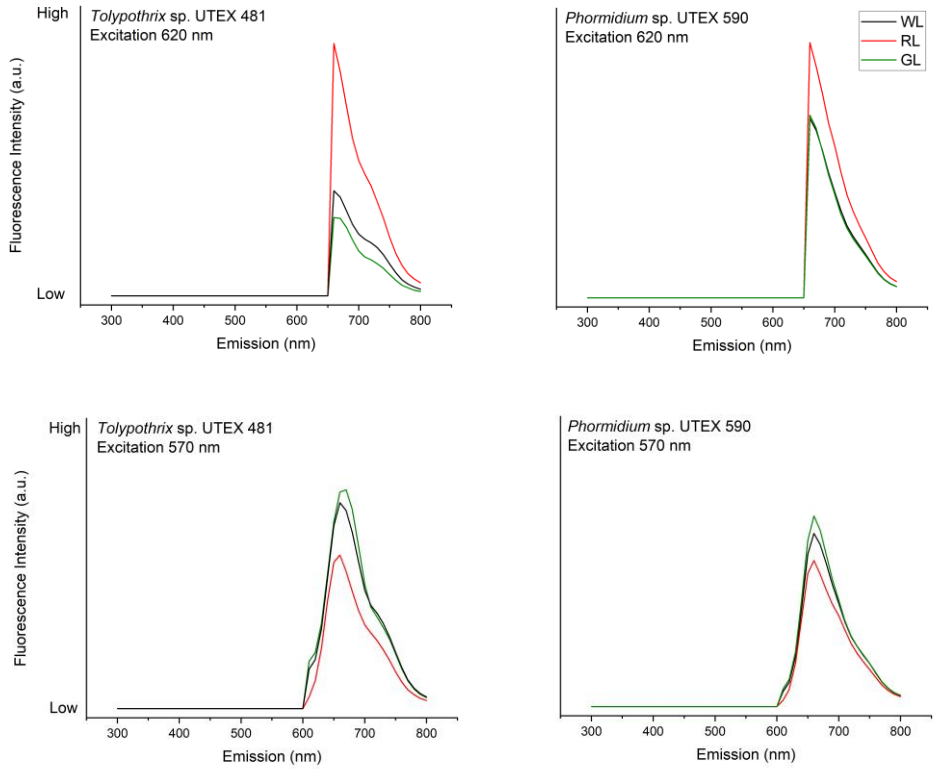

Supplementary Figure 3: Fluorescence Intensity Spectra of *Tolypothrix* sp. UTEX 481 and *Phormidium* sp. UTEX 590 at 620 nm excitation (top) and 570 nm excitation (bottom) for WL, RL, GL. Y axis is uniform for all four panels.

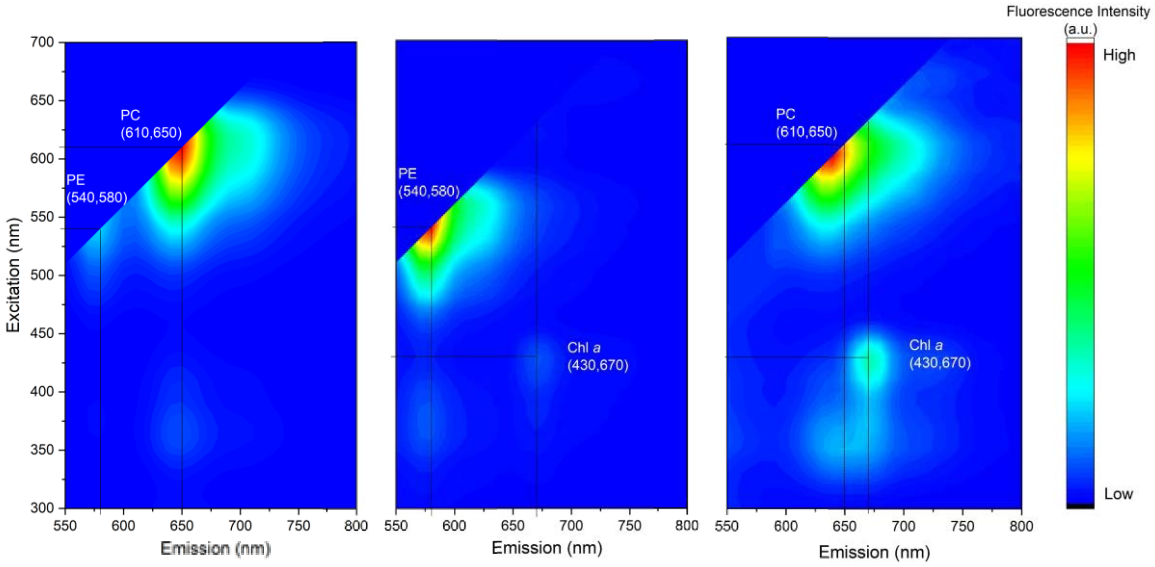

Supplementary Figure 4: Optical fingerprinting heat maps of excitation and emission matrices for pigments in combination. Pigment standards are labelled with their maximum excitation and emission point. A) PE and PC, B) PE and chl *a*, C) PC and chl *a*.

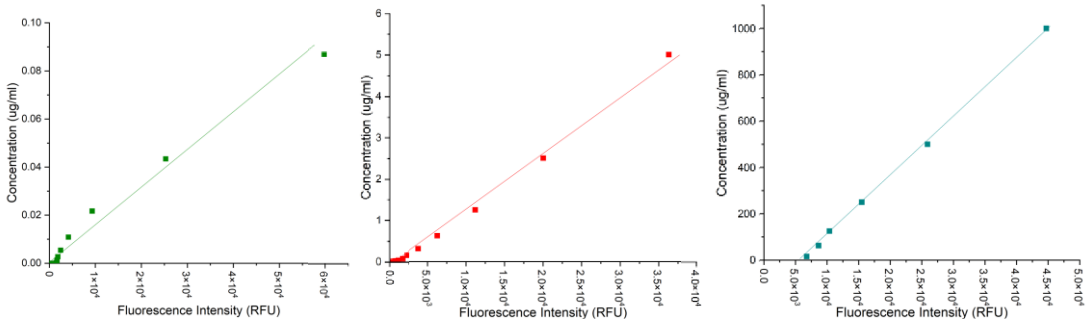

Supplementary Figure 5: Pigment standard calibration curves of a dilution series to measure fluorescence intensity (RFU) against concentration (ug/ml) for A) Chl *a* y = $2x10^{-6x}$-0.0002, R^2 = 0.9804, B) PE, y = -.0001x-0.1306, R^2 = 0.9956, C) PC, 0.0257x-154.4, R^2 = 0.9994. Standard curves used to determine the Pigment Quantities displayed in figure 4.

Supplementary Tables

Supplementary Table 1: Sequences used for the construction of the phylogenetic tree (Fig. 3)

Organism	**Sequence**
Phormidium sp. UTEX 590 obtained from RcaE primer	ANNNNNNNNANNAANTGNAAGCNGATTCTCCNNGCAGATC GCGTGCTAATTTATCATGTATTACCGGATGGTACAGGCAAA ACCATCAGCGAATCAGTTTTACCAGATTATCCCACACTGATG GATCTGGAATTTCCCCAAGAAGTTTTTCCCCAAGAGTATCAA CAACTATATGCCCAAGGAAGGGTAAGAGCGATCGCTGATGT ACATGATCCAGCCGCAGGGTTGGCGGAATGTTTGGTGGAAT TTGTCGATCAATTCCATATCAAAGCCAAATTAATTGTACCGA TTGTGCAAAACCTCAATGCCAACTCCCAGAATCAGCTTTGGG GTTTGTTAATCGCGCACCAATGCGACAGCGTTCGCCAATGG GTTGATTTTGAGTTGGAATTGATGCAGCAATTAGCAGATCAA ATCAGTATTGCTTTATCTCAAGCCCAATTATTAGGAAGATTA GAAGAGTGAGGATCCCCAT
Tolypothrix sp. UTEX 481 obtained from RcaE primer	NNNNNCTGAGATANNCATACTGATTTGATCCGCTAATTGCT GCATTAATTCCAACTCAAAATCCACCCATTGGCGAACGCTGT CGCATTGGTGGGCGATTAACAAACCCCACAGCTGATTCTGG GAGTTGGCATTGAGGTTTTGCACAATCGGTACAATTAATTTG GCTTTGATATGGAATTGATCGACAAATTCCACCAAACATTCT GCTAATCCTGCGGTTGGATCATGTACATCTGCGATCGCTCTG ACTCTTCCTTGGGCATATAGTTGTTGATATTCCTGGGGAAAA ACTTCTTGGGGAAATTCCAGATCCATGAGTGTGGGATAGTCT GGTAACACTGATTCGCTGATGGTTTTGCCTGTACCATCAGGC AATACATGATAAATTAGCACGCGATCGGCTTGGAGAATCCG CTGCACTTCTGTCACAGTGGTATGCAGAATTTCTTCCATAAT GCCAANNAC

Nostoc_carneum_NIES-2107	CTCTTCTAATCTTTCTAATAATTGGGCTTGAGATAAAGCAAT ACTGATTTGATCCGCTAATTGCTGCATCAATTCCAACTCAAA ATCTACCCATTGGCGAACGCTGTCGCATTGATGGGCGATTAA CAAACCCCAAAGTTGATTCTGGGAGTTGGCATTGAGGTTTTG CACAATTGGTACAATTAATTTGGCTTTAATATGAAATTGATC GACAAATTCCACCAAACATTCCGCTAACCCTGCGGCTGGAT CATGTACATCAGCGATCGCTCTTACCCTTCCTTGGGCATATA GTTGTTGATACTCTTGGGGAAAAACTT CTTGGGGAAATTCCAGATCGATGAGTGTGGGATAATCTGG
Fremyella_diplosiphon_putative_chromatic_adaptation_sensor_receptor	CCAGACTATCCCACACTCATGGATCTGGAATTTCCCCAAGAA GTTTTTCCCCAGGAATATCAACAACTATATGCCCAAGGAAG AGTCAGAGCGATCGCAGATGTACATGATCCAACCGCAGGAT TAGCAGAATGTTTGGTGGAATTTGTCGATCAATTCCATATCA AAGCCAAATTAATTGTACCGATTGTGCAAAACCTCAATGCC AACTCCCAGAATCAGCTGTGGGGTTTGTTAATCGCCCACCAA TGCGACAGCGTTCGCCAATGGGTGGATTTTGAGTTGGAATTA ATGCAGCAATTAGCGGATCAAATCAGTAT TGCTTTATCTCAAGCTCAACTATTAGGAAGATTAGAAGAG
Calothrix_sp._NIES-2098	TCTTCTAAGCGTTCTAGAAGTTGGGCTTGAGATAAAGCAATA CTGATTTGATCGGCTAGTTGTTGCATCAATTCCAACTCAAAA TCTACCCAATGACGCACGCTGTCGCATTGGTGGGCGATTAAC AAACCCCAAAGCTGATTTTGAGAGTTGGCATTCAGGTTTTGC ACAATCGGTACAATTAATTTGGCTTTGATCTGGAATTGATCG ACAAATCCACCAAACAATCTGCCAAGCCAGCCGCCGGATCG TGGACGTTAGCGATCGCTCTTACCCGTCCTTGGGCATATAGT TGTTGATACTCCTGGGGAAAAACTTC TTGGGGAAATTCCAGATCCATGAGTGCGGGATAATCTGG
Nostoc_commune_HK-02	CTCTTCTAAACGTTCCAGTAGTTGGGCTTGAGATAAAGCAAT ACTGATTTGATCGGCTAGTTGTTGCATCAATTCCAACTCAAA ATCTACCCAATGGCGAACGCTGTCGCATTGGTGCGCGATTA ACAAACCCCAAAGGTGATTCTGTGACTGGGCATTGAGGTTTT GCACAATCGGTACAATTAATTTGGCTTTAATCTGGAATTGAT CGACAAATTCCACCAAACAATCTGCCAAGCCAGCCGCCGGA TCGTGTACATCTGCGGTTGCACGTACCCGTCCGTGAGCATAC AGTTGTTGATACTCTTGGGGAAAAACTTCTTCAGGAAATTCT AGATCCATCAGTGTGGGATAATCTGG
Nostoc_flagelliforme_CCNUN1	CCAGATTATCCCACACTGATGGATCTGGAATTTCCTGAAGAA GTTTTTCCCCAAGAGTATCAACACCTGTATGCTCACGGACGG GTGCGTGCGACCGTAGATGTACACGATCCGGCGGCTGGCTT GGCAGATTGTTTGGTGGAATTTGTCGATCAATTCCAGATCAA AGCCAAATTAATTGTACCGATTGTGCAAAACCTCAATGCCC AGTCACAGAATCACCTTTGGGGTTTGTTAATCGCGCACCAAT GCGACAGCGTTCGCCATTGGGTAGATTTTGAGTTAGAATTGA TGCAACAACTGGCCGATCAAATCAGTATTGCTTTATCTCAAG CCCAACTACTGGAACGCTTAGAAGAG

Nostoc_sphaeroides_CCNUC1	CCAGATTATCCCACACTGATGGATCTGGAATTTCCTGAAGAA GTTTTTCCCCAAGAGTATCAACAACTGTATGCTCAGGGACGG GTGCGTGCAACCGCAGATGTCCACGATCCGGCGGCTGGCTT GGCAGATTGTTTGGTGGAATTTGTCGATCAATTCCAGGTCAA AGCCAAATTAATTGTACCAATTGTGCAAAACCTCAATGCCC AGTCACAGAATCACCTTTGGGGTTTGTTAATCGCGCACCAAT GCGACGGCGTTCGCCATTGGTAGATTTTGAGTTGGAATTGAT GCAACAACTGGCCGATCAAATCAGCATTGCTTTATCTCAAGC CCAACTATTGGAACGATTAGAAGA
Nostoc_sp._UHCC_0870	CCCGATTATCCCACGCTGATGGATCTGGAATTTCCCCAAGAA GTCTTTCCAGAGGATTATCAACAACTGTATGCTCACGGAAG GGTAAGAGCGATCGCAGATGTTCATGATCCGGCGGCTGGTT TGGCCGATTGTTTGGTGGAATTTGTCGATCAATTTCAGATCA AAGCCAAACTGATTGTCCCAATTGTGCAAAATCTCAATACC AATTTCCAAAATCAGTTATGGGGATTGTTAATCGCGCATCAA TGCAACAGCGATCGCCATTGGGTAGATTTTGAACTGGAATT GATGCAACAACTGGCAGATCAAATCAGTATTGCTTTGTCTCA AGCTCAACTCTTAGAACACTTAGAAGA
Calothrix_sp._NIES-2100	TCTTCTAAATGTTCCAGTAGTTGGGCTTGAGACAAGGCTATA CTGATTTGGTCTGCCAATTGTTGCATCAGTTCCAGTTCAAAA TCTACCCAATGGCGATCGCTACTGCATTGGTGGGCGATTAAT AAACCCCACAGCTGATTTTGGGAGTGGGCATTGAGATTTTG GACAATTGGTACAATCAGTTTGGCTTTGATTTGGAATTGATC GACAAATTCGATTAAACAATCTGCCAAACCCGCCGCCGGAT CATGGACATCAGCGATCGCTCTGACTCTTCCCTGAGCATAAA GTTGTTGATATTCTTCAGGAAAGACTTC CTGGGGAAATTCCAGATCCATCAGTGTGGGATAATCTGG
Fremyella_diplosiphon_NIES-3275	GAAATTCTGCATACCACTGTGACAGAAGTGCAGCGGATTCT CCAAGCCGATCGCGTGCTAATTTATCATGTATTGCCTGATGG TACAGGCAAAACCATCAGCGAATCAGTGTTACCAGACTATC CCACACTCATGGATCTGGAATTTCCCCAAGAAGTTTTTCCCC AGGAATATCAACAACTATATGCCCAAGGAAGAGTCAGAGCG ATCGCAGATGTACATGATCCAACCGCAGGATTAGCAGAATG TTTGGTGGAATTTGTCGATCAATTCCATATCAAAGCCAAATT AATTGTACCGATTGTGCAAAACCTCAATGCCAACTCCCAGA ATCAGCTGTGGGGTTTGTTAATCGCCCACCAATGCGACAGC GTTCGCCAATGGGTGGATTTTGAGTTGGAATTAATGCAGCA ATTAGCGG
Tolypothrix_sp._PCC_7712	GAAATTCTGCATACCACTGTGACAGAAGTGCAGCGGATTCT CCAAGCCGATCGCGTGCTAATTTATCATGTATTGCCTGATGG TACAGGCAAAACCATCAGCGAATCAGTGTTACCAGACTATC CCACACTCATGGATCTGGAATTTCCCCAAGAAGTTTTTCCCC AGGAATATCAACAACTATATGCCCAAGGAAGAGTCAGAGCG ATCGCAGATGTACATGATCCAACCGCAGGATTAGCAGAATG TTTGGTGGAATTTGTCGATCAATTCCATATCAAAGCCAAATT AATTGTACCGATTGTGCAAAACCTCAATGCCAACTCCCAGA ATCAGCTGTGGGGTTTGTTAATCGCCCACCAATGCGACAGC GTTCGCCAATGGGTGGATTTTGAGTTGGAATTAATGCAGCA ATTAGCGG

Tolypothrix_sp._PCC_7601	CTCTTCTAATCTTCCTAATAGTTGAGCTTGAGATAAAGCAAT ACTGATTTGATCCGCTAATTGCTGCATTAATTCCAACTCAAA ATCCACCCATTGGCGAACGCTGTCGCATTGGTGGGCGATTA ACAAACCCCACAGCTGATTCTGGGAGTTGGCATTGAGGTTTT GCACAATCGGTACAATTAATTTGGCTTTGATATGGAATTGAT CGACAAATTCCACCAAACATTCTGCTAATCCTGCGGTTGGAT CATGTACATCTGCGATCGCTCTGACTCTTCCTTGGGCATATA GTTGTTGATATTCCTGGGGAAAAACTTCTTGGGGAAATTCCA GATCCATGAGTGTGGGATAGTCTGG
Tolypothrix_sp._PCC_7601/1	CCAGACTATCCCACACTCATGGATCTGGAATTTCCCCAAGAA GTTTTTCCCCAGGAATATCAACAACTATATGCCCAAGGAAG AGTCAGAGCGATCGCAGATGTACATGATCCAACCGCAGGAT TAGCAGAATGTTTGGTGGAATTTGTCGATCAATTCCATATCA AAGCCAAATTAATTGTACCGATTGTGCAAAACCTCAATGCC AACTCCCAGAATCAGCTGTGGGGTTTGTTAATCGCCCACCAA TGCGACAGCGTTCGCCAATGGGTGGATTTTGAGTTGGAATTA ATGCAGCAATTAGCGGATCAAATCAGTATTGCTTTATCTCAA GCTCAACTATTAGGAAGATTAGAAGAG
Fremyella_diplosiphon_putative_chromatic_adaptation_sensor_receptor_(rcaE)_gene_complete_cds	CCAGACTATCCCACACTCATGGATCTGGAATTTCCCCAAGAA GTTTTTCCCCAGGAATATCAACAACTATATGCCCAAGGAAG AGTCAGAGCGATCGCAGATGTACATGATCCAACCGCAGGAT TAGCAGAATGTTTGGTGGAATTTGTCGATCAATTCCATATCA AAGCCAAATTAATTGTACCGATTGTGCAAAACCTCAATGCC AACTCCCAGAATCAGCTGTGGGGTTTGTTAATCGCCCACCAA TGCGACAGCGTTCGCCAATGGGTGGATTTTGAGTTGGAATTA ATGCAGCAATTAGCGGATCAAATCAGTATTGCTTTATCTCAA GCTCAACTATTAGGAAGATTAGAAGAG
Aulosira_laxa_NIES-50_DNA_nearly_complete_genome	CCAGATTATCCCACACTGATGGATCTGGAATTTCCCCAAGAA GTTTTTCCCCAAGAGTATCAACAACTATATGCCCAAGGAAG GGTAAGAGCGATCGCTGATGTACATGATCCAGCAGCGGGTT TAGCAGATTGTTTGGTGGAATTTGTTGATCAATTCCATATCA AAGCCAAATTAATTGTACCGATTGTGCAAAACCTCAATGCC AACTCCCAGAATCAGCTTTGGGGTTTGTTAATCGCGCATCAA TGTGACAGCGTGCGCCAATGGGTAGATTTTGAGTTGGAATT GATGCAGCAATTAGCGGATCAAATCAGTATTGCTTTATCTCA AGCCCAATTATTAGAAAGATTAGAAGAG
Tolypothrix_tenuis_PCC_7101_DNA_nearly_complete_genome	CTCTTCTAATCTTTCTAATAATTGGGCTTGAGATAAAGCAAT ACTGATTTGATCCGCTAATTGCTGCATCAATTCCAACTCAAA ATCTACCCATTGGCGCACGCTGTCACATTGATGCGCGATTAA CAAACCCCAAAGCTGATTCTGGGAGTTGGCATTGAGGTTTTG CACAATCGGTACAATTAATTTGGCTTTGATATGGAATTGATC AACAAATTCCACCAAACAATCTGCTAAACCCGCTGCTGGAT CATGTACATCAGCGATCGCTCTTACCCTTCCTTGGGCATATA GTTGTTGATACTCTTGGGGAAAAACTTCTTGGGGAAATTCCA GATCCATCAGTGTGGGATAATCTGG

Calothrix_brevissima_NIES-22 DNA_nearly_complete_genome	CCAGATTACCCCACACTCATGGATCTGGAATTTCCTCAAGAA GTTTTTCCCCAGGAATATCAACAATTGTATGCTCAAGGACGG GTAAGAGCGATCGCAAATGTCCACGATCCGGCGGCTGGTTT GGCAGAATGTTTGGTGGAATTTGTCGATCAATTTGCGATTAA AGCCAAATTAATTGTTCCCATCGTCCAAAATCTCAATGCCAG CGCTCAAAATCAACTTTGGGGGTTATTAATCGCCCATCAATG CAATAACTACCGCCATTGGGTAGATTTTGAATTGGAATTGAT GCAACAATTAGCCGATCAAATTAGTATTGCCTTATCTCAAGC TCAACTTTTAGAACATTTAGAAGA

Supplementary Table 2: Statistical testing results from Kolmogorov-Smirnov test with significant p-value < 0.05 in bold.

Data Set	Comparison	p-value	Statistical Test
Growth rate	WL *Tolypothrix* sp. UTEX 481 to WL *Phormidium* sp. UTEX 590	**1.26E-07**	**One-way Anova**
Growth rate	RL *Tolypothrix* sp. UTEX 481 to RL *Phormidium* sp. UTEX 590	**2.78E-06**	**One-way Anova**
Growth rate	GL *Tolypothrix* sp. UTEX 481 to GL *Phormidium* sp. UTEX 590	**3.16E-09**	**One-way Anova**
Growth rate	WL *Tolypothrix* sp. UTEX 481 to RL *Tolypothrix* sp. UTEX 481	**0.00676**	**One-way Anova**
Growth rate	WL *Tolypothrix* sp. UTEX 481 to GL *Tolypothrix* sp. UTEX 481	**0.0001**	**One-way Anova**
Growth rate	RL *Tolypothrix* sp. UTEX 481 to GL *Tolypothrix* sp. UTEX 481	**0.00525**	**One-way Anova**
Growth rate	WL *Phormidium* sp. UTEX 590 to RL *Phormidium* sp. UTEX 590	**0.00488**	**One-way Anova**
Growth rate	RL *Phormidium* sp. UTEX 590 to GL *Phormidium* sp. UTEX 590	0.65933	**One-way Anova**
Growth rate	WL *Phormidium* sp. UTEX 590 to GL *Phormidium* sp. UTEX 590	**0.00619**	**One-way Anova**
EEM	WL *Tolypothrix* sp. UTEX 481 to RL *Tolypothrix* sp. UTEX 481	0.067184281	Kolmogorov-Smirnov
EEM	WL *Tolypothrix* sp. UTEX 481 to GL *Tolypothrix* sp. UTEX 481	0.790012998	Kolmogorov-Smirnov
EEM	RL *Tolypothrix* sp. UTEX 481 to GL *Tolypothrix* sp. UTEX 481	**0.002909638**	Kolmogorov-Smirnov
EEM	WL *Phormidium* sp. UTEX 590 to RL *Phormidium* sp. UTEX 590	**0.002649949**	Kolmogorov-Smirnov
EEM	WL *Phormidium* sp. UTEX 590 to GL *Phormidium* sp. UTEX 590	0.940109339	Kolmogorov-Smirnov
EEM	RL *Phormidium* sp. UTEX 590 to GL *Phormidium* sp. UTEX 590	**0.000601965**	Kolmogorov-Smirnov
EEM	WL *Tolypothrix* sp. UTEX 481 to WL *Phormidium* sp. UTEX 590	0	Kolmogorov-Smirnov
EEM	RL *Tolypothrix* sp. UTEX 481 to RL *Phormidium* sp. UTEX 590	0	Kolmogorov-Smirnov
EEM	GL *Tolypothrix* sp. UTEX 481 to GL *Phormidium* sp. UTEX 590	0	Kolmogorov-Smirnov
rETR	WL *Tolypothrix* sp. UTEX 481 to RL *Tolypothrix* sp. UTEX 481	**$4.98E^{-05}$**	Kolmogorov-Smirnov
rETR	WL *Tolypothrix* sp. UTEX 481 to GL *Tolypothrix* sp. UTEX 481	0.108133374	Kolmogorov-Smirnov
rETR	RL *Tolypothrix* sp. UTEX 481 to GL *Tolypothrix* sp. UTEX 481	**9.58E-09**	Kolmogorov-Smirnov
rETR	WL *Phormidium* sp. UTEX 590 to RL *Phormidium* sp. UTEX 590	0.682597877	Kolmogorov-Smirnov

rETR	WL *Phormidium* sp. UTEX 590 to GL *Phormidium* sp. UTEX 590	0.969610144	Kolmogorov-Smirnov
rETR	RL *Phormidium* sp. UTEX 590 to GL *Phormidium* sp. UTEX 590	0.969610144	Kolmogorov-Smirnov
rETR	WL *Tolypothrix* sp. UTEX 481 to WL *Phormidium* sp. UTEX 590	0	Kolmogorov-Smirnov
rETR	RL *Tolypothrix* sp. UTEX 481 to RL *Phormidium* sp. UTEX 590	0	Kolmogorov-Smirnov
rETR	GL *Tolypothrix* sp. UTEX 481 to GL *Phormidium* sp. UTEX 590	0	Kolmogorov-Smirnov

Supplementary Table 3: Primer Information for PCR and DNA sequencing to distinguish the two Nostocales strains. Table includes Primer name, sequence and reference from the obtained sequence.

Primer name	**Target**	**Sequence**	**Reference**
RcaE-2	RcaE (CA regulator)	GGGGATCCTCATTGGATATTGGCGTA	Found in supplementary info. Pairs with RcaE-12 [61]
RcaE-5	RcaE (CA regulator)	GGCATATGAAGGAAATTCTGCATACC	Found in supplementary info. Pairs with RcaE-6 [61]
RcaE-6	RcaE (CA regulator)	GGGGATCCTCACTCTTCTAATCTTCCTAA	Found in supplementary info. Pairs with RcaE-5 [61]
RcaE-12	RcaE (CA regulator)	GGCATATGTCTAAAAGTTCCTCG	Found in supplementary info. Pairs with RcaE-2 [61]
IflA GAF1 F	IflA GAF Protein	GCCGAGCTCTTAACGCGCTTGACTGAGTAGGGTACT	Found in supplementary info [93]
IflA GAF1 R	IflA GAF Protein	CCAGGATCCAGAACTTAAAGAGATATTAACTACCAG	Found in supplementary info [93]
IflA GAF3 F	IflA GAF Protein	GCCGAGCTCTTAGCGACTGCTTTCATATAATTGTGC	Found in supplementary info [93]
IflA GAF3 R	IflA GAF Protein	CCAGGATCCAGACTACAAACTTACCTTGCAAACTAT	Found in supplementary info [93]
RcaE GAF expression F	RcaE GAF Expression	TTACGGATCCGAAGGAAATTCTGCATACCACTGTGA	Found in supplementary info [87]

RcaE GAF expression R	RcaE GAF Expression	TGCTGAGCTCGCGCTGCTACA ACCTCTTCTAATCT	Found in supplementary info [87]

Supplementary Table 4: Cell measurements. Cell length, filament length and cells per filament for both Nostocales strains under WL, RL and GL ± standard deviation. Letters indicate significant differences. N=20

Growth light colour	Cell Length (µm)		Filament length (µm)		Cells per filament	
	***Tolypothrix* 481**	***Phormidium* 590**	***Tolypothrix* 481**	***Phormidium* 590**	***Tolypothrix* 481**	***Phormidium* 590**
White	6.708 ± 1.10[a]	4.934 ± 0.84[b]	205.968 ± 71.77[a]	78.368 ± 30.51[b]	31.40 ± 11.62[a]	16 ± 5.13[b]
Red	6.686 ± 1.80[a]	4.529 ± 1.12[b]	199.403 ± 73.47[a]	88.617 ± 83.45[b]	30.70 ± 11.59[a]	19 ± 16.84[b]
Green	10.017 ± 2.01[c]	4.880 ± 0.71[b]	222.631 ± 74.02[a]	94.669 ± 50.17[b]	22.65 ± 7.32[c]	20 ± 10.98

Supplementary Table 5: Growth rate (OD720 Day^{-1}) for both Nostocales strains under WL, RL and GL ± standard deviation. Letters indicate significant differences. Growth rate derived from curve in figure 2 using the formula: ((OD720 Day 5 – OD720 Day 0)/6). Comparisons made across strains and across light conditions within each strain. Different letters indicate significance for the mentioned comparisons. N=10

Growth Light Colour	Growth Rate (OD720 Day^{-1})	
	***Tolypothrix* 481**	***Phormidium* 590**
White	0.0514 ± 0.02[a]	0.0219 ± 0.008[b]
Red	0.0337 ± 0.009[c]	0.0123 ± 0.004[d]
Green	0.0242 ± 0.003[e]	0.0131 ± 0.003[d]

Supplementary Table 6: Maximum fluorescent points from the Excitation / Emission heat maps in Figure 6

Organism	**Condition**	**Fluorescence Maximum (a.u.)**	**Ex / Em (nm)**
Tolypothrix sp. UTEX 481	WL	11.4	570 / 660
	RL	13.9	620 / 660

	GL	12.1	570 / 670
Phormidium sp. UTEX 590	WL	9.9	620 / 660
	RL	14.1	620 / 660
	GL	10.1	620 / 660

Supplementary Table 7: Genes commonly upregulated in both *Tolypothrix* 481 and *Phormidium* 590 as obtained from Venny in relation to Figure 8.

Regulation	**Common elements in Upregulated Genes for 481Tv481W and 590Tv590W**
U	phosphorelay signal transduction system [GO:0000160]
U	membrane [GO:0016020]
U	plasma membrane [GO:0005886]
U	metal ion binding [GO:0046872]
U	lipid biosynthetic process [GO:0008610]
U	hydrolase activity [GO:0016787]
U	carbohydrate binding [GO:0030246]; catalytic activity [GO:0003824]; carbohydrate metabolic process [GO:0005975]
U	phycobilisome [GO:0A030089]; chloride ion binding [GO:0031404]; light absorption [GO:0016037]
U	ATP binding [GO:0005524]; metal ion binding [GO:0046872]
U	oxidoreductase activity [GO:0016491]; zinc ion binding [GO:0008270]
U	membrane [GO:0016020]; transmembrane transporter activity [GO:0022857]
U	oxidoreductase activity [GO:0016491]
U	ubiquinone biosynthetic process [GO:0006744]
U	4 iron, 4 sulfur cluster binding [GO:0051539]; formate dehydrogenase (NAD+) activity [GO:0008863]; molybdenum ion binding [GO:0030151]; molybdopterin cofactor binding [GO:0043546]
U	DNA binding [GO:0003677]
U	phosphorelay sensor kinase activity [GO:0000155]

Supplementary Table 8: Genes uniquely upregulated in *Tolypothrix* 481 RL compared to WL as obtained from Venny in relation to Figure 8.

Regulation	Elements uniquely upregulated in 481Tv481W
U	plasma membrane [GO:0005886]; ammonium transmembrane transporter activity [GO:0008519]
U	2 iron, 2 sulfur cluster binding [GO:0051537]; DNA binding [GO:0003677]; metal ion binding [GO:0046872]; oxidoreductase activity [GO:0016491]
U	phosphate ion binding [GO:0042301]; phosphate ion transport [GO:0006817]
U	membrane [GO:0016020]; ATP binding [GO:0005524]; phosphorelay sensor kinase activity [GO:0000155]; protein dimerization activity [GO:0046983]; protein serine/threonine kinase activity [GO:0004674]
U	ATP binding [GO:0005524]; phosphorelay sensor kinase activity [GO:0000155]; protein serine/threonine kinase activity [GO:0004674]
U	4 iron, 4 sulfur cluster binding [GO:0051539]; catalytic activity [GO:0003824]; metal ion binding [GO:0046872]
U	enzyme activator activity [GO:0008047]; peptidase activity [GO:0008233]
U	phycobilisome [GO:0030089]; plasma membrane-derived thylakoid membrane [GO:0031676]; photosynthesis [GO:0015979]
U	membrane [GO:0016020]; protein C-terminal S-isoprenylcysteine carboxyl O-methyltransferase activity [GO:0004671]; C-terminal protein methylation [GO:0006481]
U	catalytic activity [GO:0003824]
U	ubiquitin-like modifier activating enzyme activity [GO:0008641]
U	membrane [GO:0016020]; ATP binding [GO:0005524]; ATP hydrolysis activity [GO:0016887]
U	membrane [GO:0016020]; ferrous iron transmembrane transporter activity [GO:0015093]
U	phycobilisome [GO:0030089]; plasma membrane-derived thylakoid membrane [GO:0031676]
U	membrane [GO:0016020]; monoatomic cation transmembrane transporter activity [GO:0008324]
U	ATP binding [GO:0005524]; metal ion binding [GO:0046872]; pyruvate, water dikinase activity [GO:0008986]; gluconeogenesis [GO:0006094]; phosphorylation [GO:0016310]; pyruvate metabolic process [GO:0006090]

U	GTP binding [GO:0005525]
U	cytoplasm [GO:0005737]; 4 iron, 4 sulfur cluster binding [GO:0051539]; [formate-C-acetyltransferase]-activating enzyme activity [GO:0043365]; lyase activity [GO:0016829]; metal ion binding [GO:0046872]
U	membrane [GO:0016020]; flavin adenine dinucleotide binding [GO:0050660]; hypotaurine dehydrogenase activity [GO:0047822]; N,N-dimethylaniline monooxygenase activity [GO:0004499]; NAD(P)H oxidase H2O2-forming activity [GO:0016174]; NADP binding [GO:0050661]; lipid metabolic process [GO:0006629]
U	membrane [GO:0016020]; transmembrane signaling receptor activity [GO:0004888]; chemotaxis [GO:0006935]; signal transduction [GO:0007165]
U	acetaldehyde dehydrogenase (acetylating) activity [GO:0008774]; alcohol dehydrogenase (NAD+) activity [GO:0004022]; metal ion binding [GO:0046872]; alcohol metabolic process [GO:0006066]; carbon utilization [GO:0015976]
U	plasma membrane [GO:0005886]; ATP binding [GO:0005524]; ATP hydrolysis activity [GO:0016887]; ATPase-coupled monoatomic cation transmembrane transporter activity [GO:0019829]; metal ion binding [GO:0046872]
U	DNA binding [GO:0003677]; DNA-binding transcription factor activity [GO:0003700]
U	membrane [GO:0016020]; endonuclease activity [GO:0004519]; exonuclease activity [GO:0004527]
U	helicase activity [GO:0004386]
U	membrane [GO:0016020]; lipid metabolic process [GO:0006629]
U	regulation of DNA-templated transcription [GO:0006355]
U	plasma membrane [GO:0005886]; phosphorelay sensor kinase activity [GO:0000155]
U	ATP binding [GO:0005524]; protein kinase activity [GO:0004672]; protein phosphorylation [GO:0006468]
U	membrane [GO:0016020]; ABC-type transporter activity [GO:0140359]; ATP binding [GO:0005524]; ATP hydrolysis activity [GO:0016887]
U	DNA-binding transcription factor activity [GO:0003700]; sequence-specific DNA binding [GO:0043565]

U	acyltransferase activity, transferring groups other than amino-acyl groups [GO:0016747]
U	cysteine desulfurase activity [GO:0031071]; iron-sulfur cluster binding [GO:0051536]; lyase activity [GO:0016829]; metal ion binding [GO:0046872]; pyridoxal phosphate binding [GO:0030170]; amino acid metabolic process [GO:0006520]
U	nucleic acid binding [GO:0003676]
U	cytoplasm [GO:0005737]; formate C-acetyltransferase activity [GO:0008861]; glucose metabolic process [GO:0006006]
U	metal ion binding [GO:0046872]; oxidoreductase activity, acting on single donors with incorporation of molecular oxygen, incorporation of two atoms of oxygen [GO:0016702]; lipid oxidation [GO:0034440]
U	molybdenum-iron nitrogenase complex [GO:0016612]; carbonyl sulfide nitrogenase activity [GO:0018697]; iron-sulfur cluster binding [GO:0051536]; metal ion binding [GO:0046872]; nitrogenase activity [GO:0016163]; nitrogen fixation [GO:0009399]
U	ATP binding [GO:0005524]; kinase activity [GO:0016301]; phosphorylation [GO:0016310]
U	membrane [GO:0016020]; 2 iron, 2 sulfur cluster binding [GO:0051537]; chlorophyllide a oxygenase [overall] activity [GO:0010277]; metal ion binding [GO:0046872]
U	DNA restriction-modification system [GO:0009307]

Supplementary Table 9: Genes uniquely upregulated in *Phormidium* 590 RL compared to WL as obtained by Venny in relation to Figure 8.

Regulation	**Elements uniquely upregulated in 590Tv590W**
U	double-stranded RNA binding [GO:0003725]
U	transferase activity [GO:0016740]
U	lyase activity [GO:0016829]; nickel cation binding [GO:0016151]
U	plasma membrane [GO:0005886]; nitrate transmembrane transporter activity [GO:0015112]
U	plasma membrane [GO:0005886]; magnesium ion transmembrane transporter activity [GO:0015095]; metal ion binding [GO:0046872]
U	methyltransferase activity [GO:0008168]; methylation [GO:0032259]

U	cytoplasm [GO:0005737]; RNA binding [GO:0003723]; rRNA methyltransferase activity [GO:0008649]; regulation of DNA-templated transcription [GO:0006355]
U	transferase activity [GO:0016740]; peptidoglycan biosynthetic process [GO:0009252]
U	plasma membrane [GO:0005886]; protein secretion [GO:0009306]
U	membrane [GO:0016020]; phosphorelay sensor kinase activity [GO:0000155]
U	molybdopterin cofactor binding [GO:0043546]; oxidoreductase activity [GO:0016491]
U	DNA binding [GO:0003677]; phosphorelay signal transduction system [GO:0000160]
U	membrane [GO:0016020]; signal transduction [GO:0007165]
U	ATP binding [GO:0005524]; magnesium chelatase activity [GO:0016851]; chlorophyll biosynthetic process [GO:0015995]; photosynthesis [GO:0015979]
U	membrane [GO:0016020]; thylakoid [GO:0009579]
U	heme binding [GO:0020037]; iron ion binding [GO:0005506]; monooxygenase activity [GO:0004497]; oxidoreductase activity, acting on paired donors, with incorporation or reduction of molecular oxygen [GO:0016705]
U	electron transfer activity [GO:0009055]; iron ion binding [GO:0005506]
U	membrane [GO:0016020]; transferase activity [GO:0016740]
U	thioredoxin peroxidase activity [GO:0008379]; cellular response to oxidative stress [GO:0034599]
U	ATP binding [GO:0005524]; ATP hydrolysis activity [GO:0016887]
U	ureidoglycolate hydrolase activity [GO:0004848]; ureidoglycolate lyase activity [GO:0050385]; allantoin catabolic process [GO:0000256]; purine nucleobase metabolic process [GO:0006144]
U	DNA binding [GO:0003677]; phosphorelay signal transduction system [GO:0000160]; regulation of DNA-templated transcription [GO:0006355]
U	ATP-binding cassette (ABC) transporter complex [GO:0043190]; transmembrane transport [GO:0055085]
U	glutathione hydrolase activity [GO:0036374]; hypoglycin A gamma-glutamyl transpeptidase activity [GO:0102953]; leukotriene C4 gamma-glutamyl

	transferase activity [GO:0103068]; glutathione biosynthetic process [GO:0006750]; glutathione catabolic process [GO:0006751]
U	4-hydroxyphenylpyruvate dioxygenase activity [GO:0003868]; metal ion binding [GO:0046872]; aromatic amino acid metabolic process [GO:0009072]
U	DNA binding [GO:0003677]; regulation of DNA-templated transcription [GO:0006355]
U	ATP binding [GO:0005524]; phosphorelay sensor kinase activity [GO:0000155]
U	membrane [GO:0016020]; antiporter activity [GO:0015297]; proton transmembrane transport [GO:1902600]
U	glycosyltransferase activity [GO:0016757]
U	DNA binding [GO:0003677]; DNA restriction-modification system [GO:0009307]
U	membrane [GO:0016020]; serine-type endopeptidase activity [GO:0004252]
U	ferric iron binding [GO:0008199]; oxidoreductase activity, acting on metal ions [GO:0016722]
U	cytoplasm [GO:0005737]; 4-alpha-D-(1->4)-alpha-D-glucanotrehalose trehalohydrolase activity [GO:0033942]; cation binding [GO:0043169]; glycosyltransferase activity [GO:0016757]; trehalose biosynthetic process [GO:0005992]
U	cobalamin binding [GO:0031419]; iron-sulfur cluster binding [GO:0051536]; metal ion binding [GO:0046872]; methyltransferase activity [GO:0008168]; methylation [GO:0032259]
U	anti-sigma factor antagonist activity [GO:0043856]
U	glycosyltransferase activity [GO:0016757]; carbohydrate metabolic process [GO:0005975]
U	flavin adenine dinucleotide binding [GO:0050660]; oxidoreductase activity, acting on a sulfur group of donors, NAD(P) as acceptor [GO:0016668]
U	cytoplasm [GO:0005737]; 4-alpha-D-(1->4)-alpha-D-glucanotrehalose trehalohydrolase activity [GO:0033942]; glycosyltransferase activity [GO:0016757]; trehalose biosynthetic process [GO:0005992]
U	sucrose synthase activity [GO:0016157]; sucrose metabolic process [GO:0005985]
U	DNA binding [GO:0003677]; sigma factor activity [GO:0016987]; DNA-templated transcription initiation [GO:0006352]

U	host outer membrane [GO:0044384]
U	membrane [GO:0016020]; transmembrane transporter activity [GO:0022857]; carbohydrate transport [GO:0008643]
U	protein-lysine N-methyltransferase activity [GO:0016279]; methylation [GO:0032259]
U	membrane [GO:0016020]; voltage-gated chloride channel activity [GO:0005247]
U	membrane [GO:0016020]; kinase activity [GO:0016301]; phosphorylation [GO:0016310]
U	DNA binding [GO:0003677]; site-specific DNA-methyltransferase (adenine-specific) activity [GO:0009007]
U	glutathione transferase activity [GO:0004364]
U	ATP binding [GO:0005524]; catalytic activity [GO:0003824]; metal ion binding [GO:0046872]
U	ATP binding [GO:0005524]; kinase activity [GO:0016301]; phospholipid biosynthetic process [GO:0008654]; phosphorylation [GO:0016310]
U	UDP-glucose:hexose-1-phosphate uridylyltransferase activity [GO:0008108]; zinc ion binding [GO:0008270]; galactose catabolic process via UDP-galactose [GO:0033499]
U	translation initiation factor activity [GO:0003743]
U	plasma membrane [GO:0005886]; mechanosensitive monoatomic ion channel activity [GO:0008381]
U	plasma membrane light-harvesting complex [GO:0030077]; electron transporter, transferring electrons within the cyclic electron transport pathway of photosynthesis activity [GO:0045156]; photosynthesis, light reaction [GO:0019684]
U	metal ion binding [GO:0046872]; metalloendopeptidase activity [GO:0004222]; proteolysis [GO:0006508]
U	serine-type peptidase activity [GO:0008236]; proteolysis [GO:0006508]
U	phosphopantetheine binding [GO:0031177]
U	methyltransferase activity [GO:0008168]; nucleic acid binding [GO:0003676]; macromolecule modification [GO:0043412]; methylation [GO:0032259]; nitrogen compound metabolic process [GO:0006807]; primary metabolic process [GO:0044238]
U	membrane [GO:0016020]; lipid biosynthetic process [GO:0008610]

U	ATP-binding cassette (ABC) transporter complex [GO:0043190]; ABC-type transporter activity [GO:0140359]
U	1,4-alpha-glucan branching enzyme activity [GO:0003844]; 1,4-alpha-glucan branching enzyme activity (using a glucosylated glycogenin as primer for glycogen synthesis) [GO:0102752]; cation binding [GO:0043169]; hydrolase activity, hydrolyzing O-glycosyl compounds [GO:0004553]; glycogen biosynthetic process [GO:0005978]
U	cytoplasm [GO:0005737]; phosphorelay response regulator activity [GO:0000156]; protein-glutamate methylesterase activity [GO:0008984]; chemotaxis [GO:0006935]
U	S-adenosylmethionine-dependent methyltransferase activity [GO:0008757]; methylation [GO:0032259]

Supplementary Table 10: Genes commonly downregulated in *Tolypothrix* 481 and *Phormidium* 590 as obtained by Venny in relation to Figure 8.

Regulation	**Common elements downregulated in 481Tv481W and 590Tv590W**
D	membrane [GO:0016020]
D	DNA binding [GO:0003677]

Supplementary Table 11: Genes uniquely downregulated in *Tolypothrix* 481 RL compared to WL as obtained by Venny in relation to Figure 8.

Regulation	**Elements uniquely downregulated in 481Tv481W**
D	peptidyl-prolyl cis-trans isomerase activity [GO:0003755]
D	transferase activity [GO:0016740]
D	ATP binding [GO:0005524]; protein kinase activity [GO:0004672]; protein phosphorylation [GO:0006468]; signaling [GO:0023052]
D	glycosyltransferase activity [GO:0016757]
D	plasma membrane [GO:0005886]; protein transport [GO:0015031]
D	ATP binding [GO:0005524]; ATP hydrolysis activity [GO:0016887]
D	plasma membrane [GO:0005886]; lipopolysaccharide biosynthetic process [GO:0009103]
D	helicase activity [GO:0004386]
D	isomerase activity [GO:0016853]; nucleotidyltransferase activity [GO:0016779]; polysaccharide metabolic process [GO:0005976]
D	protein transport [GO:0015031]

D	heme binding [GO:0020037]; iron ion binding [GO:0005506]; monooxygenase activity [GO:0004497]; oxidoreductase activity, acting on paired donors, with incorporation or reduction of molecular oxygen [GO:0016705]
D	membrane [GO:0016020]; potassium channel activity [GO:0005267]; proton channel activity [GO:0015252]
D	membrane [GO:0016020]; ATP binding [GO:0005524]; ATP hydrolysis activity [GO:0016887]; ATPase-coupled phosphate ion transmembrane transporter activity [GO:0015415]; inorganic phosphate transmembrane transporter activity [GO:0005315]
D	dioxygenase activity [GO:0051213]; iron ion binding [GO:0005506]; L-ascorbic acid binding [GO:0031418]; oxidoreductase activity, acting on paired donors, with incorporation or reduction of molecular oxygen [GO:0016705]
D	methyltransferase activity [GO:0008168]; methylation [GO:0032259]
D	ATP binding [GO:0005524]; protein serine/threonine kinase activity [GO:0004674]; protein phosphorylation [GO:0006468]
D	plasma membrane [GO:0005886]; transmembrane transporter activity [GO:0022857]; protein transport [GO:0015031]
D	5-formyltetrahydrofolate cyclo-ligase activity [GO:0030272]; ATP binding [GO:0005524]; metal ion binding [GO:0046872]

Supplementary Table 12: Genes uniquely downregulated in *Phormidium* 590 RL compared to WL as obtained by Venny in relation to Figure 8.

Regulation	**Elements uniquely downregulated in 590Tv590W**
D	DNA binding [GO:0003677]; N-methyltransferase activity [GO:0008170]; site-specific DNA-methyltransferase (adenine-specific) activity [GO:0009007]
D	phycobilisome [GO:0030089]; plasma membrane-derived thylakoid membrane [GO:0031676]; photosynthesis [GO:0015979]
D	cobalt ion binding [GO:0050897]; oxidoreductase activity, acting on the CH-CH group of donors, iron-sulfur protein as acceptor [GO:0016636]; phytochromobilin biosynthetic process [GO:0010024]
D	membrane [GO:0016020]; ATP binding [GO:0005524]; ATP hydrolysis activity [GO:0016887]

D	3-oxoacyl-[acyl-carrier-protein] synthase activity [GO:0004315]; phosphopantetheine binding [GO:0031177]; fatty acid biosynthetic process [GO:0006633]
D	Thylakoid membrane [GO:0042651]
D	phycobilisome [GO:0030089]; lyase activity [GO:0016829]
D	catalytic activity [GO:0003824]; iron-sulfur cluster binding [GO:0051536]; metal ion binding [GO:0046872]
D	catalytic activity [GO:0003824]; phosphopantetheine binding [GO:0031177]; lipid biosynthetic process [GO:0008610]
D	plasma membrane [GO:0005886]
D	catalytic activity [GO:0003824]; phosphopantetheine binding [GO:0031177]; amide biosynthetic process [GO:0043604]; carboxylic acid metabolic process [GO:0019752]; organonitrogen compound biosynthetic process [GO:1901566]
D	heme oxygenase (decyclizing) activity [GO:0004392]; metal ion binding [GO:0046872]; heme oxidation [GO:0006788]
D	metal ion binding [GO:0046872]; molybdate ion transport [GO:0015689]
D	plasma membrane [GO:0005886]; nitrate transmembrane transporter activity [GO:0015112]
D	dioxygenase activity [GO:0051213]
D	cell outer membrane [GO:0009279]; siderophore-iron transmembrane transporter activity [GO:0015343]; signaling receptor activity [GO:0038023]
D	plasma membrane [GO:0005886]; transmembrane transport [GO:0055085]

Supplementary Table 13: List of genes involved in the phycobilin biosynthetic pathway as referenced by a previous paper [1] accompanied by logFoldChange for *Tolypothrix* 481 RL compared to WL

Gene	Fold Change
heme oxygenase (biliverdin-producing)	1.6
Coproporphyrinogen-III oxidase	1.4
heme oxygenase (biliverdin-producing)	0.07
uroporphyrinogen-III C-methyltransferase	0.11
uroporphyrinogen-III C-methyltransferase	0.49
heme oxygenase (biliverdin-producing)	0.07
Coproporphyrinogen-III oxidase	-0.16
Uroporphyrinogen III synthase HEM4	0.06

Heme chaperone HemW	-0.27
Protoporphyrinogen IX oxidase (PPO)	0.5

Supplementary Table 14: List of Genes involved in the phycobilin biosynthetic pathway as referenced by a previous paper [1] accompanied by logFoldChange for *Phormidium* 590 RL compared to WL

Gene	**Fold Change**
uroporphyrinogen-III C-methyltransferase	-0.6
Uroporphyrinogen III synthase HEM4	-0.3
uroporphyrinogen-III C-methyltransferase	-0.3
Delta-aminolevulinic acid dehydratase	-0.5
Heme chaperone HemW	0.3
Coproporphyrinogen-III oxidase	0.4
coproporphyrin ferrochelatase	1.1
Coproporphyrinogen-III oxidase	-0.6
Protoporphyrinogen IX oxidase (PPO)	-0.03
heme oxygenase (biliverdin-producing)	**-2.3**
heme oxygenase (biliverdin-producing)	-0.5
heme oxygenase (biliverdin-producing)	-0.3